





### This is to certify that the

#### thesis entitled

# IOP MEASUREMENT USING SONIC EXCITATION AND LASER VELOCIMETRY

presented by

Jack M. Hamelink

has been accepted towards fulfillment of the requirements for

Ph.D. degree in Applied Mechanics

Gary Cloud Major professor

Date\_\_\_\_\_May 10, 1978

**O**-7639

c) 1978

JACK M. HAMELINK

ALL RIGHTS RESERVED

# IOP MEASUREMENT USING SONIC EXCITATION AND LASER VELOCIMETRY

Ву

Jack M. Hamelink

#### A DISSERTATION

Submitted to
Michigan State University
in partial fulfillment of the requirements
for the degree of

DOCTOR OF PHILOSOPHY

Department of Metallurgy, Mechanics and Materials Science

## PLEASE NOTE:

Dissertation contains glossy photographs that will not reproduce well. Filmed best way possible.

UNIVERSITY MICROFILMS

Ξ.

ε,

.

W}

Œ

e

CO

CO

is

#### ABSTRACT

## IOP MEASUREMENT USING SONIC EXCITATION AND LASER VELOCIMETRY

Ву

Jack M. Hamelink

Glaucoma, which is manifested clinically as abnormally large intraocular pressure (IOP), is an insidious eye disease which must be detected in its early stages for there to be any possibility of successful treatment. At this time, detection of glaucoma and evaluation of therapy are largely dependent upon tonometric methods which require applanation of the cornea. This dissertation describes a new method of IOP determination which is noncontacting and nonapplanating. Freshly excised lambs' eyes were stimulated by audio sound waves and the resulting corneal movements detected by the laser Doppler effect. It was observed that the response frequency shift of the cornea was a function of the IOP.

The system employed in the invitro applications is shown by Figure A-1.

Į.

IOP

and

the

fron

Valu

of d

obje

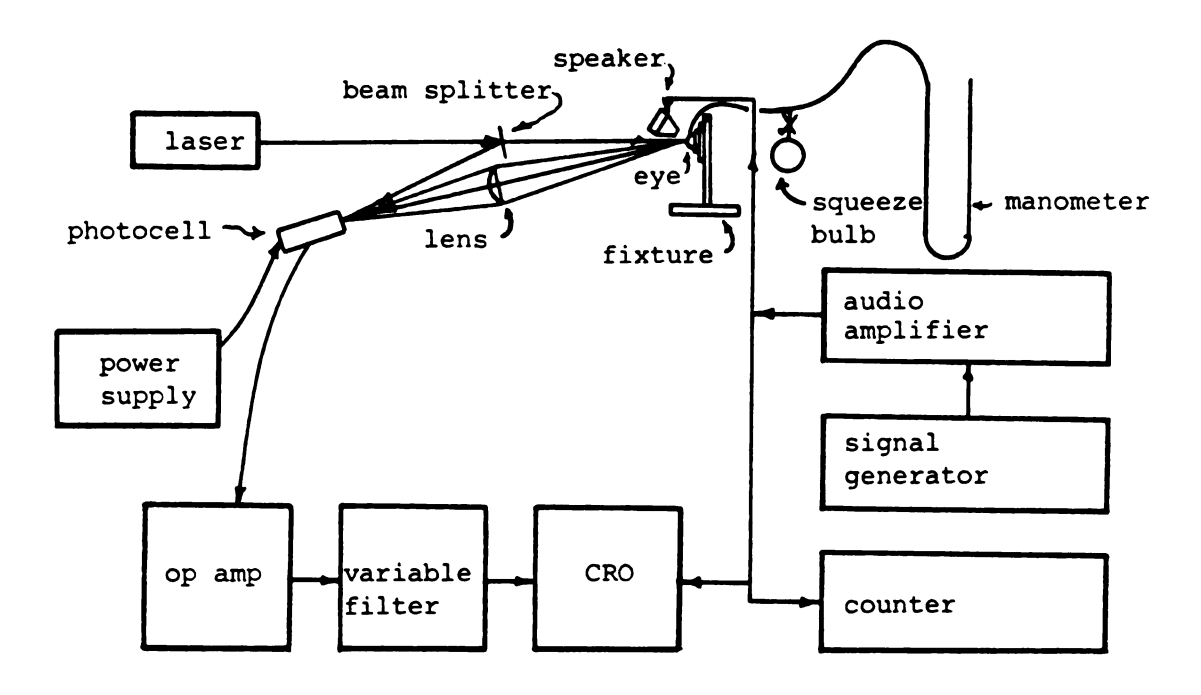


Figure A-l Data Gathering System

An empirical relationship was developed between IOP and response frequency for the lambs' eyes tested and is shown below.

 $f = 233.65 + 7.3 (ln IOP)^{\frac{1}{2}}$  in inches of H<sub>2</sub>O or  $f = 233.65 + 6.9 (ln IOP)^{\frac{1}{2}}$  in mm of Hg

The standard deviation of the data obtained in the physiological range of IOPs was  $\pm$  1.4 mm Hg. Reported values of standard deviation of existing tonometers range from about  $\pm$  1.5 mm Hg to  $\pm$  3.2 mm Hg.

High speed movies were taken of invivo applanation of dog and human eyes by three clinical tonometers. These films illustrate the reasons for the physiological blunt object trauma that exists with applanation tonometers.

No such basis for blunt object trauma exists for the posed system since there is no applanation and no physical contact with the cornea.

Invivo tests run on dogs with the proposed system showed promise for this system with certain modifications.

pe

c

w)

t

g

1

.

#### **ACKNOWLEDGMENTS**

It would be impossible for me to mention all the persons who contributed to the successful completion of this dissertation. To the unnamed persons, I humbly thank you for your interest, help, suggestions and concerns. To the persons who played a major role, I also humbly thank and would like to name as follows:

My father, the late Dr. M. H. Hamelink, M.D., who contracted glaucoma and subsequently lost most of his vision mainly due to faulty diagnosis and improper treatment of the disease and, in this way, stimulated my interest in the subject.

My committee, Drs. W. N. Sharpe, M. Potter,

E. Nordhaus and especially Dr. W. Keller who took a

great personal interest in my project and made possible

the invivo work reported within. Special thanks go to

Dr. G. L. Cloud, my major professor, who allowed me the

latitude to pursue this project and also for his direction

and encouragement when I needed it.

Mr. D. Pettigrove, photographer, G.M. Proving Grounds, General Motors Corporation, who took the high-speed films of the dogs on his own time.

My supervisor at General Motors Education and Training, Mr. H. Kipke, who allowed me time on the job to prepare the second draft of the dissertation.

And finally, my wife Jeanie and family who had to share their husband and father with this project for several years.

Of course, I would be remiss if I would not thank Almighty God who gave me the idea, the strength, the knowledge and the endurance to carry out the steps of approach and solution to the problem.

July 19/2 michile

February 15, 1978

#### DEDICATION

This dissertation is dedicated to Jeanie, my wife, my lover, and the mother of my children.

## TABLE OF CONTENTS

														Page
LIST OF	TABI	LES .	•	•	•	•	•	•		•	•	•	•	viii
LIST OF	FIGU	JRES.	•	•	•	•	•	•	•	•	•	•	•	ix
Chapter	•													
1.	INTRO	DUCT	ON	•	•	•	•	•	•	•	•	•	•	1
2.	ANATO	OMY OF	THE	E EY	E	•	•	•	•	•	•	•	•	7
		The I						•	•	•	•	•	•	7
		The A					n •	•	•	•	•	•	•	9 15
3.	SURVE	Y OF	CLIN	NICA	LI	ONO	MET	ERS	S.	•	•	•	•	18
	3.1 3.2	Appla Popul										•	•	18 23
		3.2.1	l ⋅Ma	acka	37N	iaro	ТО	non	10+0	r (	ммт	٠١		23
		3.2.2		n da	y	TON		+01		- '	1-11-1 1	. ,	•	24
		3.2.3								•	•	•	•	26
		3.2.4		ırha						•	.+~~	•	•	27
		3.2.5	5 Ar	neri ing	can	Op	tic	al	Non	con	tac	t-	•	21
		3.2.6	5 P1	(AÕT cess	) ure	Se	nsi	tiv	ve E	lec	tri	cal		28
				Pain				tic	n T	onc	met	ers	3	
			ć	and	Oth	ers	•	•	•	•	•	•	•	29
	3.3	Studi	ies d	of C	lin	ica	1 T	onc	met	ry	•	•	•	30
4.		CAL 1	гоиол	ÆTE	RS-	-A	HIG	H-S	PEE	D M	IOVI	E		
	STUD	Y.	•	•	•	•	•	•	•	•	•	•	•	33
	4.1	Intro	duct	ion	•	•	•	•		•	•	•	•	33
	4.2	Gener	cal I	roc	edu	ires		•	•		•	•	•	35
	4 3	Schio	1+7 7	lan	ana	+ 10	n m	onc	met	۵r				36

Chapter	<b>:</b>		Page
	4.4	High-Speed Filming of the EMT 20	
		Tonometer Applanating a Cornea	. 4
	4.6	Summary	. 4:
5.	EXPE	RIMENTAL SYSTEM DEVELOPMENT	. 4
	5.1		. 4
	5.2		. 48
	5.3		. 49
	5.4	Measurement System Evaluation	
	5.5	Summary	. 7
	5.6	Summary	
		Tonometer System	. 83
	5.7	Tonometer System	. 8!
		The second series of the second secon	
		5.7.1 Introduction	. 85
		5.7.2 Procedures	. 85
6.	EXPE	RIMENTAL EQUIPMENT AND PROCEDURES	
		ITRO	. 93
	6.1	Experimental Fixture	. 93
		Speciman Preparation	. 9
	6.3	Stimulation System	. 9
	6.4	Detection System	. 9
		Doppler Velocimeter	. 9
	0.5	boppier verocimeter	•
		6.5.1 Introduction	. 9
		6.5.2 Doppler Phenomenon	. 9
		6.5.3 Measurement of Doppler Fre-	
		quency Shift	. 10
		quency success to the transfer	
	6.6	Modifier System	. 110
		Experimental Procedures	. 11
	• • •		
7.	DATA	ANALYSIS AND RESULTS	. 119
	7.1	Data Analysis	. 119
	7.2	Data Analysis	. 13
	7.3	Discussion of Data Scatter	. 13
	7.4	Summary	. 13
8.	A PRI	ELIMINARY INVIVO STUDY ON DOGS	. 13
	8.1	Introduction	. 13
	8.2	General Procedures	. 13
		Invivo Data	
		Summary	. 14

Cł	napte	r														Page
	9.	CONCLUSIONS AND RECOMMENDATIONS										•	145			
		9.1 9.2 9.3	Rec	omme	sions endat ord.				•	•	•	•	•	•	•	145 147 151
AI	PEND	ICES														
ΑI	PEND	IX														
	A.	THE	11 G	LAUC	OMA	RUL	ES	•	•	•	•	•	•	•	•	152
	В.	EQUI	PMEN	T LI	ST.	•	•	•	•	•	•	•	•	•	•	154
	c.	CALC	ULAT	IONS	ANI	ні	STO	GRAI	MS	•	•	•	•	•	•	155
	D.	DIAP	HRAG	M IC	P DA	ATA	•	•	•	•	•	•	•	•	•	168
	E.	BASI	C VA	LIDI	TY C	F A	PPR	OAC	H T	EST	•		•	•		171
BI	BLIO	GRAPH'	Y													174

## LIST OF TABLES

Table		Page
1.	Sample Data Sheet	64
2.	Mean Frequencies for Lamb Eye Data	120
3.	Sample Calculations	126
4.	Mean, Standard Deviation and Standard Error	129
5.	Normal Response Frequency for Dogs, Run Invivo	143
D-1.	Diaphragm IOP Data	168

## LIST OF FIGURES

Figur	e	Page
1.	Anatomy of the Eye	8
2.	An Eye Model	10
3.	The Anterior Region	11
4.	Transverse Section of the Cornea	12
5.	Applanation	19
6.	Initial Contact of Mackay-Marg Tonometer Plunger with Cornea	23
7.	Mackay-Marg Tonometer Applanating Cornea	24
8.	Prism of the Goldmann Tonometer Applanating Cornea	25
9.	Plunger of Schiotz Tonometer Applanating Cornea	27
10.	Durham Pneumatic Tonometer	28
11.	American Optical Noncontacting Tonometer	29
12.	Pressure Sensitive Paint Transducer	30
13.	Preliminary Camera Set-Up	34
14.	Determination of Distance and Field of Vision	34
15.	Final Check and Lens Opening Determination .	35
16.	Preparation of Canines for Examination	36
17.	Schiotz Tonometer Applanting a Cornea	37
18.	Initial Contact of Schiotz Tonometer Plunger with Cornea	38

Figur	e	Page
19.	Contact of Schiotz Tonometer Foot with Eye Globe	39
20.	Close-up of EMT 20 Applanating Cornea	40
21.	High-Speed Filming of the EMT 20 Tonometer Applanating a Cornea	41
22.	High-Speed Film Clip of EMT 20 Applanating a Cornea	42
23.	High-Speed Film Clip of the AOT Applanating Cornea	44
24.	Discrepancies of Figure 23, Frame 2 Enlarged	45
25.	Data Gathering System	49
26.	Anterior Portion of the Eye	50
27.	Assembly Drawing of Model Fixture	52
28.	Diaphragm with Strain Gage Tab Glued in Place	53
29.	Mounted Diaphragm with Pressure Variation Apparatus	54
30.	Preliminary Speaker Calibration Apparatus	55
31.	Improved Speaker Calibration System	57
32.	Speaker Calibration Curve	58
33.	Experimental Test Set Up #1	59
34.	Experimental Test Set Up #2	61
35.	Experimental Test Set Up #3	62
36.	Frequency-IOP Plot, Experimental Set Up #1 .	65
37.	Normal Response Plot, Set Up #1, 5" H <sub>2</sub> O	66
38.	Normal Response Plot, Set Up #1, 7.5" H <sub>2</sub> O	67
39.	Normal Response Plot, Set Up #1, 10" H <sub>2</sub> O	68

Figur	e	I	age
40.	Normal Response Plot, Set Up #1, 12.5" H <sub>2</sub> O	•	69
41.	Frequency-IOP Plot, Experimental Set Up #2	•	70
42.	Normal Response Plot, Set Up #2, 5" H <sub>2</sub> O .	•	71
43.	Normal Response Plot, Set Up #2, 7.5" H <sub>2</sub> O	•	72
44.	Normal Response Plot, Set Up #2, 10" H <sub>2</sub> O.	•	73
45.	Normal Response Plot, Set Up #2, 12.5" H <sub>2</sub> O	•	74
46.	Normal Response Plot, Set Up #3, 5" H <sub>2</sub> O .	•	76
47.	Normal Response Plot, Set Up #3, 7.5" H <sub>2</sub> O	•	77
48.	Normal Response Plot, Set Up #3, 10" H <sub>2</sub> O.	•	78
49.	Normal Response Plot, Set Up #3, 12.5" H <sub>2</sub> O	•	79
50.	Frequency-IOP Plot, Set Up #3	•	80
51.	Set Ups in Comparison	•	80
52.	High-Speed Film Clip of the Proposed Tonometer System	•	83
53.	Enlargement of a Frame from Figure 52	•	84
54.	Film Clip Showing Timing Marks	•	87
55.	High-Speed Film Clip of Lamb Cornea Recovery	•	89
56.	Enlargement of Applanation Dimple of Figure 55	•	90
57.	IOP Control Measurement System	•	92
58.	Corneal Stimulation System	•	94
59.	Cone Speaker System	•	95
60.	Audio Amplifier Output Curve	•	96
61.	Laser Doppler Velocimeter	•	97
62.	Source Stationary Pathway	•	99

Figur	re	Page
63.	Source Stationary Distance/Wave Length Relationship	99
64.	Source Moving Pathway	100
65.	Source Moving, Distance/Wave Length Relationship	100
66.	Simple Doppler Frequency Shift Measurement Apparatus	103
67.	Incoming Waves to Photo Diode	104
68.	Component and Combined Output from Photo Diode	111
69.	Variable Filter Characteristics in the Band Pass Mode	112
70.	Signal Modifier System	113
71.	Instruments for Eye Removal	115
72.	Invitro IOP Measurement Apparatus	118
73.	Frequency vs IOP for 20 Lamb Eyes	125
74.	Histogram, 5" H <sub>2</sub> O (9.34 mm Hg) IOP	128
75.	Response Frequency vs IOP	130
76.	Linearized Data Plot	132
77.	Lamb Eye Frequency Response	134
78.	IOP Instrumentation for Invivo Measurements	140
79.	Preparation of Eye for Examination	140
80.	Inserting Needle into Anterior Chamber	142
81.	Pressure Monitoring System	142
82.	Cross-Section through Barone's Reflector .	149
83	Possible System for Invivo Investigation	150

Fig

C-1

C-2

C-3

C-4

C-5

E-]

E-2

Figur	е												Page
C-1.	Histogram,	5" I	H <sub>2</sub> O ]	OP	•	•	•		•	•	•	•	165
C-2.	Histogram,	10"	н <sub>2</sub> о	IOI	٠.	•	•	•	•	•	•	•	165
C-3.	Histogram,	15"	н <sub>2</sub> о	IOI	₽.	•	•	•	•	•	•	•	166
C-4.	Histogram,	25"	н <sub>2</sub> о	IOI	·	•	•	•	•	•	•	•	166
C-5.	Histogram,	35"	H <sub>2</sub> O	IOI	·	•	•	•	•	•	•	•	167
E-1.	Calibration	n Cui	rve,	4 "	Spe	ake	er	•	•	•	•	•	172
E-2.	Basic Valid	dity	Expe	erin	nent	al	Sys	sten	α.	•		•	173

#### CHAPTER 1

#### INTRODUCTION

Glaucoma, which is manifested clinically as abnormally high IOP (intraocular pressure), is an insidious eye disease which must be detected in its early stages for there to be any possibility of successful treatment. Currently, glaucoma detection and evaluation of therapy are largely dependent upon tonometry (pressure measurement) methods which require applanation (flattening a known area) of the cornea. The clinical tonometers in popular use yield readings with standard deviations of  $\pm$  1.4 mm Hg to  $\pm$  3 mm Hg or more depending upon the tonometer used and the experimenter reporting (31, 34, 48, 53). This standard deviation is of minor importance to persons with normal eyes or to known glaucoma patients who are undergoing continuous treatment, but it is of major importance to persons with borderline glaucoma. Normal eyes in humans will have an IOP from 12 mm Hg to 19 mm Hg while glaucomatous eyes will have an IOP ranging from 21-25 mm Hg to 60 mm Hg or more. Almost any tonometry method could be used successfully for the

detection of high pressures (a trained person could detect these high pressures with his fingers alone) but for the person with borderline glaucoma and an IOP of 21 mm Hg the measurement is critical. A ± 3 mm Hg standard deviation could place a person with borderline glaucoma into the "normal" pressure range causing a delay of necessary treatment. An error in diagnosis even with the most careful of ophthalmologists making the measurement is possible. Since glaucoma is the number one cause of blindness in the United States today, it would appear that sufficiently early detection is not happening.

The standard deviations reported (31, 34, 48, 53) with the popular clinical devices are attributed to various causes including the following:

- 1. Blunt object trauma.
- Patient apprehension of the measurement process.
- Non-normal positioning of the tonometer probe on the eye.
- Surface tension variation caused by tear layer and anesthetic.
- 5. Difficulties within the instrument.

If a tonometer system could be devised that would not applanate the eye, would not touch the eye, would not cause any discomfort (or could be performed without the patient being made aware of the measurement),

would not require the use of an anesthetic and yet be capable of accurate measurements, most of the above difficulties would be circumvented. In addition, if the system could easily be used by a trained technician and not require the services of an ophthamologist, the clinical applications would be significant.

Previous studies of tonometric processes have been concerned primarily with the effects of tissue mechanical properties and/or changes of these properties upon applanation. In viscoelastic tissue, material parameters such as Young's Modulus and Poisson's ratio are variables dependent upon factors including strain level, length of time at a strain level and strain history; therefore, application of the simplifications necessary to arrive at a solution are not completely satisfactory.

The proposed tonometer system requires a fresh look at the entire pressure measurement procedure. One approach is to consider the eye to be a thin walled spherical pressure vessel filled with a moderately gelatinous fluid subjected to a weak vibrational forcing function. This pressure vessel is hypothesized to have "normal response frequencies" which are related to the internal pressure. It was theorized that if the vibrational characteristics of the eye were examined

with respect to the measurement of IOP, limitations of existing IOP measurement schemes might be avoided.

This dissertation describes such a new method of IOP determination which is nonapplanting and noncontacting. The new technique requires that eyes be stimulated by low frequency sound waves and the resulting corneal movements detected by the laser Doppler effect. Testing of the hypothesis and basic technique were carried out with freshly excised lambs' eyes. The objectives of the investigation were three and are as follows:

- Develop an apparatus and procedure for exploring the vibrational response of enucleated lambs' eyes (Chapters 5 and 6).
- Establish an empirical relationship between vibrational response and IOP (Chapter 7).
- 3. Use the data and model to establish parameters for invivo tests (Chapters 4, 8 and 9).

The following is the order of presentation of this dissertation along with a brief description of the chapters.

 Chapter 2 is entitled "Anatomy of the Eye" and is included to help the reader whose background is insufficient to understand the bio-engineering nature of this dissertation.

- 2. Next is "Survey of Clinical Tonometers," which begins with a brief treatment of the theory behind applanation tonometers and then moves into a description of several popular clinical devices.
- 3. Experimental observations of some clinical tonometers using a high-speed movie study is the subject for Chapter 4. Several high-speed film clips are used to support evidence discussed in the next chapter.
- 4. Chapter 5, "Experimental System Development," follows the system metastasis from criteria to evaluation with the steps in between.
- 5. The experimental equipment and the procedures used to obtain the data from freshly excised lambs' eyes are presented in Chapter 6.
- 6. In Chapter 7 is presented the data analysis and results including the empirical equation generated from the lambs' eye data. A discussion of the data scatter including a comparison of the standard deviations from this investigation with those of clinical devices is also a part of Chapter 7.

- 7. Chapter 8, "A Preliminary Invivo Study on Dogs," illustrates through photographs and text the procedures used in the application of the proposed tonometer system to live dogs.
- 8. The final chapter, "Conclusions and Recommendations," summarizes the findings and makes specific suggestions for future experimental work in this area.

While the concept used in the reported research is unique, it appears to be practical. It is hoped that this idea will develop into a tool that will aid in the detection of glaucoma as well as in the evaluation of therapy.

#### CHAPTER 2

#### ANATOMY OF THE EYE

## 2.1 The Eyeball

The eye, within its protective socket, has a layer of receptors, a lens system for focusing light on these receptors and a system of nerves and other bodies (lateral geniculate bodies) for conducting impulses from the receptors to the occipital cortex. The outer protective coating, the sclera (Figure 1) is modified anteriorly to form the transparent cornea through which the light enters the eye. Inside the sclera is the choroid layer whose function is to nourish the structures in the eyeball. Lining the posterior two-thirds of the choroid is the retina, the tissue containing the light receptor cells. The lens is a transparent structure held in place by a circular lens ligament or zonula. The zonula is attached to the thickened anterior part of the choroid, the ciliary body. The ciliary body contains circular muscle fibers and longitudinal fibers which attach near the corneo-scleral junction. In front of the lens is the pigmented and opaque iris, the colored

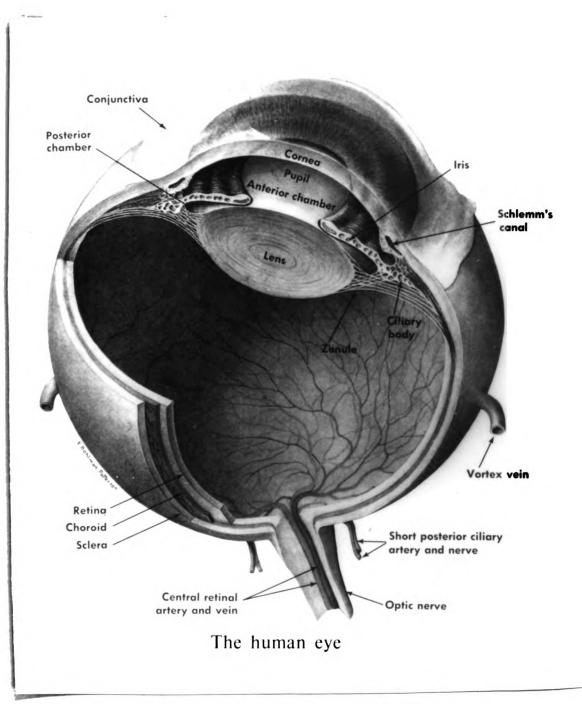


Figure 1 Anatomy of the Eye

Reproduced with permission from Newell, Frank W., and Ernest, J. Terry: Ophthalmology, ed. 3, 1974; copyrighted by the C. V. Mosby Co., St. Louis, Mo.

portion of the eye. The iris contains circular muscle fibers which constrict the pupil and radial fibers which dilate it. The anterior chamber of the eye between the cornea and the lens is filled with aqueous humor secreted by the ciliary process. The space between the lens and the retina contains a clear gelatinous material called the vitreous humor. Eye movements are basically rotations and are caused by muscles attached to the tough scleral shell just behind the ciliary body.

Except for variations in size, pupil geometry and retinal construction, the anatomy of the human eye and that of domestic animals is similar. The size variation in different animals depends chiefly on the necessity for acuteness of vision in various lighting conditions rather than on the size of the animal. The size of the eye in homo sapiens varies little. The eyes of the human male are slightly larger than the female. Eye shape is that of a somewhat flattened spheroid with a transverse major diameter of about 23.6 mm. Some investigators (27, 35, 40) model the eye as two nonconcentric spheres with the corneal diameter one-half that of the eye globe (see Figure 2).

### 2.2 The Anterior Region

The anterior region consisting of the cornea, anterior chamber, iris, lens, ciliary body, posterior chamber and the canal of Schlemm will be considered in

detail because of its importance to this investigation. Figure 3 (page 11) is a sketch of the anterior region of the eye.

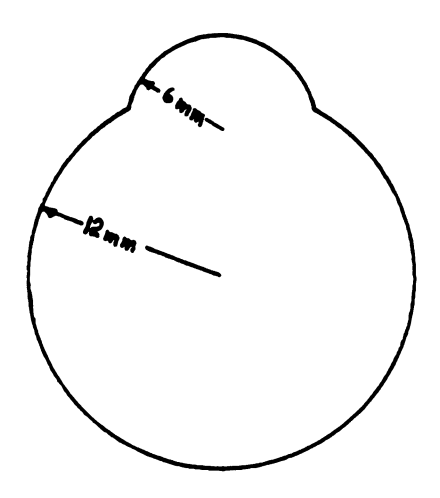


Figure 2 An Eye Model

The cornea, which is a transparent extension of the sclera, is the window through which light passes into the eye. Because the difference of indices of refraction between air (1) and the cornea (1.33) is greater than between the aqueous humor (1.33) and the lens (1.42), the greatest refraction occurs in the cornea. The cornea forms the anterior one-fifth of the fibrous tunic of the eyeball and has a varying anterior diameter between 11.0 mm and 15.6 mm. The posterior diameter is nearly constant at 13 mm accounting for the uneven thickness of the corneal tissue. The

<sup>\*</sup>Indices of refraction for the cornea, aqueous humor and vitrous humor are the same at 1.33.

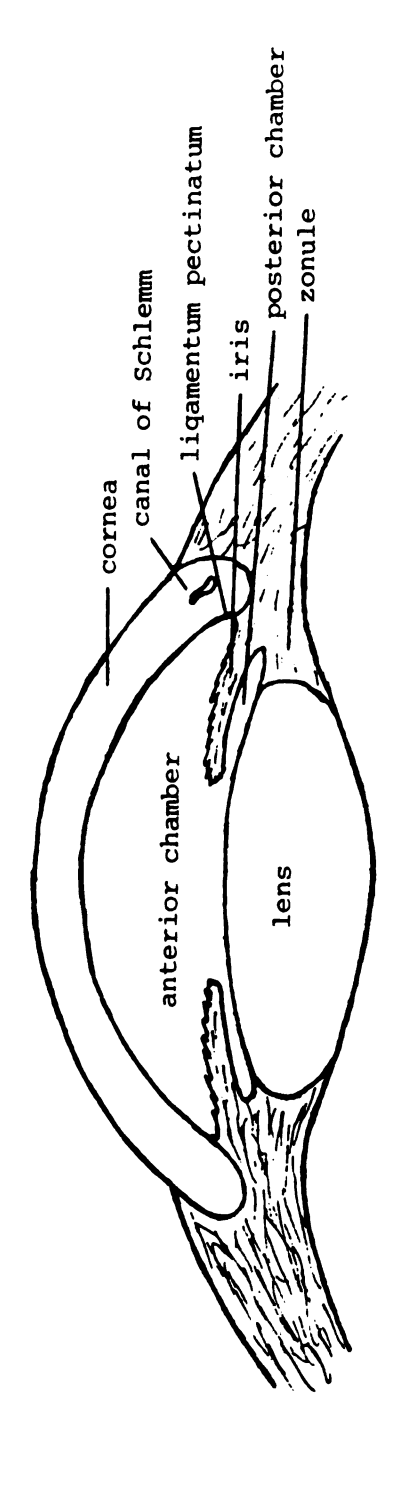


Figure 3 The Anterior Region

cornea is thinnest in the center (.6 to .8 mm) and thickens to 1.1 mm at the periphery. The radius of curvature of the cornea varies in different individuals and at different periods of life. Refer to the sketch presented in Figure 4 illustrating the following five distinct layers of the cornea:

- 1. Anterior epithelium
- 2. Anterior limiting membrane (Bowman's membrane)
- 3. Substantia propria (stroma)
- 4. Posterior limiting membrane (Descemet's membrane)
- Posterior endothelium

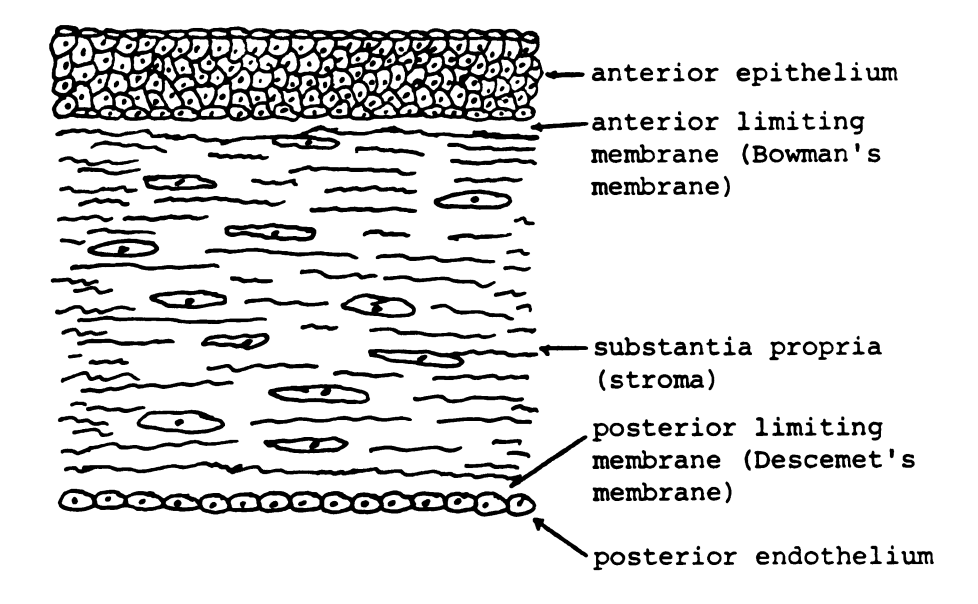


Figure 4 Transverse Section of the Cornea

The anterior epithelium of the cornea is usually five cells deep in man, and measures .045 mm at the center and .8 mm deep at the periphery. The deepest cells, or basal cells, are columnar in form with broad

basal plates resting upon the anterior limiting membrane. The outer parts of the basal cells fit into corresponding depressions in the cells of the superimposed layers. The middle layers are composed of irregular polyhedral cells. The superficial layers consist of flattened cells which lie parallel to the free surface.

The anterior limiting membrane is situated immediately below the epithelium and appears as a homogeneous band about .02 mm in thickness at the center and thinner at the periphery.

The stroma constitutes the main portion of the cornea and is made up of interlacing bundles of connective tissue which are directly continuous with those of adjacent sclera. The bundles are composed of fine fibrilla and are arranged so as to make regular layers. The stroma consists of about sixty layers of these bundles held together by connective tissue.

The posterior limiting membrane is a practically homogeneous band varying in thickness from .006 mm at the center to .012 mm at the periphery. It resembles elastic tissue and is very firm and resistant to injury or perforation.

Finally, the posterior endothelium is reached.

It is a single layer of flattened polygonal cells which are connected by delicate protoplasmic processes and which are continuous with the cells lining the anterior surface of the iris.

There are no blood vessels in the cornea. The cells apparently receive adequate nutrition as they heal readily under favorable conditions. Injury, in most situations, however, causes the cornea to become opaque or to form striations.

Immediately behind the cornea is the anterior chamber which is the major reservoir of the aqueous humor. The intraocular pressure (IOP) is usually measured in the anterior chamber of the eye.

The iris forms the anterior segment of the choroid or vascular tunic and is visible through the cornea. Slightly to the inner side of its center is an approximately circular opening called the pupil. Through the action of the iris, the pupil size varies from 1 mm to 8 mm in diameter with considerable individual variation. The "color" of the eye is partially dependent upon the amount of pigment within the iris stroma and partly upon the density of the pigmentation of the cells on its posterior surface.

The lens is a biconvex completely transparent body situated on a level with the anterior plane of the ciliary body. It is suspended between the anterior surface of the vitrous humor and the posterior surface of the aqueous humor by the suspensory ligament. A healthy lens gives the pupil a black color when viewed from the front. The convexity of the lens changes with age and

with eye accommodation to various distance objects.

Important pathological diseases of the eye including glaucoma generally cause the lens to become translucent or opaque, seriously reducing the visual acuity of the individual.

The ciliary body is generally divided into three parts by function: ciliary muscle, ciliary process and ciliary ring. Of the three, the ciliary process is of greatest interest to this investigation. The ciliary process consists of an annular series of folds, about 70 in number which act as points of attachment of the suspensory ligament. The aqueous humor is produced chiefly by the blood-vessels of the ciliary process. The aqueous flow is from the ciliary process to the region behind the iris in front of the lens which is called the posterior chamber. From the posterior chamber, the aqueous humor flows through the pupil to the anterior chamber. Finally, the aqueous humor escapes in the angle formed by the iris and the cornea by passing through the lymph-spaces in the ligamentum pectinatum and by diffusion reaches the canal of Schlemm. The aqueous humor then passes out of the eye by the anterior ciliary veins.

# 2.3 Glaucoma

Glaucoma is evidenced by excessive intraocular pressure which, unless relieved, progressively increases

until the eye is destroyed. Glaucoma in one eye is almost always indicative of glaucoma in the other eye. The abnormal tension is believed to be the result of one of two possible phenomological occurrences.

- 1. The inflow of the aqueous humor is increased and the IOP must be increased to increase the diffusion rate of the aqueous into the canal of Schlemm.
- 2. The outflow resistance of the aqueous humor is increased due to a pathological change in the lymph-channels through which the aqueous humor must pass. This would increase the IOP.

Important symptoms in the glaucomatous eye include:

- 1. Increase in corneal tension.
- 2. Pathological cupping of the optic disc (blind spot).
- 3. Distended retinal veins.

Generally, great pain accompanies advanced cases of glaucoma. The pain is thought to be due to the compression of the sensory nerves of the ciliary body and iris against the unyielding sclera. The distended retinal veins can be easily observed using an opthalmoscope.

Progressing glaucoma causes serious and irreversible pathological changes in the cornea and lens. If left untreated, the retina will detach and the optic nerve will be destroyed, leaving the individual totally blind.

Eleven glaucoma rules written by Dr. Theodore Schmidt are included in Appendix A for a better understanding of a widely accepted clinical diagnostic procedure.

This investigation addresses the efficient detection of increased IOP.

#### CHAPTER 3

#### SURVEY OF CLINICAL TONOMETERS

# 3.1 Applanation Model

At this time, detection of glaucoma and evaluation of therapy are largely dependent upon tonometric methods which require applanation of the cornea. All of the significant analytical and conceptual model developments center upon the applanation type of tonometer system, rather than upon the development of a general system model. Primarily these models were developed to show the basic validity of applanation tonometers in certain controlled clinical situations.

The first recorded model of an eye being applanated was described by Imbert and Fick sometime before 1876. The Imbert-Fick maxim states that the pressure in a spherical vessel filled with fluid and surrounded by an infinitely thin elastic membrane can be measured through determination of the counter pressure which flattens part of the membrane to a plane (Figure 5). This theory is still basic to all applanation tonometers.

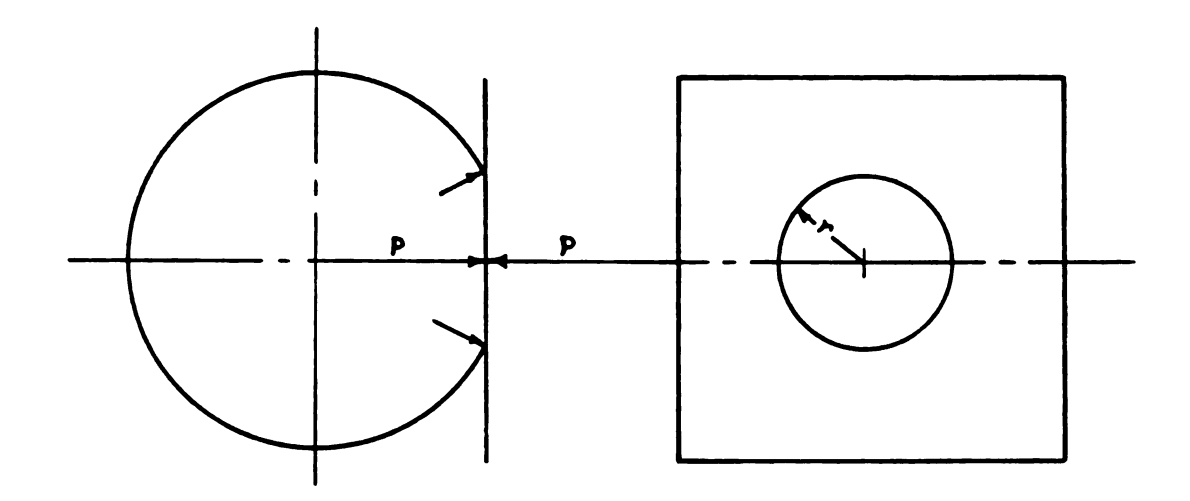


Figure 5 Applanation

Since applanation tonometry reduces the effective volume of the applanated eye, pressure recorded by an applanation tonometer is always higher than the actual IOP. An improvement to the basic model was put on a theoretical basis by Friedenwald in his defining of a term "ocular or scleral rigidity." Ocular rigidity is defined mathematically by Friedenwald (12) as

$$K = \frac{1}{\Delta v} \text{ Log } \frac{P}{P_O}$$
 (3-1)

where  $\Delta v$  is the change in volume due to tonometer applanation,  $P_O$  is pressure in the eye before applanation and P is the pressure measured by the tonometer.

Conceptually, ocular rigidity could be described as "stretchability" of the scleral or corneal tissue.

Ocular rigidity variation between different eyes can account for significant deviations between applanation

tonometer readings and actual IOP. Every applanation tonometer reading is affected to varying degrees by ocular rigidity. Ocular rigidity in general increases with age (12) and decreases with increased IOP (15, 55). Ocular rigidity coefficients reported by different investigators (12, 15, 16, 45, 55) vary from 0.69 to 4.13  $\mu mm^{-1}$  in normal (nonglaucomatous) eyes, while eyes with glaucoma can have higher, lower or the same value of ocular rigidity as normal eyes (12). "In acute congestive glaucoma, the ocular rigidity is highly variable, sometimes showing extreme fluctuations during the course of illness. Apparently, the great IOP congestion in these cases tends to reduce the rigidity coefficient as the result of the increased compressibility of the intraocular vascular bed while long-standing high pressure tends to increase the rigidity of the scleral coat" (12).

Friedenwald (12) theorized that the IOP when measured by a tonometer consisted of the original IOP plus a change of pressure caused by the volume change resulting from applanation. He supposed a linear relationship between depth of indentation of the tonometer plunger and the radius of the indented area to be

R = a + bD

where R is the radius of the plunger, D is the depth of indentation and a, b are constants.

The effective area is then

$$A = \pi (a + bD)^2$$

Applanation force, using the Imbert-Fick law now can be expressed as

$$F = P\pi (a + bD)^2$$
 (3-2)

Using a heuristic argument and the Schiotz charts of 1924, Friedenwald arrives at a volume of

$$V = \frac{\pi}{3} [(1.62 + D)^3 - (1.62)^3]$$
 (3-3)

This volume and the equation for ocular rigidity (3-1) can be used to correct the tonometer readings. The correction factor (3-3) does <u>not</u> correct for resistance to bending, but only for cornea stretching.

Mow (35) approached the eye model problem from a slightly different aspect by assuming it to be a "sand-wich" structure consisting of the epithelium, stroma and endothelium. He also assumed that the properties of the two face layers (epithelium and endothelium) have significantly different properties from the core (stroma) layer; the cornea material is linearly elastic; the two faces have the same thickness, and the thickness of the cornea is much less than the radius of the cornea.

Mow developed his model in an attempt to show how the stresses are distributed between the membranes

and transmitted across the stroma. He feels that his theory can be applied to applanation tonometry with some degree of success even with the linearly elastic assumption. He admits that his model is only an attempt at a better model, and the validity of the model will be proven only when the mechanical properties of the Bowman's and Descement's membrane and the properties of the stroma are measured.

Kobayashi, Woo (24, 54) and others have attempted the finite element approach to the eye model. Woo (54) reports a modeling technique that appears to give close correlation with experimental results in some clinical applications if problem parameter values are allowed to vary by as much as two orders of magnitude.

Others have modeled the eye as a rubber ball filled with fluid (55) and have applanated this ball to determine its IOP.

To summarize, no completely satisfactory model has yet been devised. The lack of success results from the lack of consistent values for the material properties of corneal tissue, and from the lack of a full understanding of the physical and physiological processes associated with applanation. Therefore, several questions about the validity of the applanation approach remain.

# 3.2 Popular Clinical Tonometers

# 3.2.1 Mackay-Marg Tonometer (MMT)

The Mackay-Marg tonometer is a constant indentation tonometer. Its design and function are pictured in Figures 6 and 7. This tonometer measures the reaction forces of a tonometer plunger which is pushed a constant known depth into the eye. When the probe is first brought into contact with the eye, the cornea flattens. The force necessary to maintain a constant depth of plunger is theorized to consist of corneal bending forces and the intraocular force.

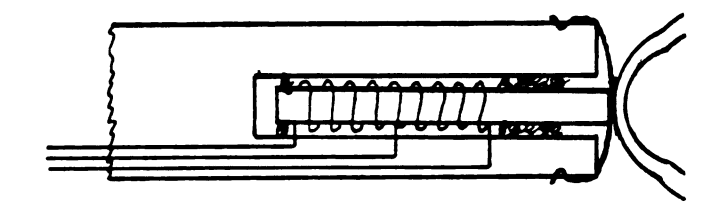


Figure 6 Initial Contact of Mackay-Marg Tonometer Plunger with Cornea

As the probe is brought into firmer contact with the eye, the bending forces are assumed to be carried by the probe, and the plunger is theorized to measure simply the IOP. However, it was noted by Stepanide (47), Moses (23), Hilton (21) and others that the readings from the MMT were in general higher than the Goldmann applanation tonometer. This discrepancy, Stepanide suggests, is a result of the displaced aqueous humor caused by the deformation of the cornea by the MMT probe. Other

experimenters such as Kobayashi and Staberg (24) and Tierncy and Rubin (49) also noted the consistently higher readings for the MMT as compared to readings from the Goldmann tonometer. Both tonometers displace fluid, but it was shown that the MMT displaced more fluid due to its larger probe size. Possibly the larger probe size also causes greater trauma and sympathetic hypotony in the opposite eye as is sometimes noted.

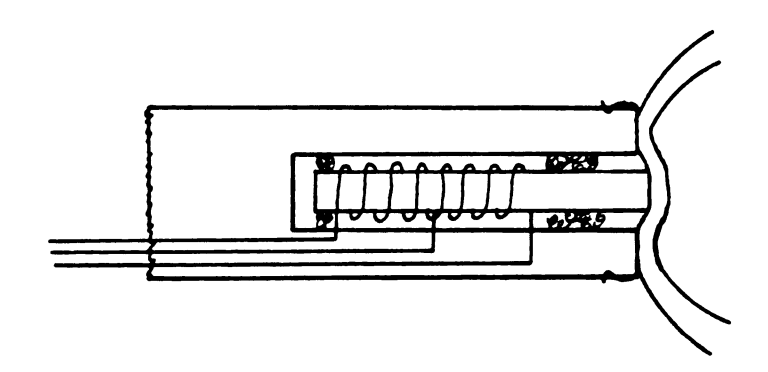


Figure 7 Mackay-Marg Tonometer Applanating Cornea

# 3.2.2 Goldman Tonometer

The Goldmann applanation tonometer (Figure 8) is a contacting tonometer which measures the force necessary to flatten a known area of the cornea being applanated.

The procedure that is followed for the Goldman tonometer will be described as it is one of the most widely used and accepted clinical systems. Also, most

<sup>\*</sup>From "Use of the Goldman Applanation Tonometer 870."

other systems adhere to a procedure similar to the Goldmann procedure.

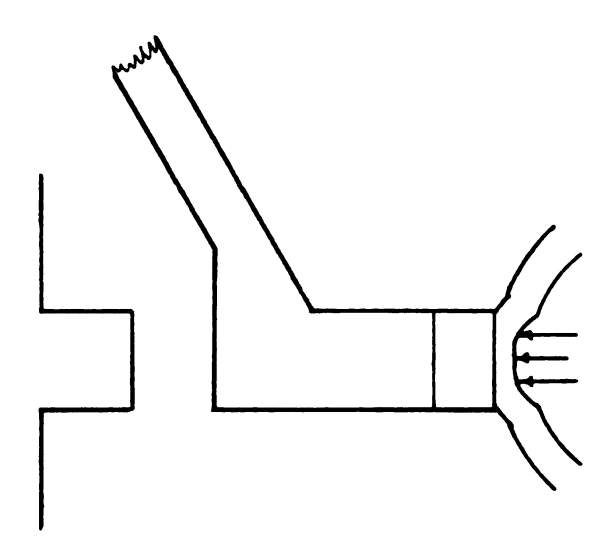


Figure 8 Prism of the Goldmann Tonometer Applanating Cornea

- Both eyes are anesthetized with 2-3 drops of Novesine (Dorsacaine) of 0.2 or 0.4% within 15 seconds of each other. Both eyes are always anesthetized to prevent movement of the lids during prolonged examination.
- 2. In the case of the Goldmann tonometric examination, an eye drop solution containing 0.25 to 0.5% sodium fluorescein is used to enable the examiner to observe the visible flourescein ring upon contact of the tonometer eye piece with the cornea. This ring indicates whether proper applanation of the cornea is taking place.
- The patient is asked to press his head firmly on the chin and forehead rest of the slit lamp.
- 4. The patient is instructed to look straight ahead. The fixation lamp can be used to steady the eyes.
- 5. The patient must be repeatedly asked to keep his eyes wide open during the examination. If necessary, the examiner may have to hold open the lids of the eye being examined.
- 6. Immediately before measurement the patient should blink for a moment so that the cornea is well moistened with lacrimal fluid and flourescein.

- 7. The measuring prism is then brought into contact in the center of the cornea on the pupillary area.
- 8. The pressure on the eye is then increased by turning the measuring drum on the Goldmann tonometer until the pressure without is exactly balanced by the pressure within as evidenced by the flourescein ring pattern.
  It is recommended that several measurements be made on each eye. When three measurements on each eye agree within ± 0.5 mm the reading will be accepted as correct. If the readings do not agree within ± 0.5 mm, repeated measurements will be made until three in a row agree within ± 0.5 mm for each eye.

The pressure reading obtained from this measurement includes not only the IOP but also the indicated pressure caused by the bending forces of the cornea. The tonometer reading is also subject to errors due to surface tension of the fluid film on the cornea. Surface tension tables for various eye anesthetics (12) are available to help correct these errors. Finally, the Goldmann tonometer is greatly dependent upon the skill of the ophthamologist (45).

### 3.2.3 Schiotz Tonometer

The Schiotz tonometer (Figure 9) is one of the simplest applanation tonometers in use. It too is a device which flattens a known area of the cornea. The plunger deforms the cornea because the pressure it exerts is greater than the resisting pressure. The plunger will continue to sink into the cornea until the elastic tension resists further deformation. The lower the plunger sinks, the larger the scale reading. When the system comes

into equilibrium, the operator uses the reading and a calibration chart to determine the IOP.

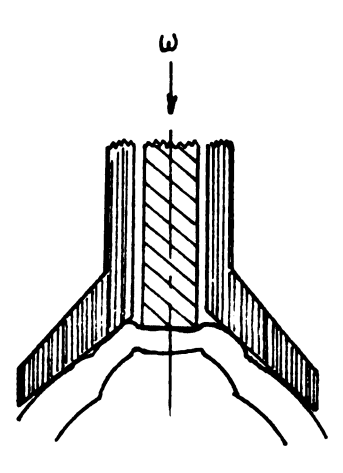


Figure 9 Plunger of Schiotz Tonometer Applanating Cornea

Although this system is susceptible to variation of scleral rigidity, tear surface tension, etc., it continues to be used extensively for evaluation of scleral rigidity in addition to measurement of IOP.

## 3.2.4 Durham Pneumatic Tonometer

The Durham pneumatic tonometer, pictured in Figure 10, employs the same basic force-area relationship during applanation as do the tonometers previously discussed. IOP is estimated with the Durham system by measuring the force required to applanate a calibrated area of the cornea. Walker and Litovitz (51) show the relationship between estimated values of IOP, measured

air flow volume and chamber pressure. Uncertainties due to membrane rigidity and membrane tension plague the Durham device as well as the Goldmann and Schiotz devices.

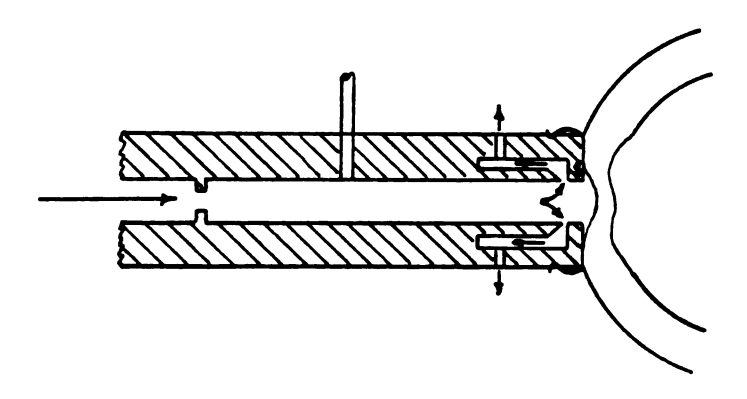


Figure 10 Durham Pneumatic Tonometer

# 3.2.5 American Optical Noncontacting Applanation Tonometer (AOT)

A noncontacting applanation tonometer system was developed by American Optical Corporation. It is pictured in Figure 11. An air jet is utilized to perform the applanation and an electronic counter and automatic optics system are used to determine precisely when applanation occurs. The counter reading, when compared with a pressure vs time curve, can be used to determine the amount of air pressure required to applanate the cornea at the instant of applanation. Through careful calibration, the pressure necessary for applanation (or time to reach that pressure) can be used to determine IOP.

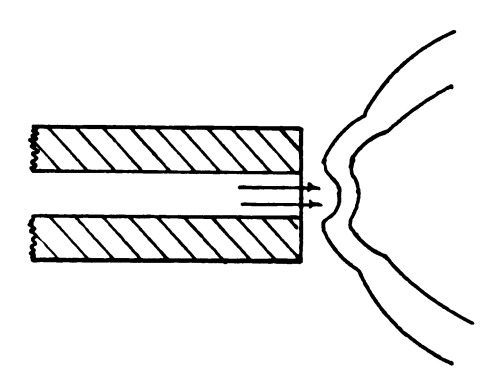


Figure 11 American Optical Noncontacting Tonometer

The AOT is also susceptible to error due to bending forces and scleral rigidity. Of all the tonometers studied, the AOT causes the least amount of trauma to the eye. However, since it employs the applanation principle, some trauma and resulting hypotony are still evident (53). Hypotony is increased with this device because the startling air blast causes a reflex reaction in the patient. Marked variation (usually reduction) of the IOP in the opposite eye takes place (53) possibly as a result of the reaction.

# 3.2.6 Pressure Sensitive Electrical Paint Applanation Tonometers and Others

Mackay and Marg (27) discuss the advantages of several fast, automatic, electronic tonometers including a device that uses pressure sensitive paint as its primary transducer (see Figure 12). These devices will not be

discussed separately as they still rely on the applanation principle; however, the reason for the collective study of them is relevant.

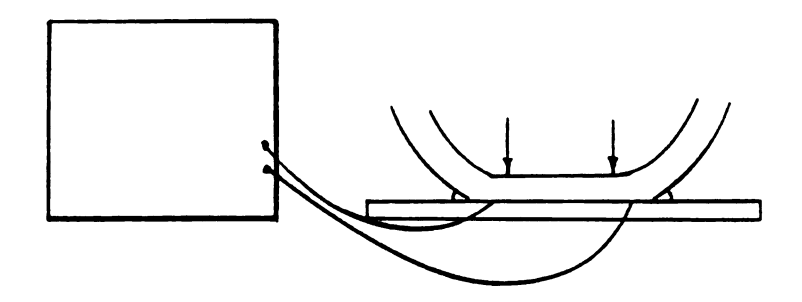


Figure 12 Pressure Sensitive Paint Transducer

The study by Mackay and Marg (27) was in response to the need for a fast, automatic, direct-reading tonometer which is accurate, repeatable and gentle. The existing instruments may have one or two of these characteristics but none exists with all of them. Such an instrument would be of great value not only to the ophthalmologist in his diagnosis and treatment of glaucoma, but also to the optometrist who would be able to determine IOP in his patients without using the anesthetics that the present corneal tonometers demand.\*

# 3.3 Studies of Clinical Tonometry

Tonometry has been refined considerably from the weighted cylinder system devised by Maklanhoff in 1885,

An exception is the AOT. It does not require the use of an anesthetic, although one is sometimes employed.

but the trauma associated with all applanation apparatus is still a serious problem (31, 34, 39).

Moses (31) noted that repeated applanation with the Goldmann tonometer resulted in the lowering of the IOP by approximately 2.5 mm Hg in right eyes and 1.5 mm Hg in left eyes when readings were taken first on the right eye and then on the left eye. When the procedure was reversed, the IOP reductions were reversed. In most cases, the second eye to be measured had a lower pressure than the first eye. There was no plateau pressure recorded in the right eye, but a plateau appeared to be reached with the left eye. Part of this variation of IOP estimate is attributed to the anesthetic, part to the trauma anticipated by the patient and part to the viscoelastic flow of the cornea with repeated applanation.

Moses and Tiu (35) report a standard deviation of more than ± 3 mm Hg when using the Goldmann applanation tonometer. They noted that in 35% of the 148 eyes tested, the difference between two tonometric readings on the same eye after a wait of four minutes between readings was 2 mm Hg or more. It was also noted that if the decrease in applanation pressure estimate was 2 mm Hg, the aqueous flow range value would have to vary by 300%! This tends to suggest that the variation in IOP during applanation is from causes other than variations in the aqueous flow.

Using the Mueller electronic tonometer, Stocker (48) noted that the variation between readings on the same eye averaged 2.72 mm Hg. The variation did not appear to be caused by the increase in aqueous humor outflow resulting from pressures which were elevated by applanation.

That the blunt object trauma caused marked hypotony is well documented by experimenters (31, 34, 49, 53). All applanation tonometers are subject to this limitation to varying degrees.

All applanation tonometer measurements seem to be affected by the blunt object trauma, scleral rigidity, bending rigidity of corneal tissue and surface tension of tear film. A tonometer system not based on applanation would probably circumvent most, if not all, of these problems. Some other problems connected with applanation such as myopia, hypermetropia, hypotonia, astigmatism and corneal scarring perhaps could also be overcome by a new approach.

#### CHAPTER 4

# CLINICAL TONOMETERS--A HIGH-SPEED MOVIE STUDY

# 4.1 Introduction

High-speed films were taken of three tonometers applanating corneas of dogs and humans in the Veterinary Clinic at Michigan State University. These movies were taken to aid in the investigation of the phenomenon associated with applanation. The motion pictures were taken both with "Low Cam" and "Fastax" high-speed movie cameras at an exposure rate of approximately 500 frames per second. Both black and white and color reversal process film were used at f stops and lighting appropriate to each.

Figures 13, 14 and 15 illustrate the procedures used by the photographer in preparation for the high-speed filming of the canines.



Figure 13 Preliminary Camera Set-Up



Figure 14 Determination of Distance and Field of Vision



Figure 15 Final Check and Lens Opening Determination

#### 4.2 General Procedures

Dogs used for the filming were anesthetized with a barbiturate (phenobarbital) \* immediately prior to examination. Clamps and sutures were used to keep the eyes open during examination (see Figure 16). Since the examination period lasted as long as an hour for some dogs, their eyes required repeated moistening with an isotonic lacrimal fluid such as "Tearsol" by Alcon Laboratories. After the tonometric examination, the

It was observed that the baseline IOP of the dogs decreased from normal (12-15 mm Hg) to about 5 mm of Hg when they were anesthetized with phenobarbital. This decrease, however, did not invalidate the results since the methodology and not the IOP's were of interest in the high-speed film study.

sutures and clamps were removed and the dogs were returned to their kennels to recover from the effects of the anesthetic.



Figure 16 Preparation of Canines for Examination

#### 4.3 Schiotz Applanation Tonometer

The first of the clinical tonometers investigated was the Schiotz applanation tonometer. The Schiotz tonometer was selected because of its simplicity, availability, adaptability to canines and wide acceptance in clinical circles. High-speed filming of the Schiotz tonometer applanting a cornea is illustrated in Figure 17.

<sup>\*</sup>High-speed films of the canines were taken by Mr. David Pettigrove, General Motors Proving Grounds, General Motors Corporation.



Figure 17 Schiotz Tonometer Applanting a Cornea

In Figures 18 and 19 are shown the initial contact of the Schiotz tonometer plunger with cornea and contact of tonometer foot with eye globe (indicating that the IOP measurement can be taken off tonometer scale), respectively.

Note the wrinkles formed in the cornea during applanation (see arrow in Figure 18) in addition to the deformation caused by the plunger. It was observed during review of the films that even with a skilled ophthalmologist performing the applanation, considerable rubbing of the corneal surface took place. It was also noted that an actual displacement of the eye globe and

<sup>\*</sup>Copyright applied for.



Figure 18 Initial Contact of Schiotz Tonometer Plunger with Cornea



Figure 19 Contact of Schiotz Tonometer Foot with Eye Globe

distortion of the globe occurred when the tonometer foot contacted the cornea. These observed phenomena contributed to the total trauma experienced by the eye during applanation.

#### 4.4 EMT 20 Digital Applanation Tonometer

The second applanation tonometer selected was the EMT 20 tonometer. The EMT 20 was chosen because of its availability and applicability to anesthetized dogs. The EMT 20 applanating a cornea is illustrated in Figure 20.



Figure 20 Close-up of EMT 20 Applanating Cornea

A photograph of the actual high-speed filming of the EMT 20 tonometer applanating a cornea is presented in Figure 21. As with the Schiotz applanation tonometer, physical evidence of trauma inducing deformations caused by the tonometer is clearly observable from examination of the high-speed films. Globe displacement and distortion, cornea wrinkling and flattening and corneal rubbing occur with this tonometer. An action sequence of actual disturbances during applanation can be seen if the film is reviewed. A clip of the high-speed film of the EMT 20 applanating a cornea is presented in Figure 22.



Figure 21 High-Speed Filming of the EMT 20 Tonometer Applanating a Cornea

#### 4.5 American Optical Applanation Tonometer (AOT)

A tonometer utilizing an air jet for applanation was the third device selected. The AOT was selected because of its availability, its unique applanation



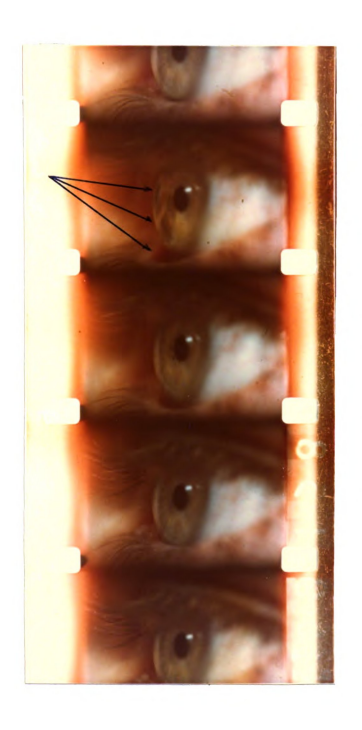
Figure 22 High-Speed Film Clip of EMT 20 Applanting a Cornea

procedure and its alleged superiority of measurement. Since the AOT, as well as other optical types (such as the Goldmann) considered, required focusing of the total eye, a human subject was necessary. Shown in Figure 23 is a high-speed film clip of the AOT applanting the cornea of a human eye. Note the darkened line at the end of the arrow drawn on the photograph. This darkened line, since appearing only after the air jet applanation, could possibly be a wrinkle in the corneal surface, a bow wave in the corneal surface, an index of refraction change in the cornea or aqueous or some other phenomenon; it is clearly related to the air blast. The dimple caused by the same blast is easily seen. Depth of the dimple can be estimated by comparing it with the corneal thickness. Notice also the lid separation which is readily observable in Figure 23. Finally, when the film was viewed in motion, it was observed that the patient's recoil from the air blast nearly removed him from the field of vision of the camera.

In Figure 24 is shown more clearly the discrepancies outlined in the second frame of Figure 23.

# 4.6 Summary

The high-speed films showed that even with a skilled operator applanating the cornea, considerable rubbing and corneal wrinkling occurred during applanation



High-Speed Film Clip of the AOT Applanating Cornea Figure 23



Figure 24 Discrepancies of Figure 23, Frame 2 Enlarged

with both of the contacting tonometers. The films indicated an additional probable cause of the variation of readings on the same eye with contacting tonometers. This variation is due in part to non-normal positioning of the tonometer probe on the corneal surface, tonometers which require focusing of the whole eye, however, are not as susceptible to this type of error. Most tonometer manufacturers recognize the possibility of non-normal positioning error and recommend repeated readings and averaging or repeated readings and selection of the lowest reading (Section 3.2) instead of a single reading for each eye. The noncontacting air jet tonometer did not cause wrinkling in the corneal tissue but did apparently generate an index of refraction variation in the cornea in addition to the applanation dimple. apparent variation in the index of refraction of the corneal material and/or aqueous humor could be either a shock wave generated by the sudden blast of air dimpling the cornea or a corneal ripple similar to the bow wave of a boat or the ripple generated by a pebble tossed into a puddle. What is important, however, is that the pressure wave that caused the alleged index of refraction variation exists and could be partly responsible for the observed variation in IOP measurements made with the AOT on the same eye (53).

All applanation devices in fact deform the eye and displace both corneal tissue and aqueous.

#### CHAPTER 5

#### EXPERIMENTAL SYSTEM DEVELOPMENT

# 5.1 Criteria for Measurement System

The following criteria were considered in the selection of a measurement system for invitro and invivo IOP determination.

- Ease of measurement. Measurement procedure should be simple and easy to follow.
- 2. Speed of measurement. If the system is to be applicable to invivo tests, the time required for a measurement should be in the neighborhood of a few seconds.
- 3. Form of data desired. The data should be in a form which is easily understood. The system should yield hard copy of the results for keeping in a patient's file.
- 4. Availability of equipment. For this investigation, the use of readily available equipment was imperative because of the lack of a large equipment budget. It was felt that general purpose

"off the shelf" equipment could be used to provide criteria for selecting instrumentation for subsequent invivo testing.

- 5. Reliability of measurements. Measurements should be free as possible of systematic errors so random errors could be minimized using statistical methods.
- 6. Strength of output signal. The signal should be of sufficient strength to be easily separated from signal noise. This criterion was a major factor in the final selection process.

Other criteria considered which almost goes without comment include resolution and accuracy, for if
instrumentation is repeatable but wrong, where is the
value of the measurement.

## 5.2 System Selected

The apparatus selected for invitro tests in this investigation is diagrammed in Figure 25.

Of the three systems evaluated, the one shown in Figure 25 most closely satisfied the selection criteria listed in Section 5.1. While the system will require modification to be satisfactory for further invivo IOP measurements, it yielded good invitro IOP data.

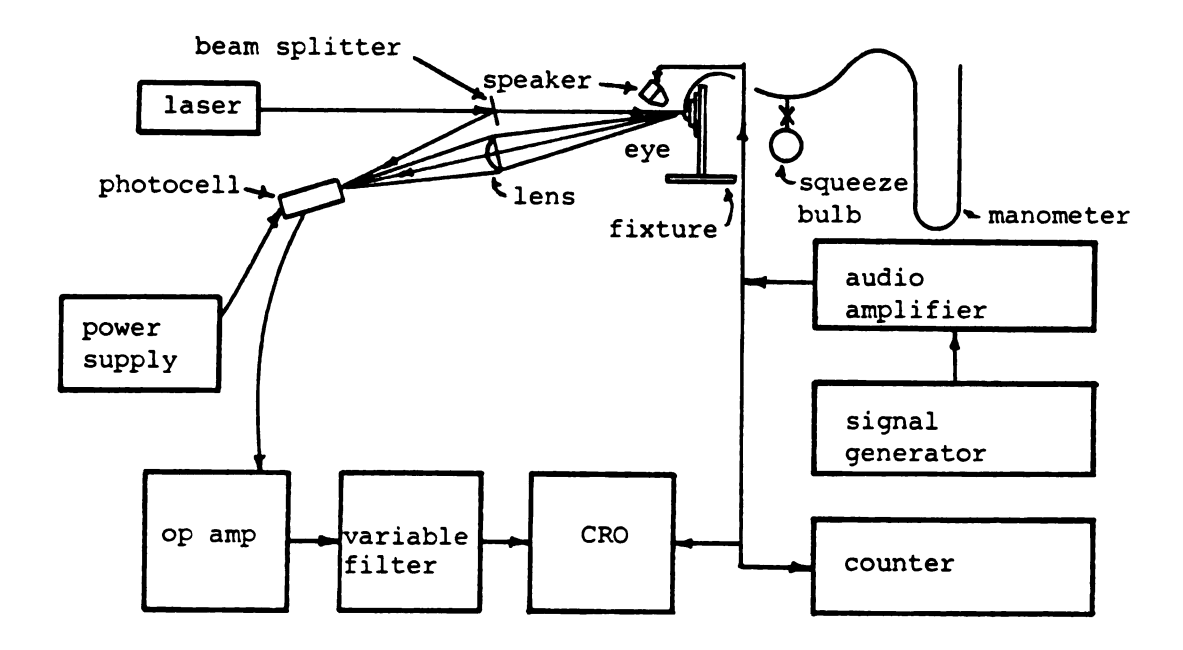


Figure 25 Data Gathering System

The remainder of the chapter details the investigation and evaluation of the three systems considered using a latex diaphragm as a model. It was felt that if the measurement system would perform satisfactorily for the diaphragm model, it should be satisfactory for invitro investigations.

# 5.3 Preliminary Investigation

The selection of a data acquisition system required considerable preliminary investigation. An experimental model of the anterior region of the eye was developed. The data from three modifier systems using the model furnished the information on which to base the selection of the final system.

The portion of the eye modeled consisted of the cornea, anterior chamber, lens and ciliary body. The globe of the eye was omitted (see Figure 26).

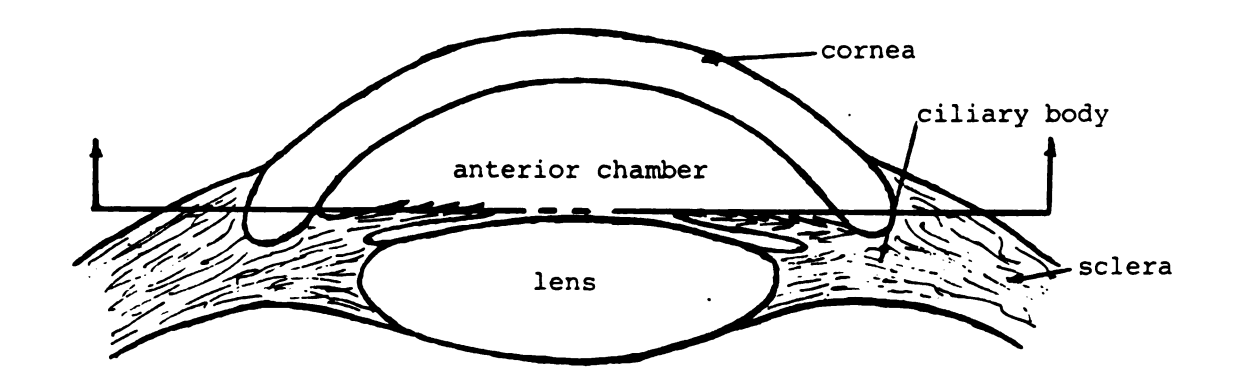


Figure 26 Anterior Portion of the Eye

The experimental model chosen for this phase of the investigation was based on a number of criteria including the following:

- 1. Availability
- 2. Cost
- 3. Flexibility of material
- 4. Contour to be similar to that of the cornea
- 5. Quality of material
- 6. Similarity to eye

Since the model was going to be used to aid in the selection and calibration of the instrumentation package, criteria number six was not felt to be as important as the first five. The model selected was a

thin latex female contraceptive diaphragm 80 mm in diameter with a radius of curvature of about 50 mm. Although the size of the diaphragm was the main factor determining the model fixture specifications, the following criteria were also considered:

- 1. Ease of removal of the diaphragm from the fixture.
- Light enough to be portable, but yet of sufficient strength not to be affected by the diaphragm or speaker-induced vibrations.
- Air-tight seal between diaphragm and model fixture.
- 4. Ability to easily vary diaphragm cavity pressure.
- 5. Can be converted to hold excised eyes.

The fixture design is shown in Figure 27. The fixture frame was a 4" by 10" hot rolled steel plate 1/2" thick. The diaphragm holding ring was machined from aluminum.\*

After many unsuccessful attempts to put a reflective surface on the latex rubber diaphragm, a strain gage tab was snipped off a foil type resistance strain gage and glued to the diaphragm surface with G. E. Silicone Rubber (see Figure 28). The tab was then carefully

<sup>\*</sup>The fixture was built in the machine shop of General Motors Institute, Flint, Michigan.

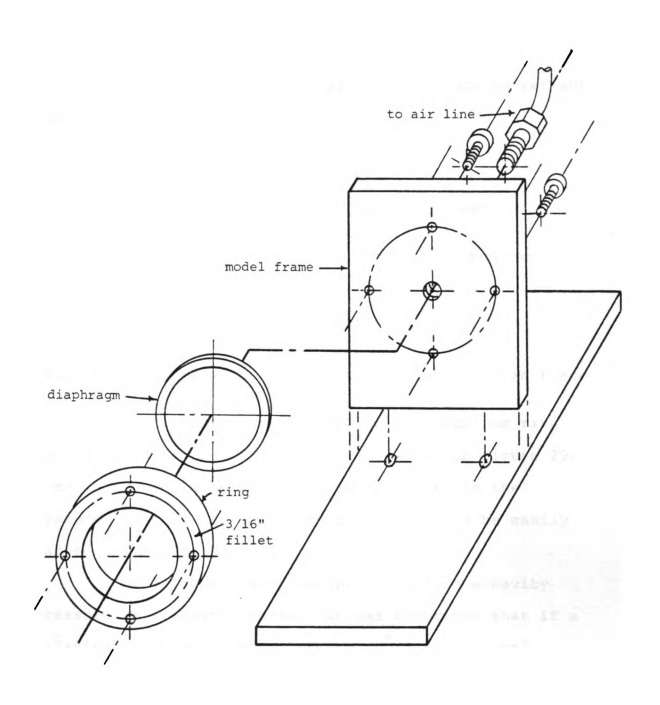


Figure 27 Assembly Drawing of Model Fixture

cleaned. Since there was still significant scattering of reflected light, the tab was coated with clear finger nail polish making a very satisfactory surface to reflect laser light.

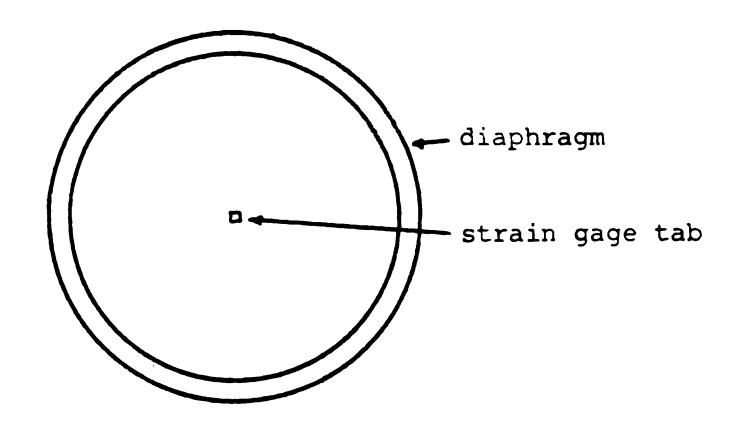


Figure 28 Diaphragm with Strain Gage Tab Glued in Place

The diaphragm was mounted in the aluminum ring and fastened to the fixture frame as shown in Figure 29. A manometer and squeeze bulb were connected to the fixture frame so the diaphragm pressure could be easily varied and monitored.

The apparatus was designed to obtain a cavity pressure vs frequency curve. It was theorized that if a relationship between normal response frequency and cavity pressure could be obtained with the measurement

<sup>\*</sup>Normal response frequency was used because it is observable and is defined to be that frequency to which the eye responds with a maximum output for a minimum input. The exact resonance frequency cannot be experimentally determined without knowing the damping coefficient of the system.

system employed for the diaphragm model, the same could be obtained for the eye.



Figure 29 Mounted Diaphragm with Pressure Variation Apparatus

The pressurized latex diaphragm was excited by an inexpensive radio speaker with a mirror fragment glued on its cone and driven by an audio oscillator.

In Figure 30 is a sketch of the system used to calibrate the speaker in terms of frequency and amplitude. The detection system is a laser Doppler velocimeter system and is covered in detail in Sections 6.4 and 6.5.

The data obtained for the calibration of the speaker, light and detector was speaker input frequency,

speaker input amplitude and photocell output amplitude. It was planned to normalize the speaker amplitude data throughout the test frequency range. The input signal frequency was monitored by the counter and the amplitude by the cathode ray oscillscope (CRO). Observation of the wave forms of the output signal from the photocell indicated substantial wave distortion. Meaningful normalization could not be performed without further signal modification. The distortion was attributed to the speaker's nonlinear characteristics.

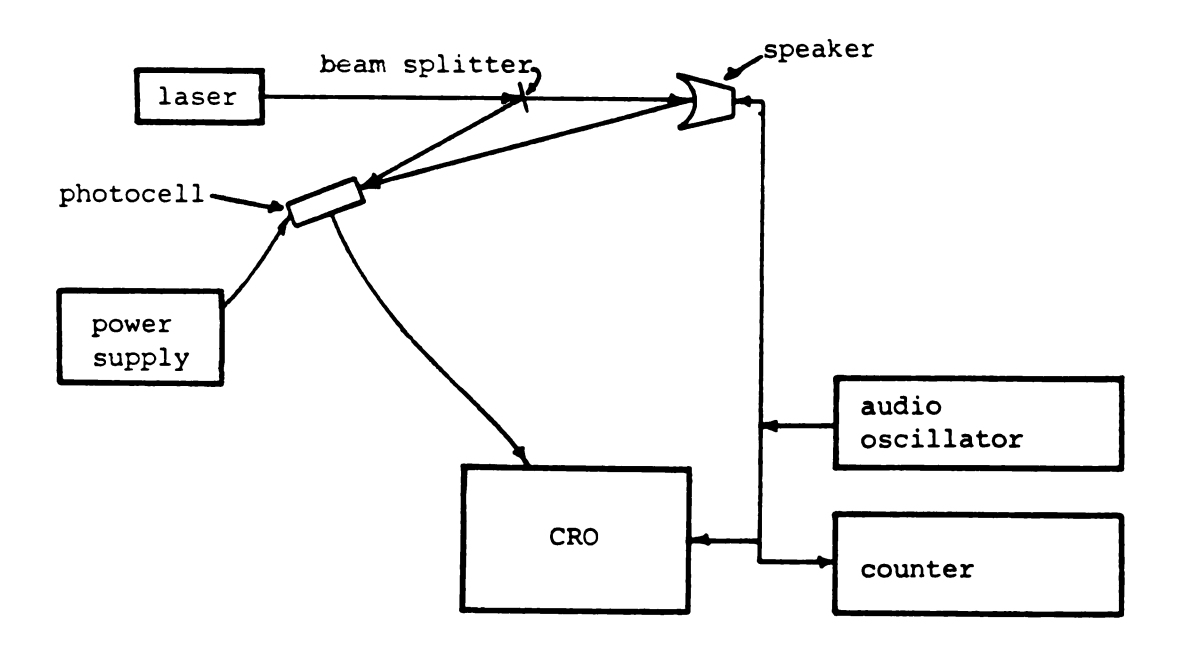


Figure 30 Preliminary Speaker Calibration Apparatus

The audio oscillator output amplitude was then reduced. A Kronhite \* variable filter was used to pass

A complete list of test equipment will be found in Appendix B.

only the audio oscillator frequency. The filter was adjusted to the "band pass" function, the low pass and high pass settings were tuned to the audio oscillator frequency and the amplification set to the + 20 db position. The output from the variable filter was the input to a Tektronix 555 dual beam oscilloscope (see Figure 31). The procedure for speaker calibration is listed as follows:

- Adjust audio oscillator output amplitude to a predetermined value (for final calibration, an amplitude of "50" was used).
- 2. Adjust audio oscillator to 100 Hz.
- 3. Fine tune audio oscillator frequency using the electronic counter as the readout.
- Adjust high pass and low pass settings of the variable filter to the audio oscillator frequency.
- 5. Measure the output amplitude of the photocell on the CRO.
- 6. Measure the output amplitude of the audio oscillator on the CRO.
- 7. Re-adjust audio oscillator to previous reading plus 10 Hz.
- 8. Repeat steps 3 through 8 until the calibration range has been covered.

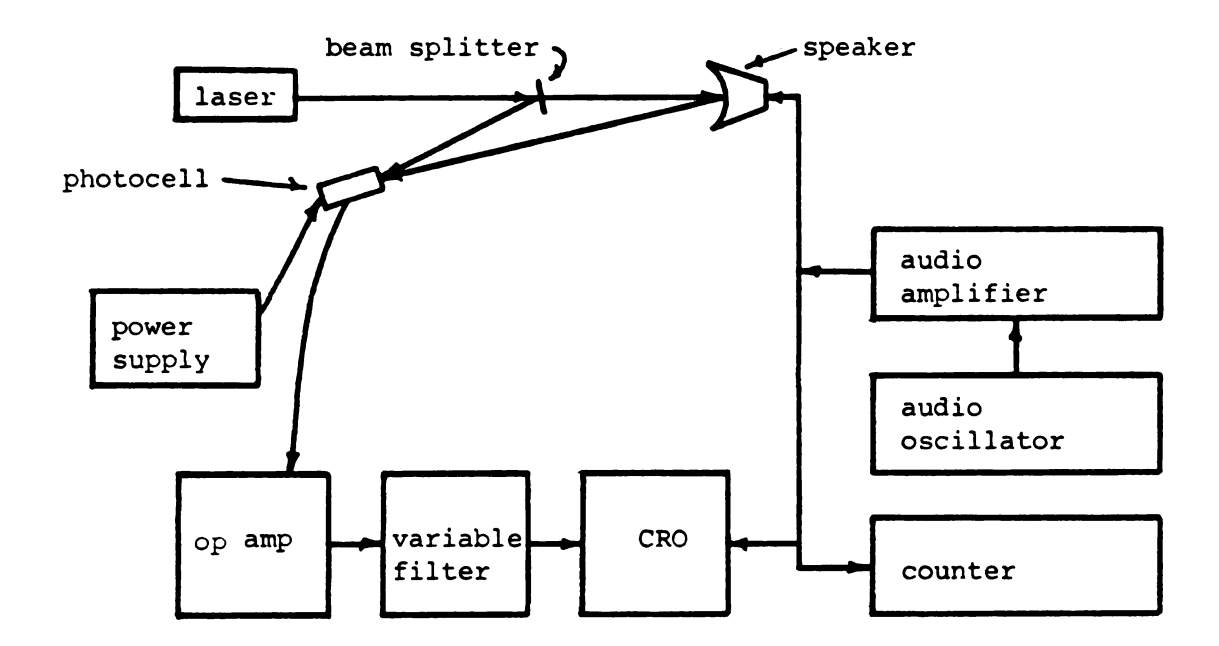


Figure 31 Improved Speaker Calibration System

After perfecting the calibration procedure and sequence, further modification of the instrumentation was necessary to eliminate audio oscillator loading and to strengthen the output from the photocell.

An audio amplifier in line between the oscillator and speaker eliminated oscillator loading and thereby removed the need to normalize the speaker input signal. The resulting speaker calibration curves are displayed on Figure 32.

After calibration of the speaker system, the diaphragm fixture was placed on the lab jack, positioned and then clamped in place. Next, the calibrated speaker was located where it could provide the diaphragm

<sup>\*</sup>Data can be found in Appendix D.

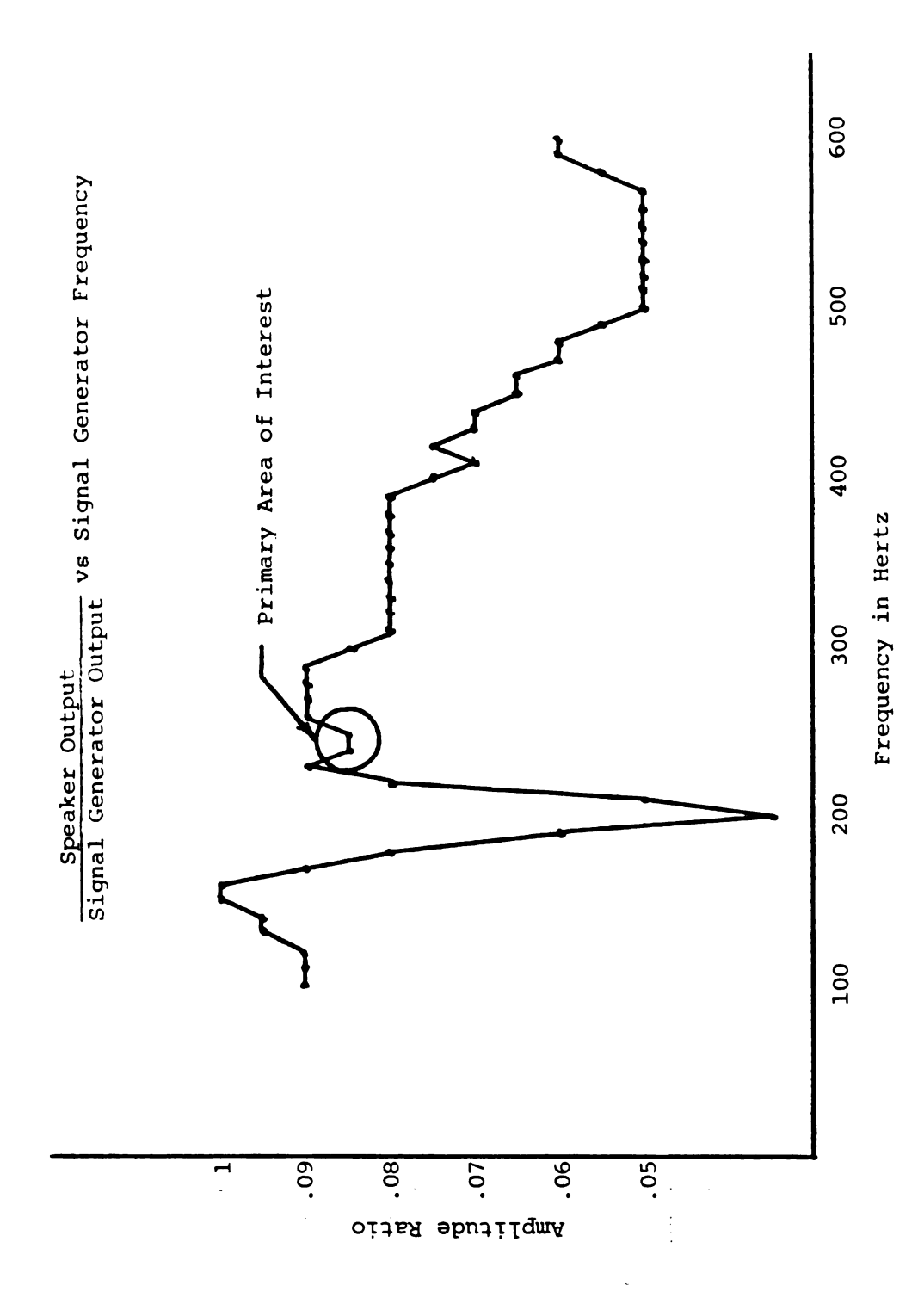


Figure 32 Speaker Calibration Curve

excitation, and yet not interfere with the incident or reflected laser beam. When all leads were properly connected, the audio oscillator and variable filter were adjusted to the natural frequency (about 150 Hz) of the speaker. The signal amplitude on the CRO was adjusted to about 2 cm at 0.2 V/cm vertical sensitivity. In Figure 33 is displayed the Experimental Set Up #1 for diaphragm data.

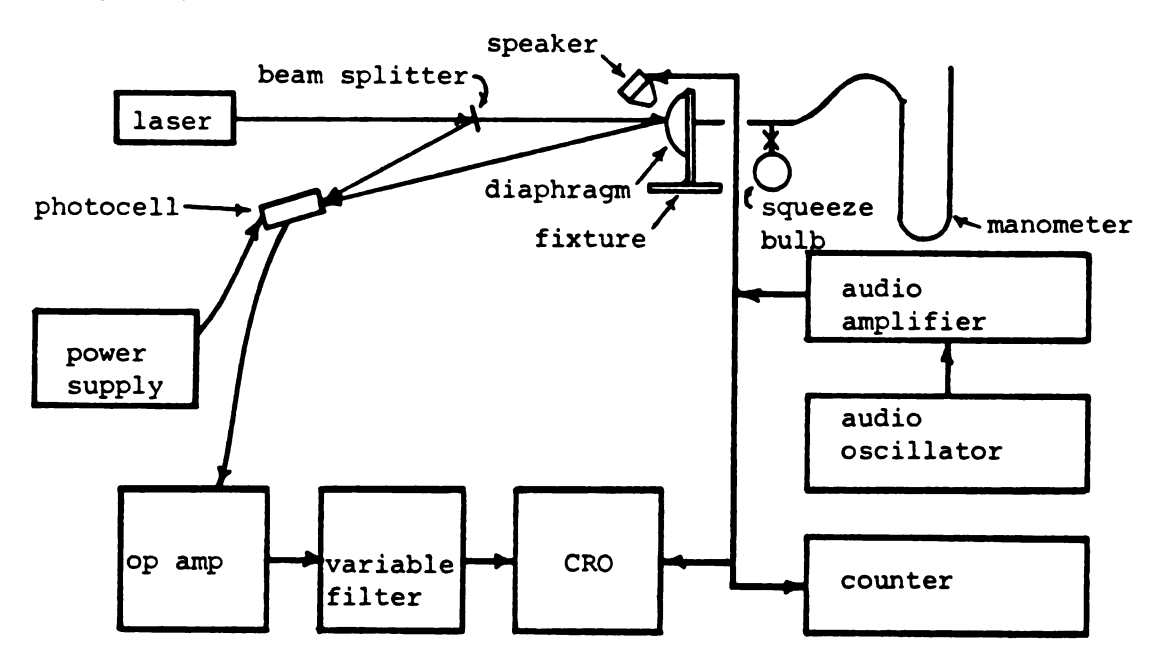


Figure 33 Experimental Test Set Up #1

The following procedure was developed to obtain data for each diaphragm cavity pressure:

- Adjust audio oscillator output amplitude to the value used for speaker calibration.
- 2. Adjust audio oscillator frequency to 100 Hz.

- 3. Fine tune audio oscillator using the electronic counter as the guide.
- 4. Adjust high pass and low pass settings of the variable filter to the audio oscillator frequency.
- 5. Measure photocell output amplitude on the CRO.
- 6. Readjust audio oscillator frequency to previous setting plus 10 Hz.
- 7. Repeat steps 3 through 7 throughout the calibration range of the speaker.

At this time, the diaphragm cavity pressure was re-adjusted with the squeeze bulb, and the test was repeated.

Since an objective of the project was to develop some design criteria for invivo testing of suspected glaucomatous eyes in humans, further investigation into modifier systems and procedures was undertaken. With the present instrumentation and procedures it required approximately 12 hours to obtain and plot the data for five data points on a pressure vs frequency curve for the diaphragm. The need for streamlining the data acquisition procedure was indicated.

A white noise or random noise generator was substituted for the audio oscillator and a Quantech Wave

Analyzer and XY plotter were substituted for the variable

filter and CRO. With these changes in instrumentation (see Figure 34), a complete set of data for one diaphragm cavity pressure could be obtained in one minute or ten minutes, depending on the sampling rate selected on the wave analyzer.

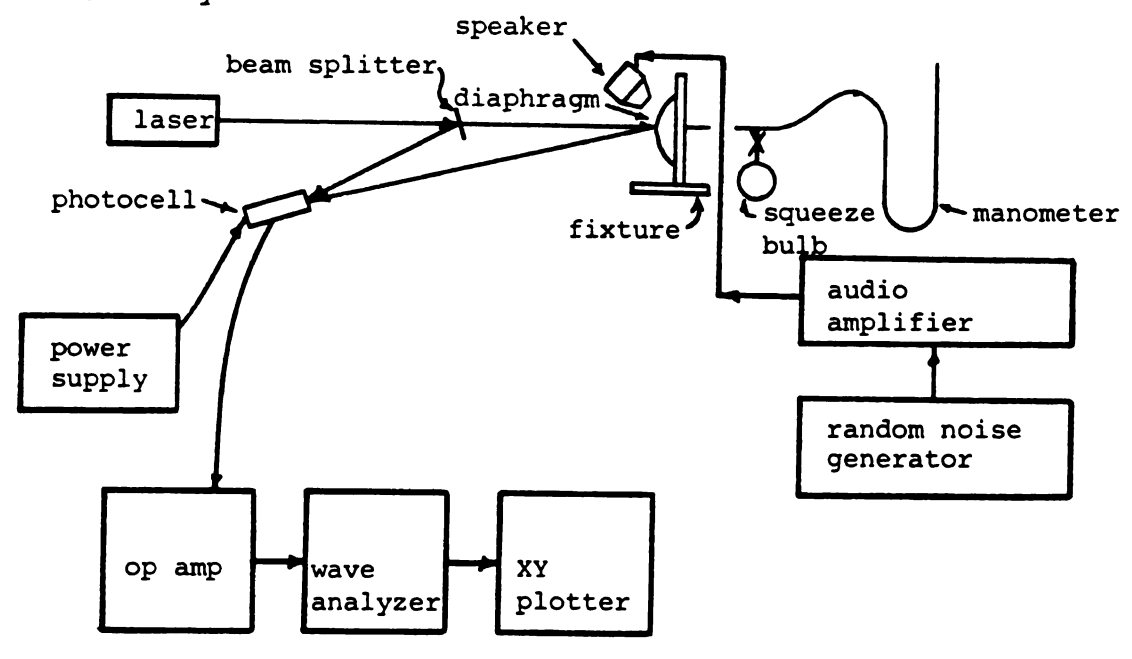


Figure 34 Experimental Test Set Up #2

Two limitations of the Quantech Analyzer were noted and are listed as follows:

- 1. Lack of normalization capability. (If the normal response frequency and cross-over frequency of the exciter system is out of the range of the normal response frequency of the system to be excited, this limitation is not significant.)
- Cannot be used if a transient excitation is to be employed.

The final instrumentation system investigated was selected in response to the problem of transient measurements. It is shown in Figure 35. In this system, the Quantech analyzer and XY plotter were replaced with a Federal Scientific Fourier wave analyzer. The Fourier analyzer, when used in conjunction with the random noise generator, could gather a complete set of information at one diaphragm cavity pressure in about 10 seconds. The information could be obtained in paper form in less than one minute. With further modifications, the time could be further reduced.

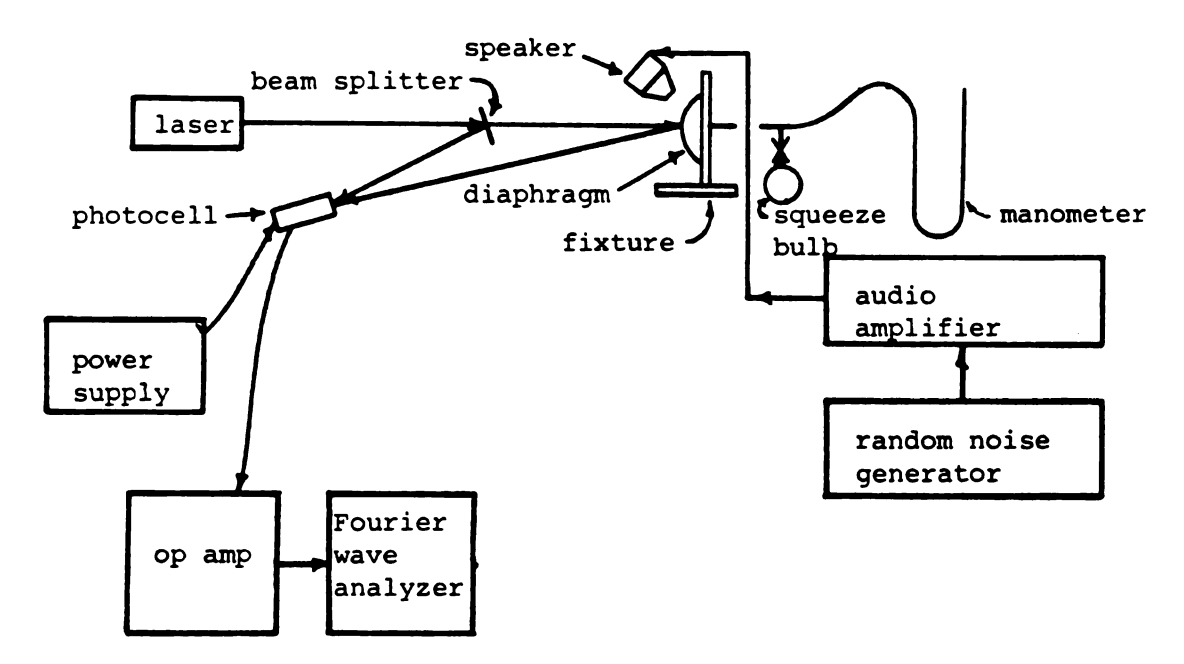


Figure 35 Experimental Test Set Up #3

# 5.4 Measurement System Evaluation

The three modified systems described in Section 5.3 were evaluated. The data from these three systems as

applied to the diaphragm model were compared and the advantages and disadvantages of each system are listed in Section 5.5.

Using the Experimental Set Up #1 as presented by the sketch in Figure 33, a frequency sweep was made for each of several diaphragm cavity pressures. The data taken for each pressure included frequency, photocell output amplitude and speaker input amplitude are shown in Table 1.

The amplitude data obtained was normalized on the speaker output and plotted versus audio oscillator frequency. The peaks in the amplitude ratio curve represent normal response frequencies for the diaphragm. Because the latex diaphragm is an infinite degree-of-freedom system, it is difficult to predict from the data which frequency is the fundamental. Since the diaphragm model was used primarily to test the measurement system and to show variations in normal response frequency with variations in pressure, no theoretical analysis was performed to isolate the fundamental frequencies. The first observed one or two well-developed and pronounced amplitude ratio peaks were used for the comparison. See

<sup>\*</sup>A complete listing of these data will be found in Appendix D.

Table 1 Sample Data Sheet

September 26, 1975 Experimental Set U	6, 1975 1 Set Up #1	Diaphragm Model		Data Set	I-B	
Frequency	(2V/cm) Speaker Input	(.2V/cm) Speaker Output	Ratio	5" Head	7.5" Head	10" Head
100	2 cm	1.8 cm	60.	;	! 	ł
110	2 cm	1.8 cm	60.	.2	}	.2
120	2 cm	1.8 cm	60.	4.	.2	.2
130	2 cm	1.9	.095	9.	. 4	4.
140	2 cm	1.9	.095	<b>∞</b> .	9.	4.
150	2 cm	2.0	.1	9.	.2	4.
160	2 cm	2.0	.1	4.	.2	.2
170	2 cm	1.8	60.	.2	.2	.2
180	2 cm	1.6	.08	.2	.2	4.
190	2 cm	1.2	90.	.2	.2	4.
200	2 cm	۲.	.035	4.	4.	9.
210	2 cm	1.0	.05	4	4.	1.2

The frequencies corresponding to the amplitude ratio peaks designated by the "+" for the various diaphragm cavity pressures were plotted. This plot clearly illustrates the dependence of the normal response frequency on the cavity pressure (see Figure 36) for Set Up #1.

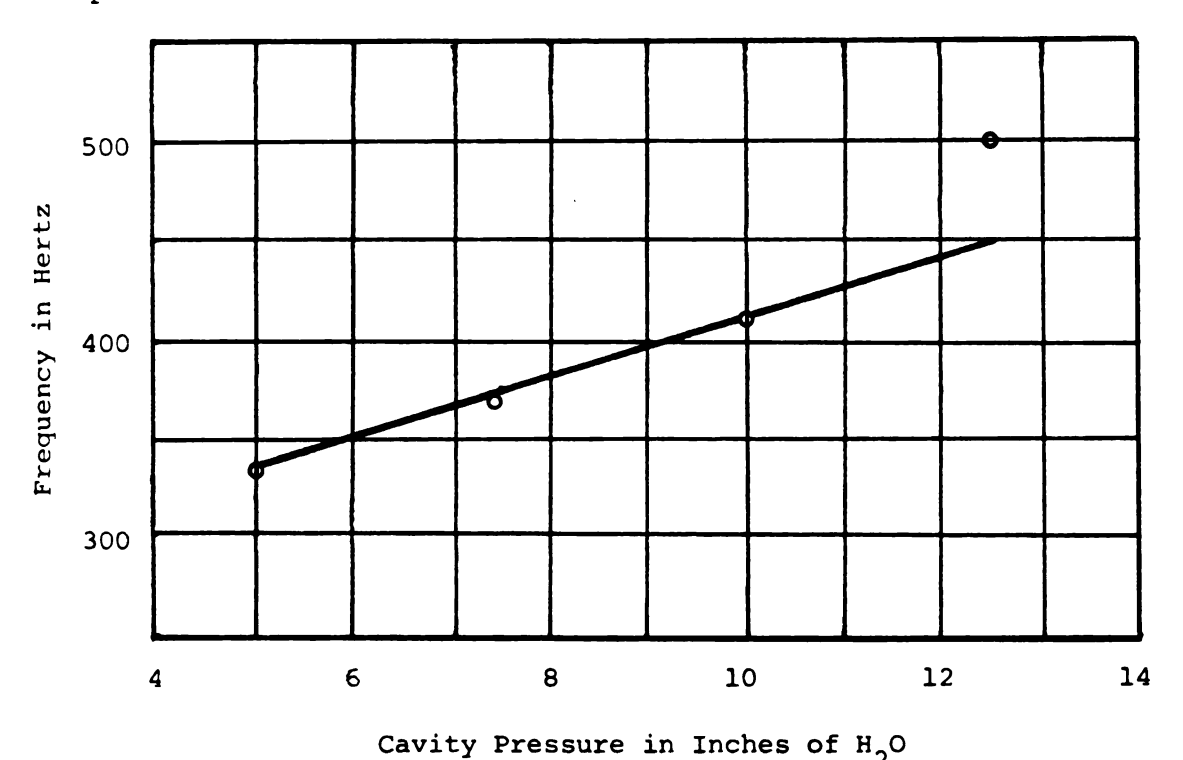


Figure 36 Frequency-IOP Plot, Experimental Set Up #1

The Quantech wave analyzer and XY plotter from

Set Up #2 replaced the variable filter and the CRO in

Set Up #1. Also, the audio oscillator and counter were

replaced by a white or random noise generator. The

function of the wave analyzer was to sweep the frequency

range (100 to 600 Hz) and to provide an amplitude-frequency

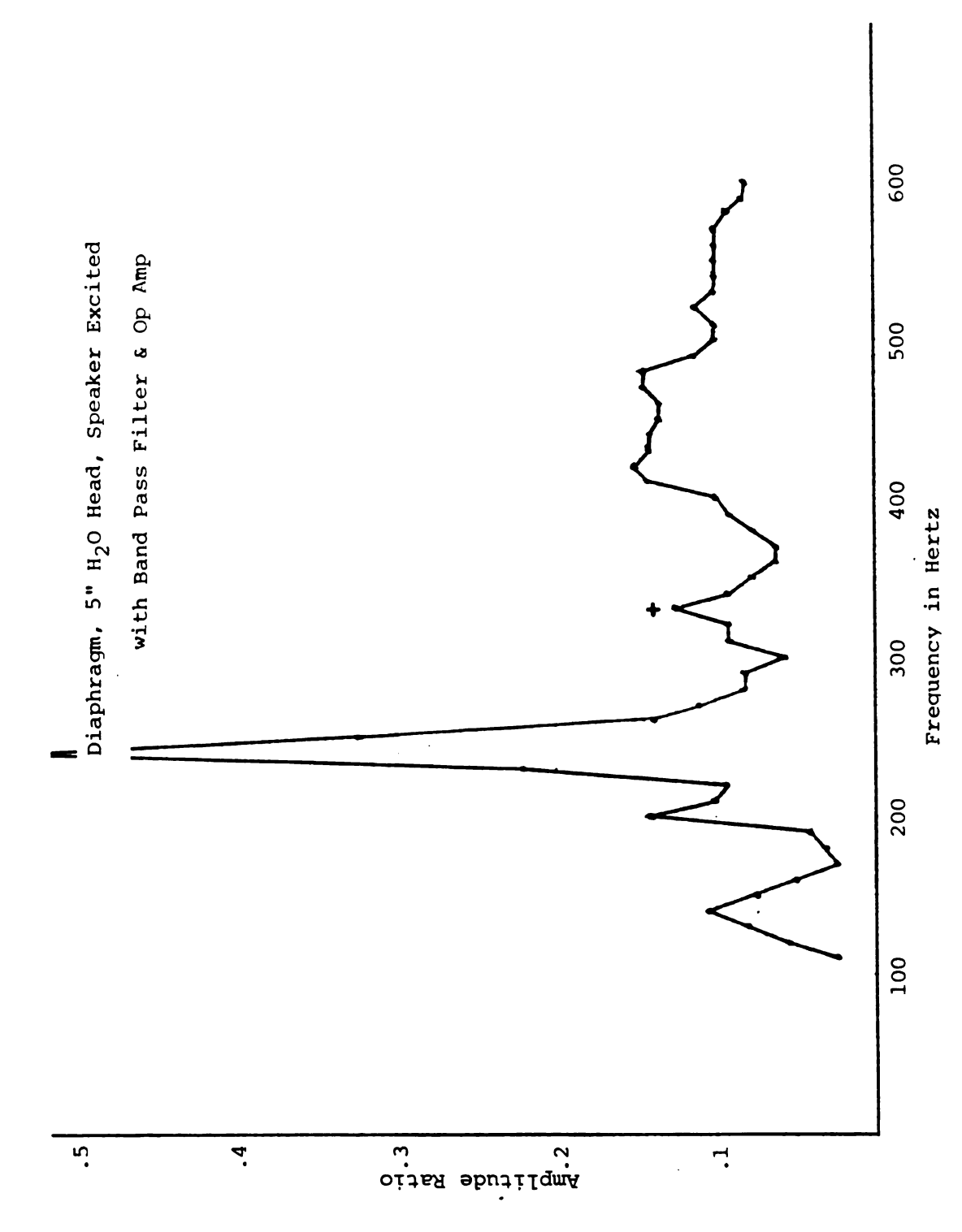


Figure 37 Normal Response Plot, Set Up #1, 5"  $\mathrm{H}_2\mathrm{O}$ 

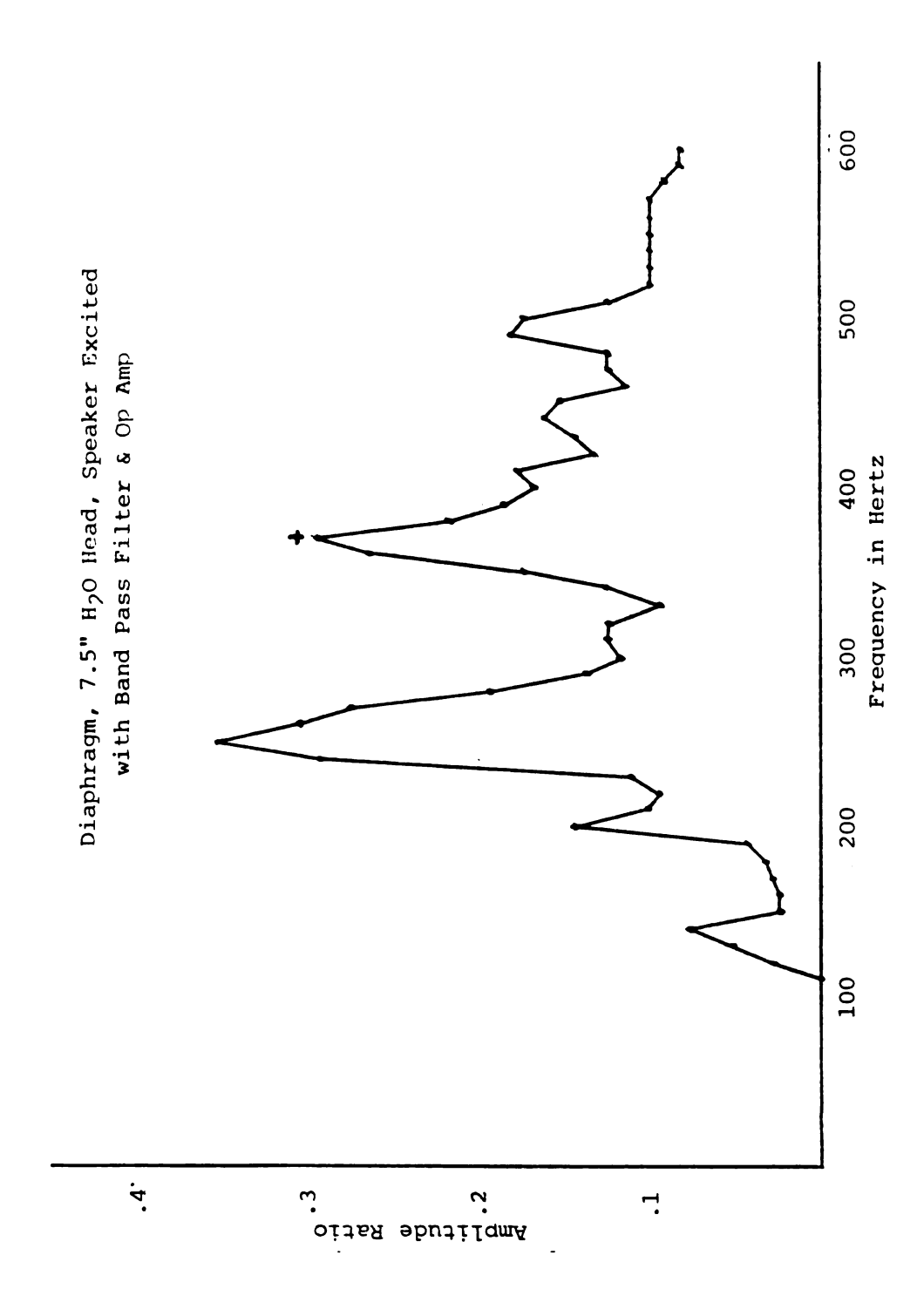
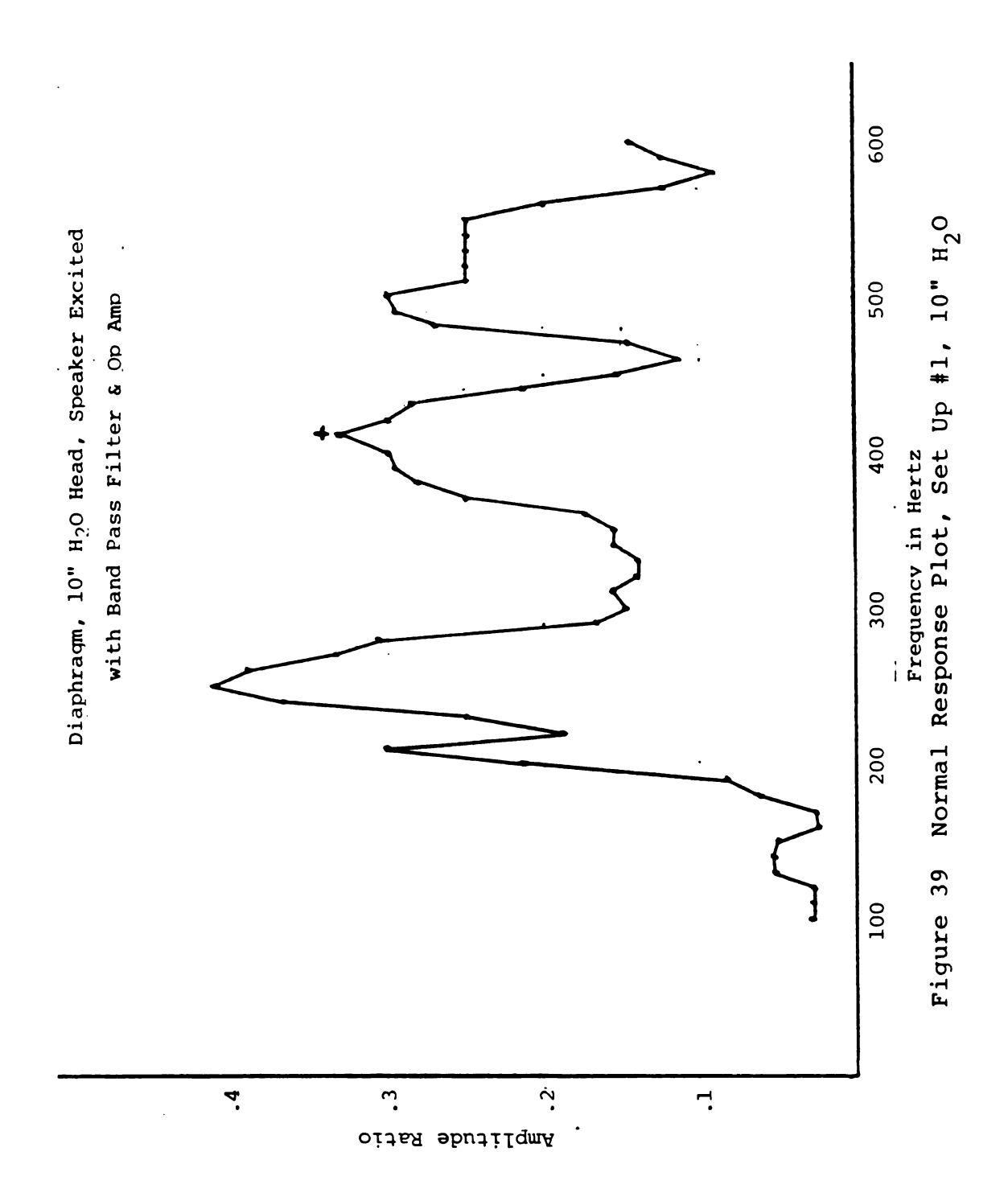
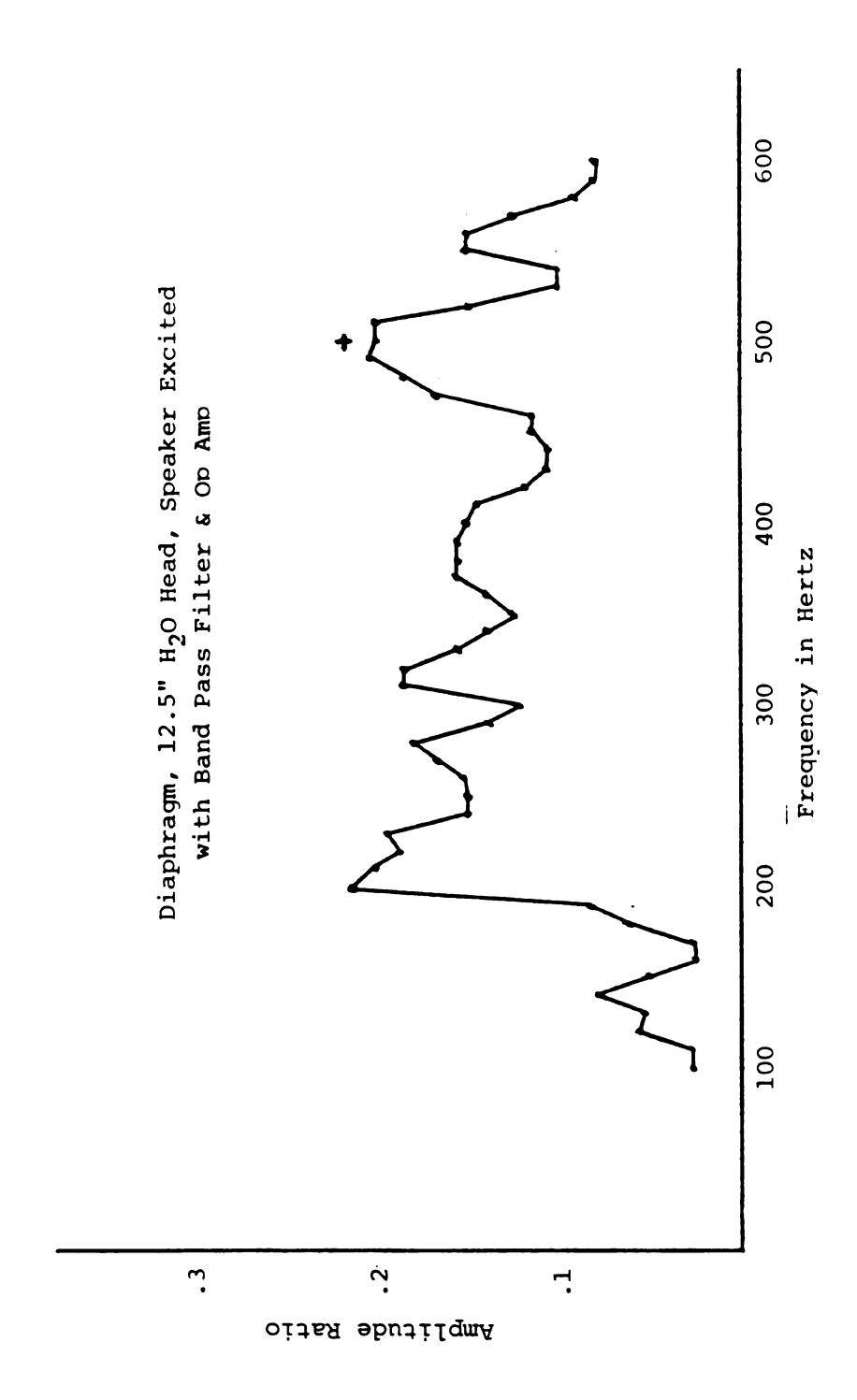


Figure 38 Normal Response Plot, Set Up #1, 7.5"  $\mathrm{H}_2\mathrm{O}$ 





Normal Response Plot, Set Up #1, 12.5"  $\mathrm{H_2O}$ Figure 40

signal for the XY plotter. The XY plotter simply plotted the output from the wave analyzer.

The sweep output from the wave analyzer was calibrated in inches and served as the X input for the plotter. Therefore, the XY plotter could generate an amplitude versus frequency plot as the analyzer swept the pre-set frequency range. See Figures 42-45 for representative curves from Experimental Set Up #2.

The frequencies corresponding to the amplitude peaks designated by the "+" for the various cavity pressures are plotted on Figure 41. This plot also illustrates the dependence of normal response frequency on cavity pressure.

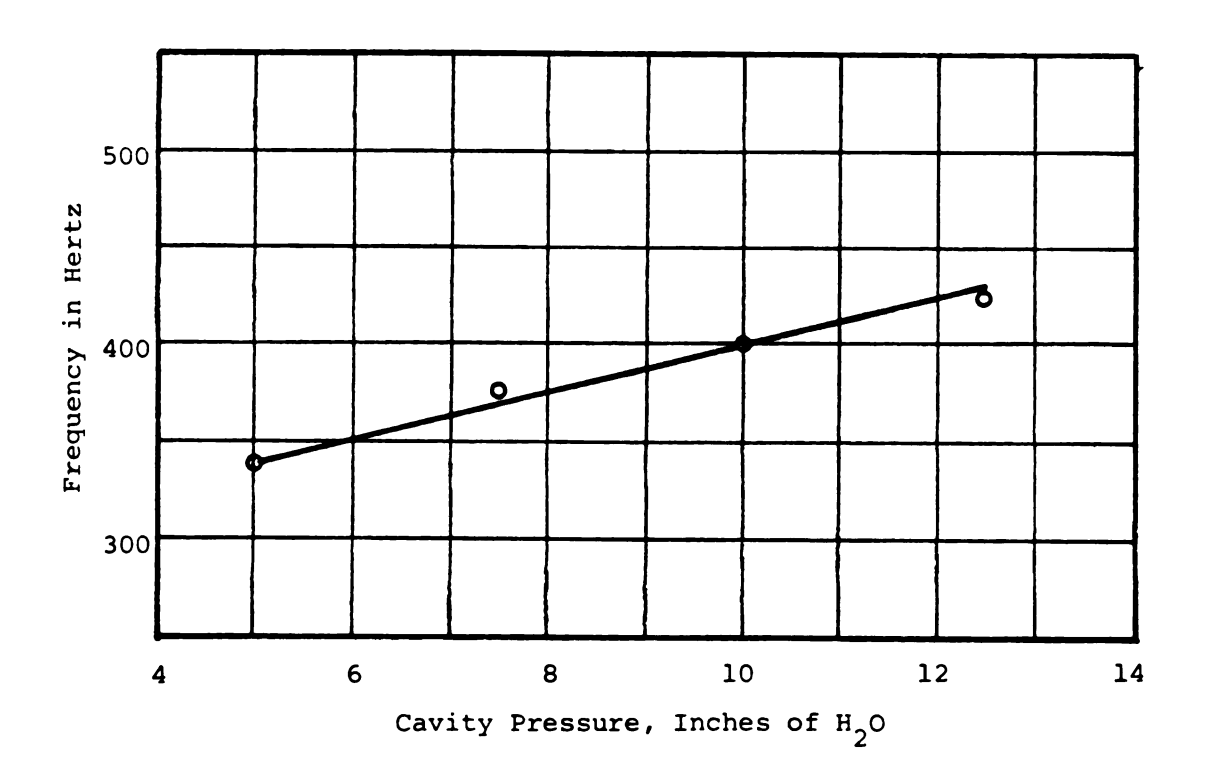
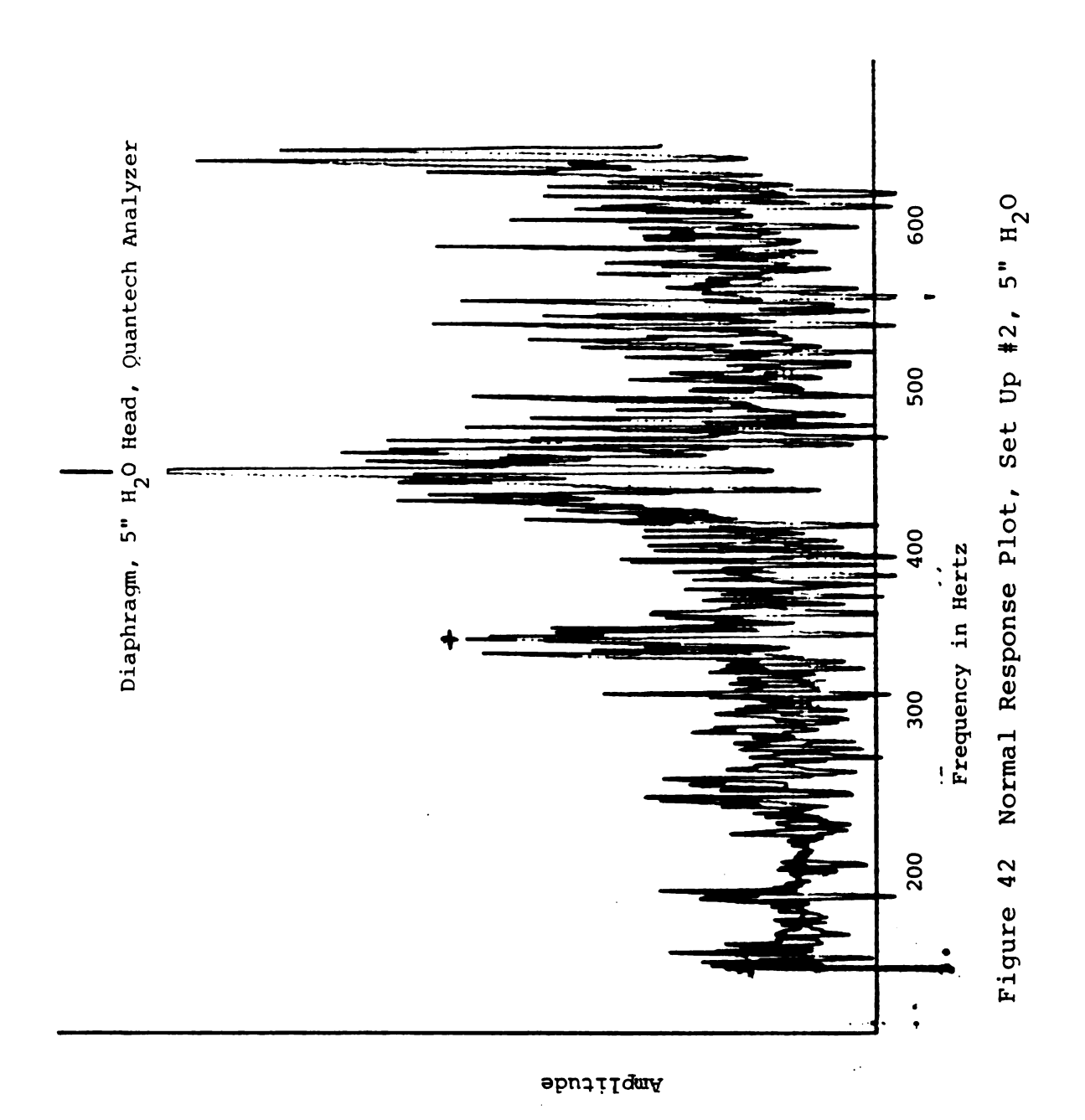
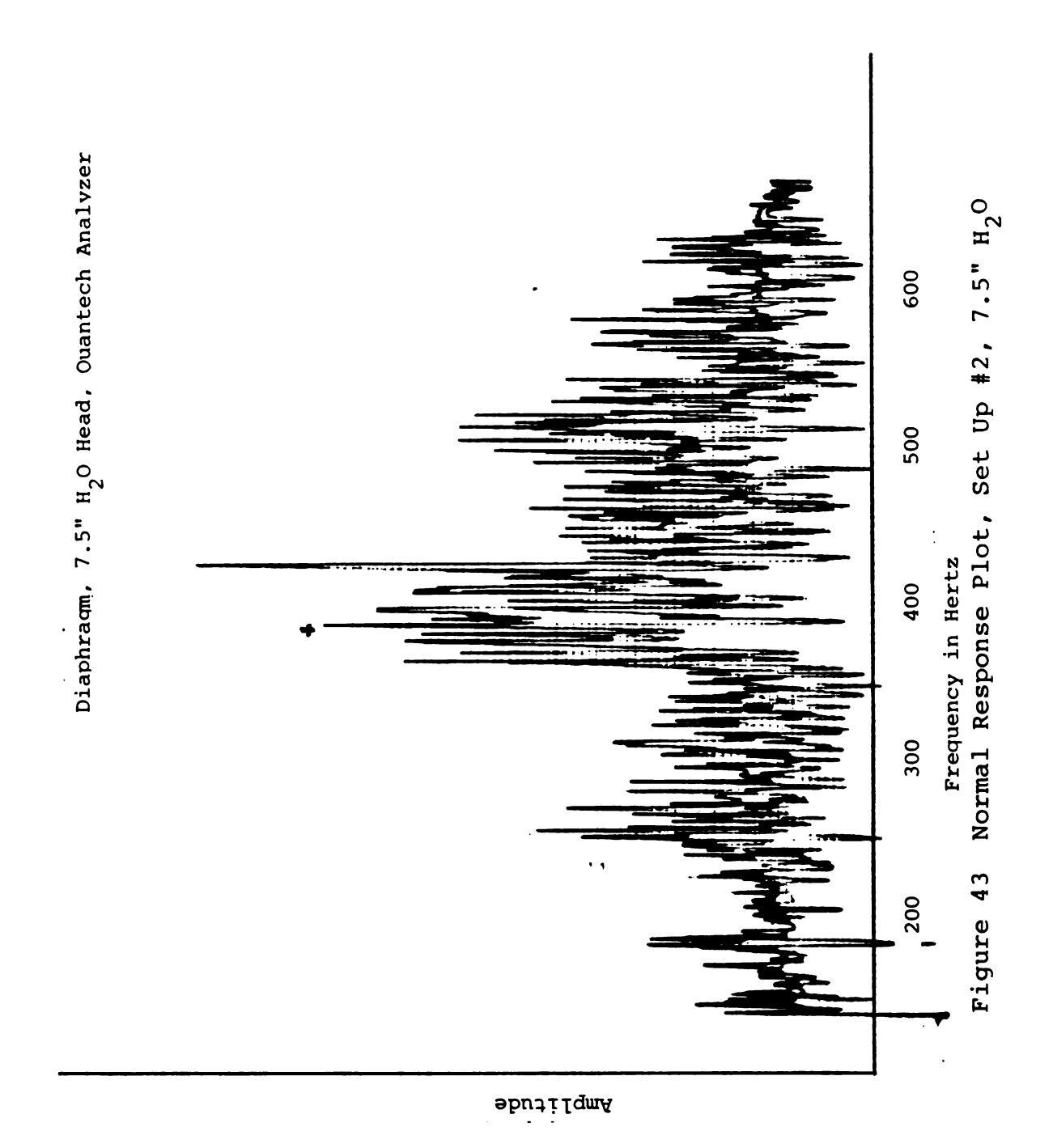


Figure 41 Frequency-IOP Plot, Experimental Set Up #2





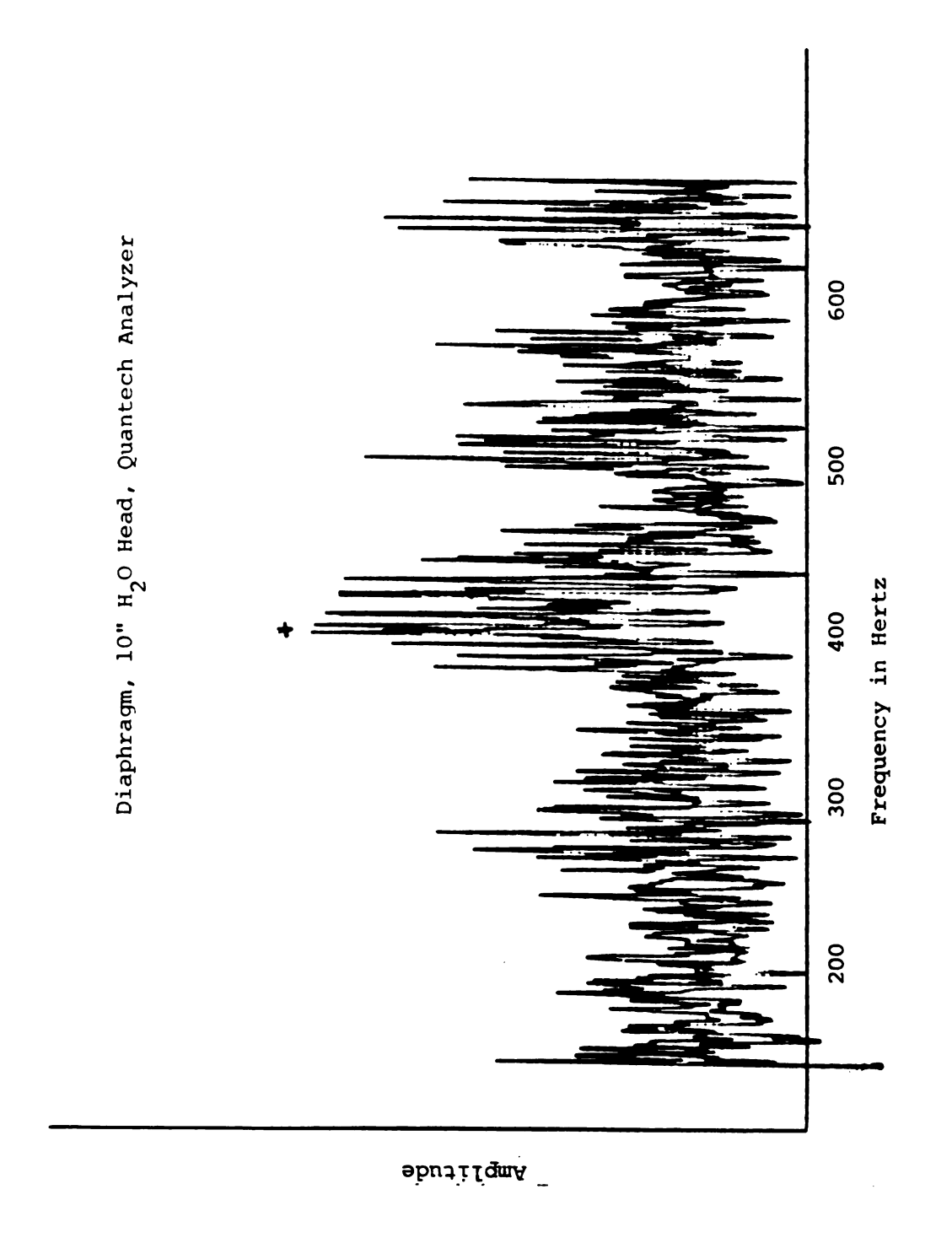
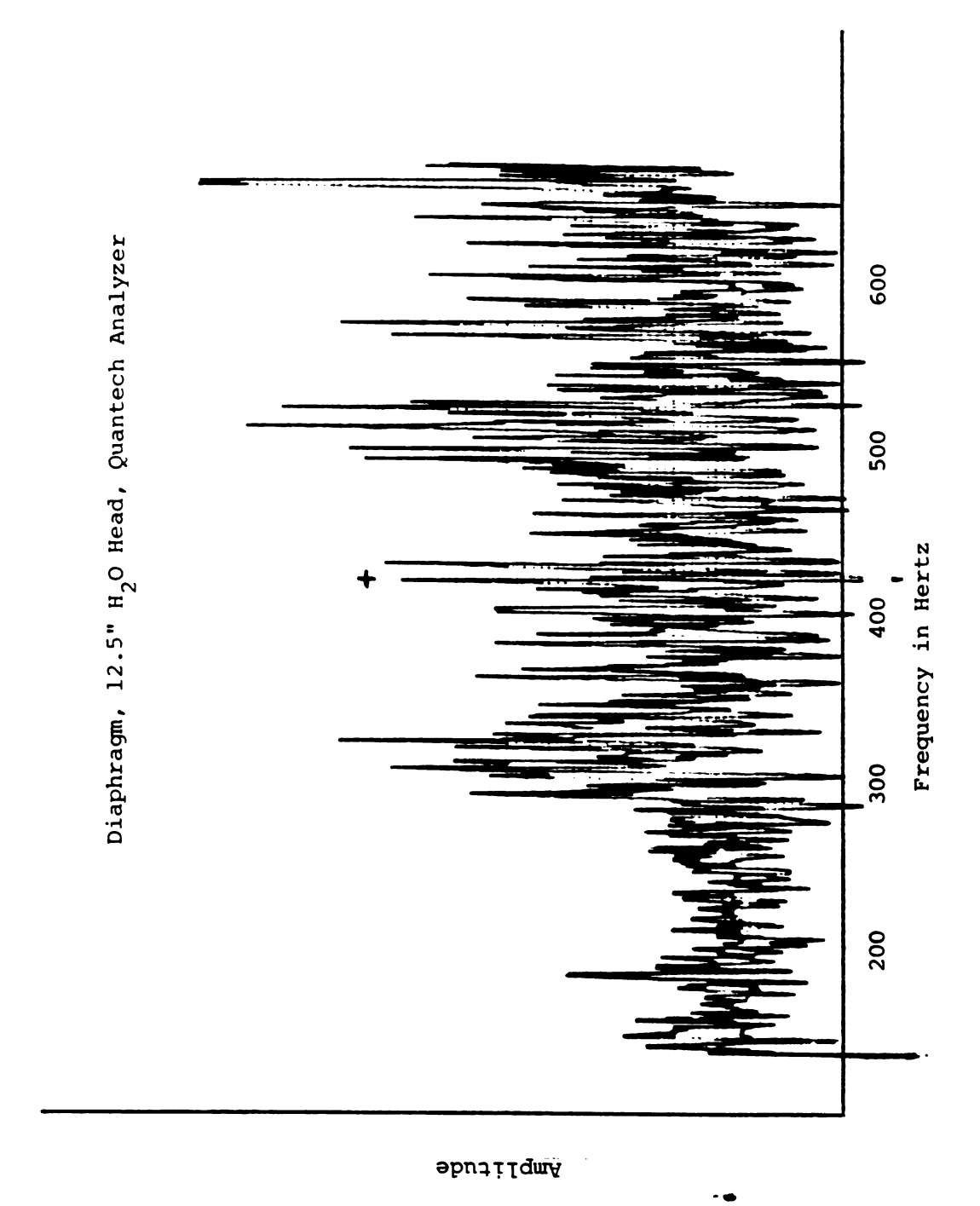


Figure 44 Normal Response Plot, Set Up #2, 10"  $\mathrm{H}_2\mathrm{O}$ 



Normal Response Plot, Set Up #2, 12.5"  $\rm H_2O$ Figure 45

The final measurement system investigated was also a modification of Experimental Set Up #1. The Federal Scientific Spectrum Analyzer replaced the variable filter and CRO of Set Up #1 while the audio oscillator and counter of Set Up #1 were replaced by a random noise generator. This variation, Experimental Set Up #3, was chosen mainly to utilize a system that could handle a random or pulse input. Possibly, an invivo eye test would require the use of a pulse stimulation or detection system. Figures 46-49 present the response data from Set Up #3. As with Set Ups #1 and #2, the frequencies corresponding to the amplitude peaks designated by the "+" are plotted for Set Up #3 (see Figure 50).

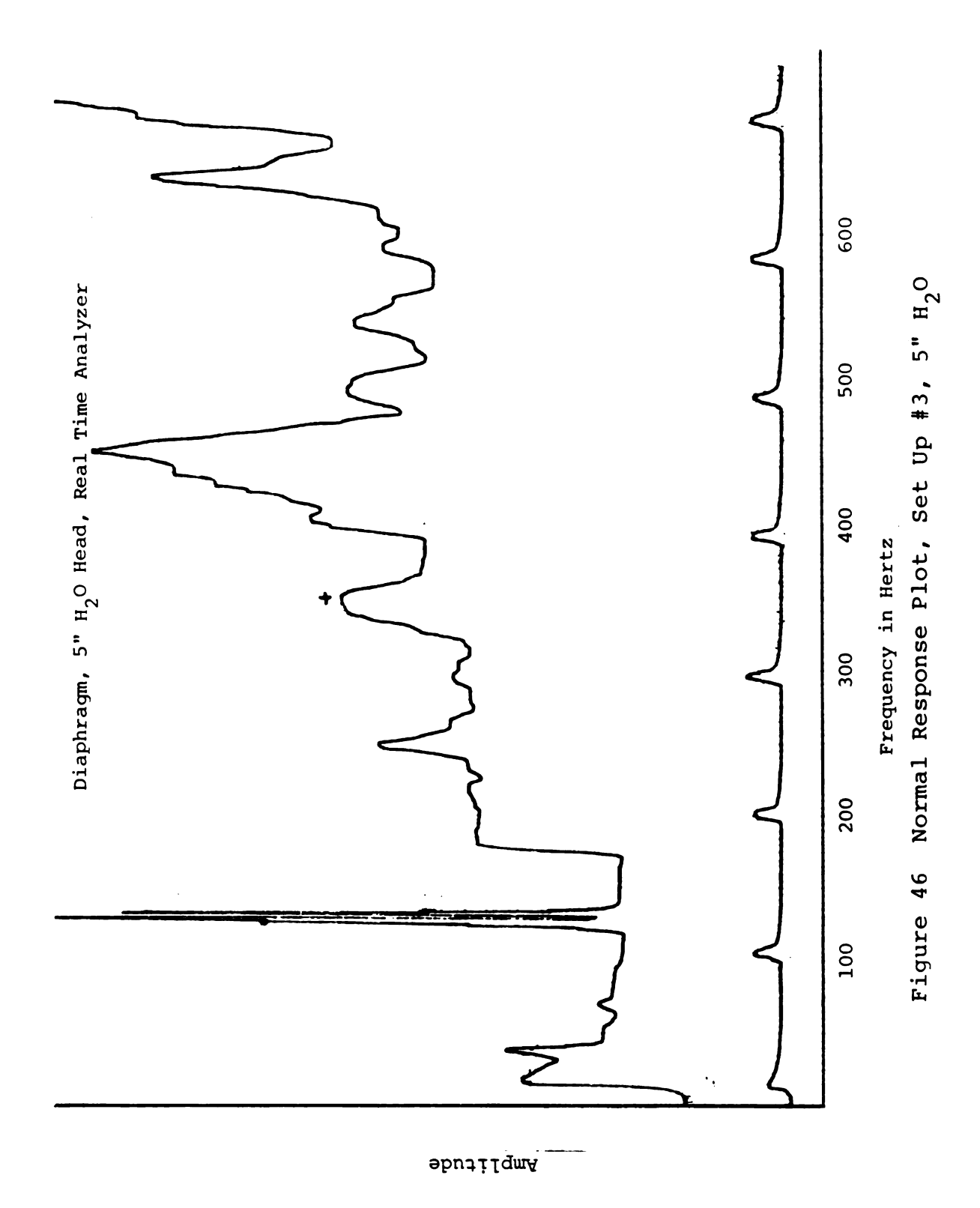
### 5.5 Summary

The similarities, shown in Figure 51, between the three experimental set ups' curves signify that the systems appear to be free of systematic errors of the modifier systems and that any of the three systems could be expected to yield reasonably valid data.

The relative merits of each set up based on the criteria presented in Section 5.1 are listed as follows:

#### Set Up #1

 Procedure is easy to use once the system is operational.



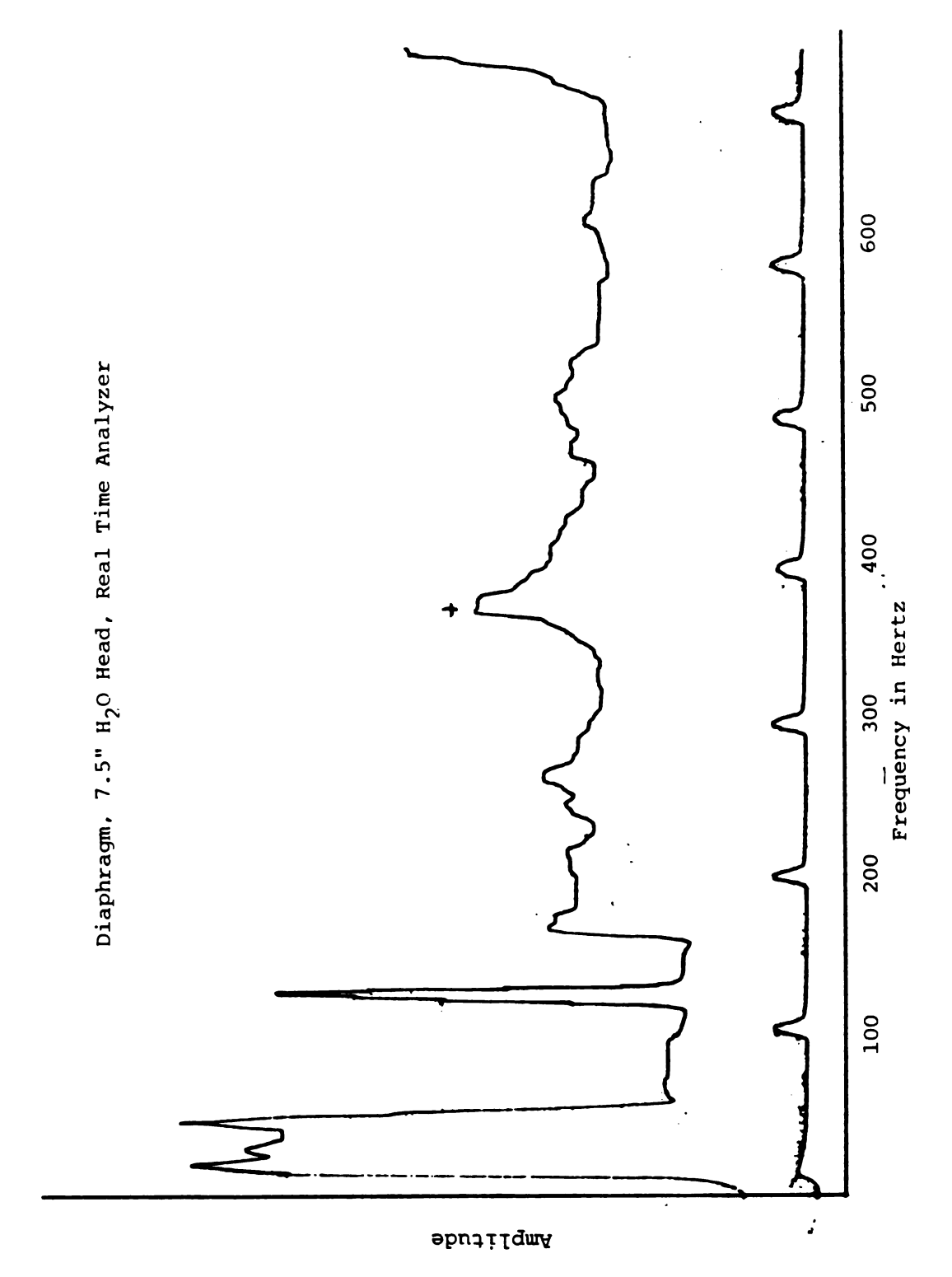


Figure 47 Normal Response Plot, Set Up #3, 7.5"  $\mathrm{H}_2\mathrm{O}$ 

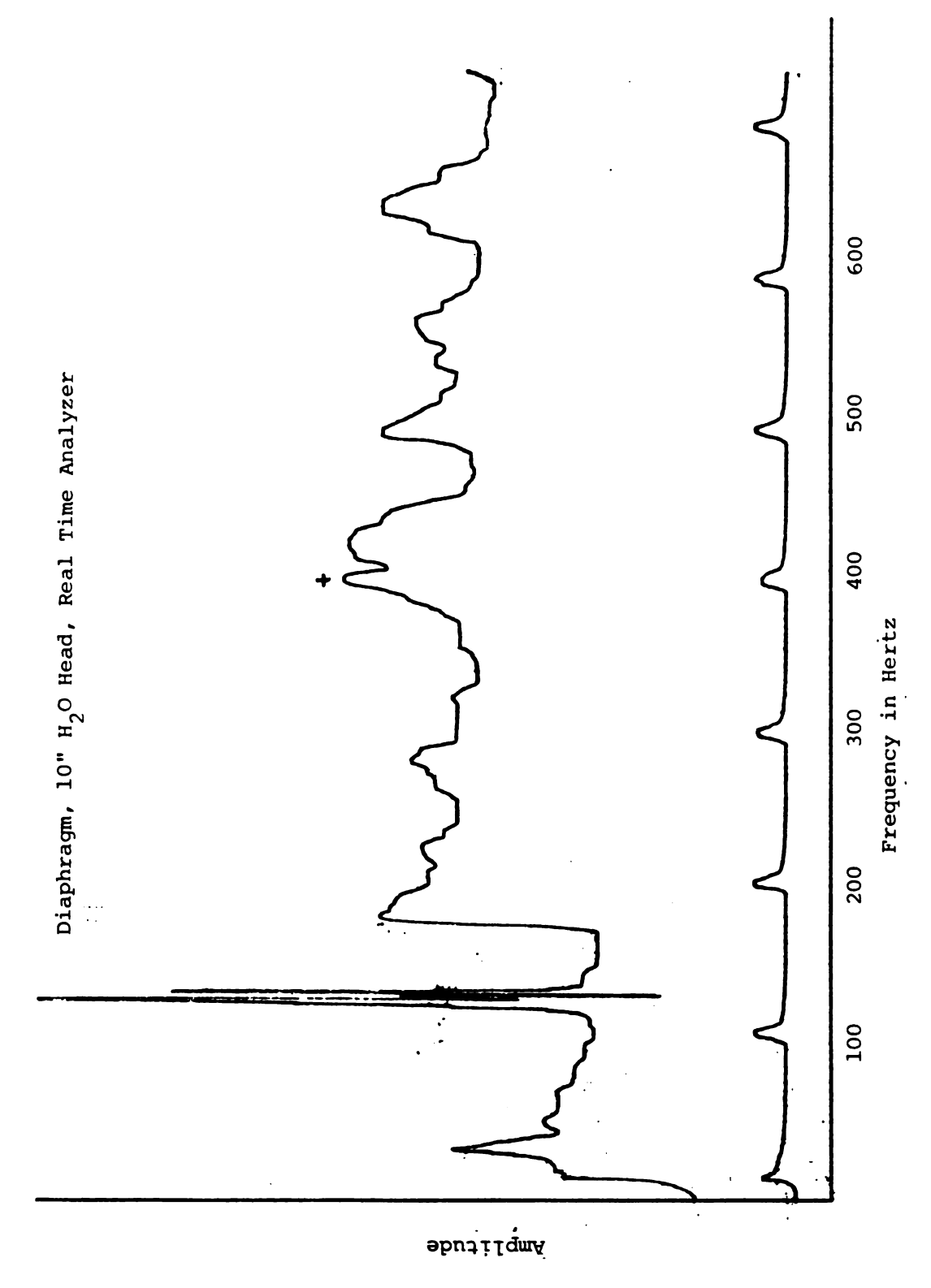


Figure 48 Normal Response Plot, Set Up #3, 10"  $\mathrm{H}_2\mathrm{O}$ 

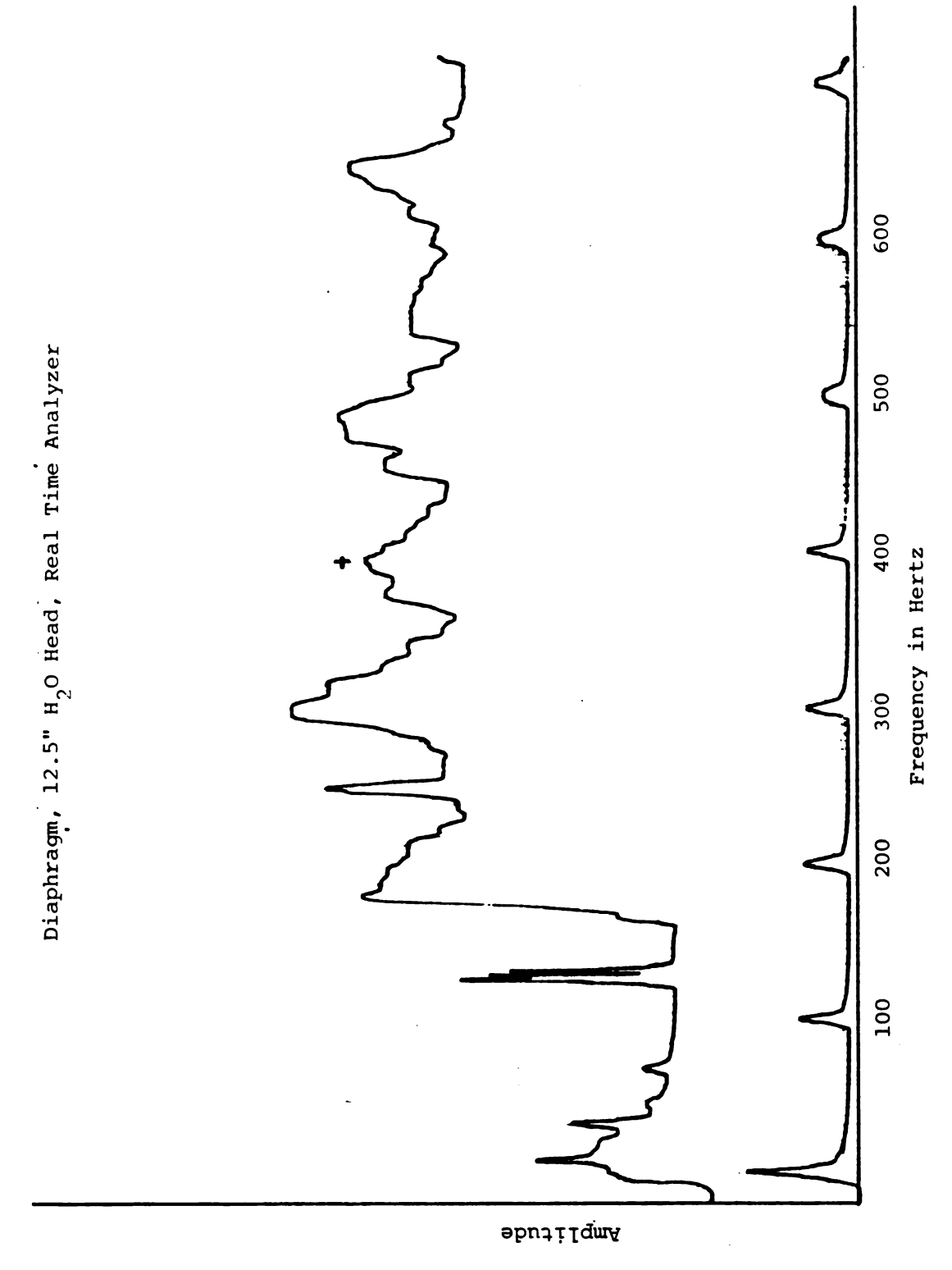


Figure 49 Normal Response Plot, Set Up #3, 12.5"  $\rm H_2O$ 

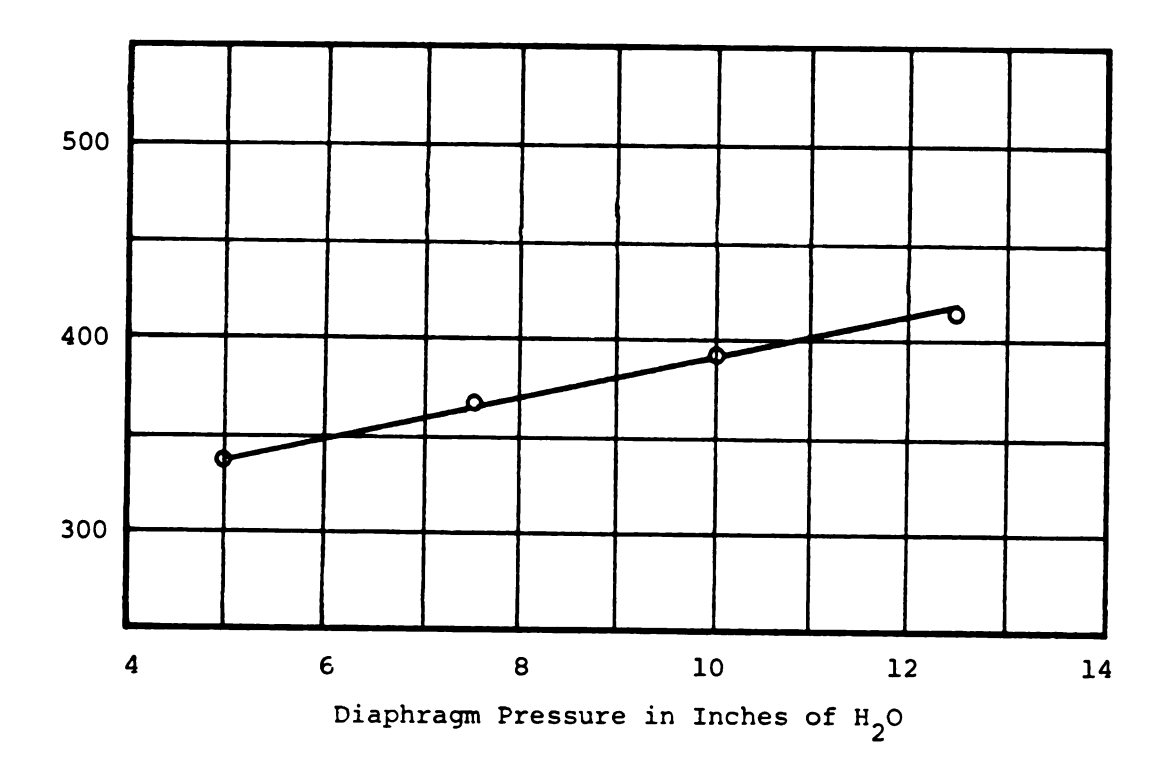


Figure 50 Frequency-IOP Plot, Set Up #3

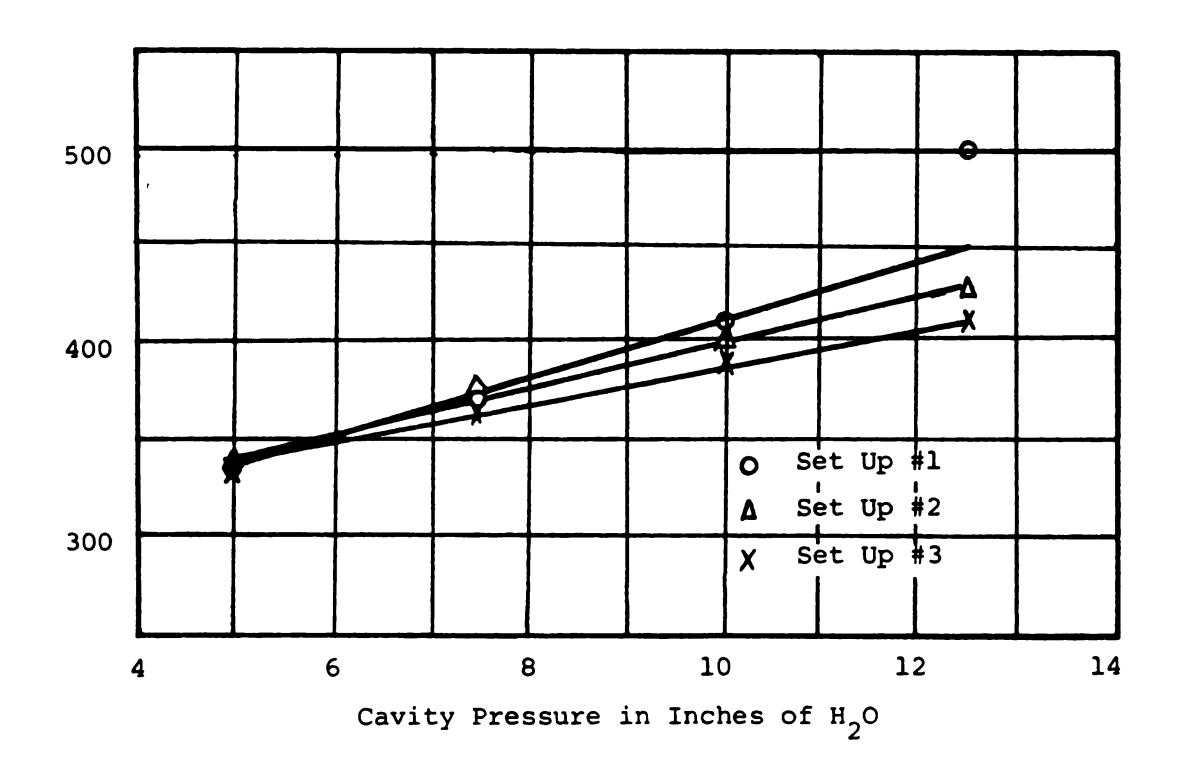


Figure 51 Set Ups in Comparison

- 2. Adjustments are manual (while exact frequencies could be dialed and held, considerable time was required to make measurements).
- 3. Data are in correct format.
- 4. Input signal is in correct format.
- 5. Equipment is readily available.
- 6. Large input energy in discrete frequency bands is available.

# Set Up #2

- 1. Procedure is easy to use.
- 2. Adjustments are automatic or manual.
- 3. Data are in correct format.
- 4. Input signal is in correct format.
- 5. Equipment is available.
- 6. Sufficient input signal strength was not available in any discrete frequency.

## Set Up #3

- Procedure is easy to use once the system is operational.
- 2. Adjustments are automatic.
- 3. Data are in correct format.
- 4. Input signal is in correct format.

- 5. Equipment scheduling is difficult.
- 6. Sufficient input signal strength was not available in any discrete frequency.

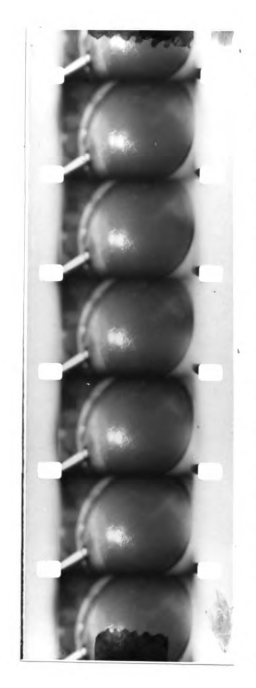
All of the experimental set ups evaluated have limitations. However, all three set ups were adequate with the experimental model. Since Set Up #1 had superior signal strength and its procedure could be optimized to reduce the time required to obtain a set of data from hours to minutes, it was selected for invitro measurements in this investigation.

## 5.6 High-Speed Film Study of Proposed Tonometer System

High-speed movies were taken of the proposed tonometer system to determine if the system caused any visually observable physical disturbances to the eye being tested as did the clinical systems presented in Sections 4.1.2 - 4.1.4. Since no applanation took place, no observable evidence was expected. Figure 52 is a high-speed film clip of an eye being examined by the proposed tonometer system.

See Figure 53 for an enlargement of one frame of Figure 52. Even with an enlargement, no physical evidence of eye deformation can be observed.

The high-speed clip shown is of an invitro lamb eye. While work was done invivo with the proposed system on dogs (see Chapter 8), high-speed films were not taken



High-Speed Film Clip of the Proposed Tonometer System Figure 52



Figure 53 Enlargement of a Frame from Figure 52

of this work because the photographer and equipment were unavailable at that time. It was felt while IOP comparisons between live and dead eyes could not be made, observable physical disturbances such as those that would be recorded on film could be obtained and compared.

### 5.7 An Invitro High-Speed Study

#### 5.7.1 Introduction

Since it was desired to stimulate the cornea with a low-energy vibration that could easily be adapted to an invivo setting, a sound wave with air as the medium was considered to be ideal. However, the normal response frequency of the eye was unknown. Suppose that the time required for the eye to recover from a small air-induced dimple deformation could be measured. Twice that time then might be considered a reasonable normal response period for that eye. The inverse of this normal response period should then yield the normal response frequency. The procedure outlined in Section 5.7.2 was based on the above suppositions.

#### 5.7.2 Procedures

A Fastax high-speed movie camera with a 2" Raptar lens with extension (to give necessary field of vision) with required accessories was borrowed from General Motors Institute. The GMI camera was used since it had a timing accessory that would place 120 timing marks per

second on the edge of the film. It would then be a simple matter to count the frames between the timing marks and thereby closely determine the film speed in frames per second. A dimple was induced in the lamb cornea by a blast of air from a can of dry air.

In Figure 54 is a film clip clearly illustrating the timing marks on the edge of the film.

Since there are 5 frames between the timing marks in this film clip, an estimate of the film speed would be calculated as follows:

The film speed in this clip is approximately 600 frames per second.

If timing marks could be observed, then the lamb cornea recovery time could be determined using the following equation:

Recovery time = 
$$\frac{1}{\text{film speed (frames/second)}}$$
  
X frames to recovery (5.1)

An estimate of the normal response frequency to a vibrational input was obtained by doubling the time required for corneal recovery from an air-induced applanation dimple. No precise timing of corneal tissue



Figure 54 Film Clip Showing Timing Marks

recovery is claimed; however, it was hypothesized that these measured times would yield a satisfactory initial value. The response frequency is given by

Normal Response Frequency (NRF) = 
$$\frac{1}{\text{Recovery}}$$
 (5.2)

or

$$NRF = \frac{\text{film speed (frames/second})}{\text{frames (to recovery)}} \times 2$$
 (5.3)

A high-speed clip of a lamb cornea recovering from an air blast is shown in Figure 55. The arrows drawn on the film border point to the timing marks while the arrows drawn on the film point to the applanation dimple. The dimple appears as a faint shadow on the film.

Figure 56 shows with greater clarity the applanation dimple observed in Figure 55.

The frequency calculated was approximately 30 Hz for lamb corneas. It was felt that the 30 Hz value would be within one order of magnitude of the normal response frequency of an eye responding to a vibrational stimulus and would supply a numerical basis from which to begin.

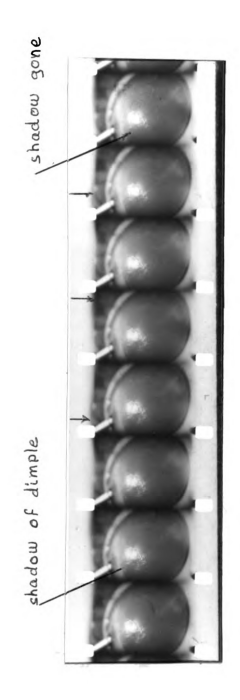


Figure 55 High-Speed Film Clip of Lamb Cornea Recovery



Figure 56 Enlargement of Applanation Dimple of Figure 55

#### CHAPTER 6

# EXPERIMENTAL EQUIPMENT AND PROCEDURES--INVITRO

#### 6.1 Experimental Fixture

The model fixture shown in Figures 27 and 29 was designed to hold the selected diaphragm and, with minor modifications, to hold an excised lamb's eye. The cup used to hold the excised eye in the loading frame was made of hot rolled steel lined with silicone rubber. The eye was held in the silicone rubber socket with white petroleum jelly both to minimize direct contact with the rubber socket and to hold the eye in position with its tenacity. It was thought that the jelly contact would not be unlike the fatty tissue contact in the invivo setting. The eye cup was clamped in place with the same ring that provided the diaphragm clamping reported in Chapter 5. See Figure 57 for the IOP control measurement system.

#### 6.2 Speciman Preparation

Eyes were obtained from humanely killed lambs in the "Meats Laboratory" of the Food Science Department at



Figure 57 IOP Control Measurement System

. . .

Michigan State University. These eyes were enucleated within an hour after death and placed immediately in warm Ringer's solution. All excised eye data presented in this dissertation came from eyes that were used immediately after removal without intermediate refrigeration. No eyes were over six hours old at the conclusion of the test. Immediately before use, the eyes were rinsed in distilled water, dried and placed in the loading frame. A twenty gage, 25 mm hypodermic needle was placed in the anterior chamber of the eye. The manometer and connective tubing were filled with distilled water. Previously, Ringer's solution was used until it was noted that it caused deposits in the tubing and brass valving.

#### 6.3 Stimulation System

Since the normal response frequency of lambs' eyes appeared to be below 1000 Hz (see Section 5.7.2), it was decided that a general purpose radio speaker operating in the audio range could provide the low energy stimulation. A sketch of the corneal stimulation system is shown in Figure 58.

A mirror fragment was glued to the cone of the selected speaker and the speaker was calibrated using the procedure described in Section 5.3. See Figure 32

<sup>\*</sup>Distilled water has been used instead of an isotonic fluid in direct pressure measurements before with no reported ill effects (33, 34).

for the calibration curve. After calibration, the speaker was placed in a wooden frame and fitted with a cone to direct the sound toward the eye. The speaker's calibration was checked and it was determined that no change in its characteristics occurred in the frequency range of interest. While it is realized that the cone did not actually focus the sound on the cornea, the db value at the corneal surface increased from 90 to 110 through the use of the cone. Fiberglass insulation was stuffed in the back of the speaker to reduce the external noise in the laboratory. Ear protection was used by the experimentor during extended testing periods. See Figure 59 for a photograph of the speaker system (page 95).

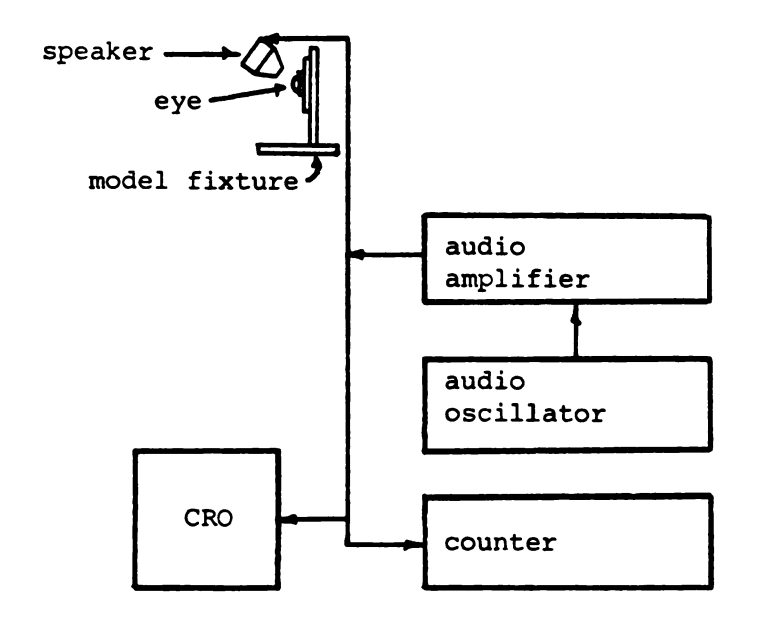


Figure 58 Corneal Stimulation System

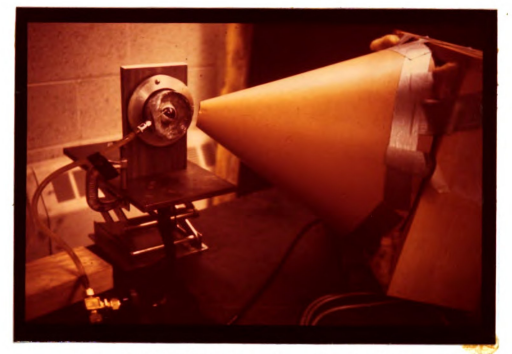


Figure 59 Cone Speaker System

The audio oscillator coupled with the audio amplifier produced an output signal that was constant throughout the frequency range investigated. The audio amplifier output curve is displayed in Figure 60.

#### 6.4 Detection System

Laser Doppler velocimetry was used to measure corneal velocities. See Figure 61 for a sketch of the instrumentation system used. It was felt that with proper signal modifiers, the Doppler method would be practical for invivo measurements for the following reasons:

- 1. Insensitive to low frequency eye movements.
- All but desired frequencies can be easily eliminated.

- 3. Can make precise measurements with conventional electronic instrumentation.
- 4. Sensitive to existing small amplitudes of corneal tissue displacement.
- 5. Will not induce blunt object trauma.

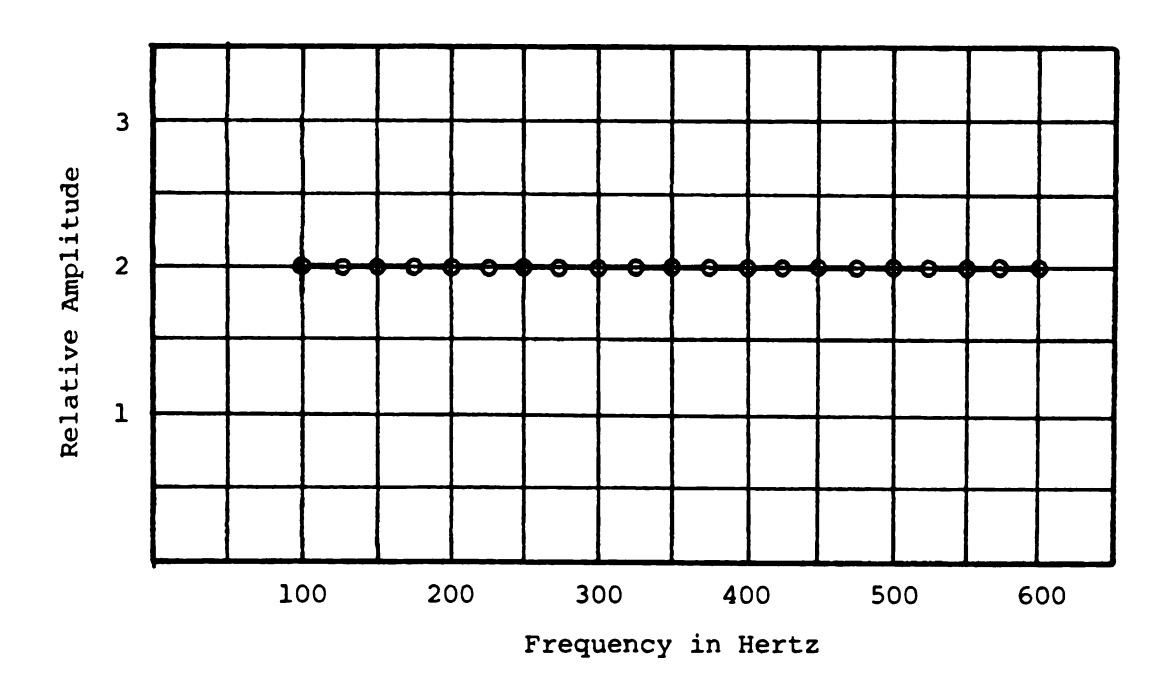


Figure 60 Audio Amplifier Output Curve

The laser used in the investigation was a Spectra Physics Model 134, 4.8 m watt Ne He laser. The Photocell unit was designed and built by G. Cloud (5) and was powered by a Harrison Laboratories No. 6204 D.C. Power Supply.

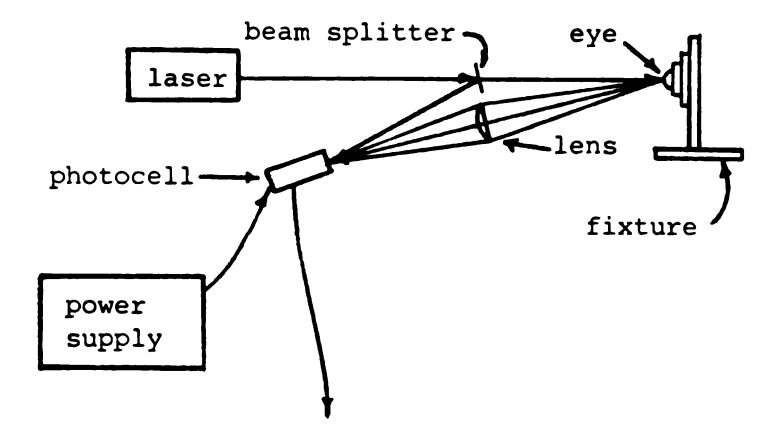


Figure 61 Laser Doppler Velocimeter

#### 6.5 Doppler Velocimeter

#### 6.5.1 Introduction

As mentioned previously, laser Doppler velocimetry was used for observation of velocity and amplitude of corneal vibrations. The basis of the laser Doppler effect is outlined below, and correlation of Doppler frequency shift with cornea vibration is established. The nature of the output of the photodetection system is derived for the apparatus configuration employed.

#### 6.5.2 Doppler Phenomenon

It is well known that the frequency of electromagnetic or acoustic radiation which would be measured
by an observer is dependent upon the velocities of the
observer and the radiation source. Attention here is
confined to the case where the source, including any
sort of mirror or scattering source, is moving and the

observer is fixed. Also only coherent light, as from a laser, is being used.

Consider the Doppler effect. If the optical path length is a constant (source stationary) as it is when the beam is reflected from a beam splitter to a photocell, relationships between the number of cycles, the wave length and the distance traveled by the laser beam can be written. Figures 62 and 63 contain the "source stationary" illustrations of the pathway and the distance/wave length relationships.

If the path length is a variable (source moving) as it is when the beam is reflected from the vibrating cornea (see Figure 64), relationships between the number of cycles and distance traveled must include the corneal velocity as illustrated in Figure 65.

Phase changes upon reflection from the nonvibrating cornea and beam splitter can be assumed constant and,
therefore, neglected, so we have after reflection for
the moving cornea,

$$n\lambda^1 = t (c - v)$$

or

$$n = \frac{t}{\lambda^{1}} (c - v)$$

where n = number of cycles

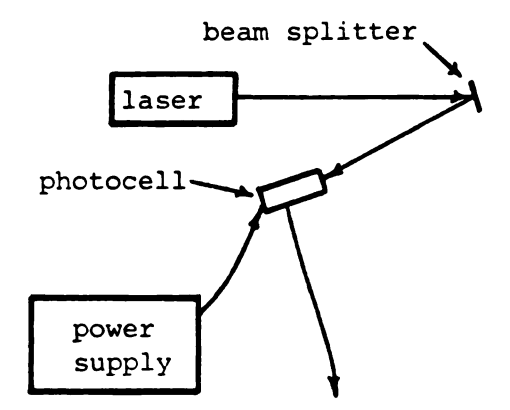


Figure 62 Source Stationary Pathway

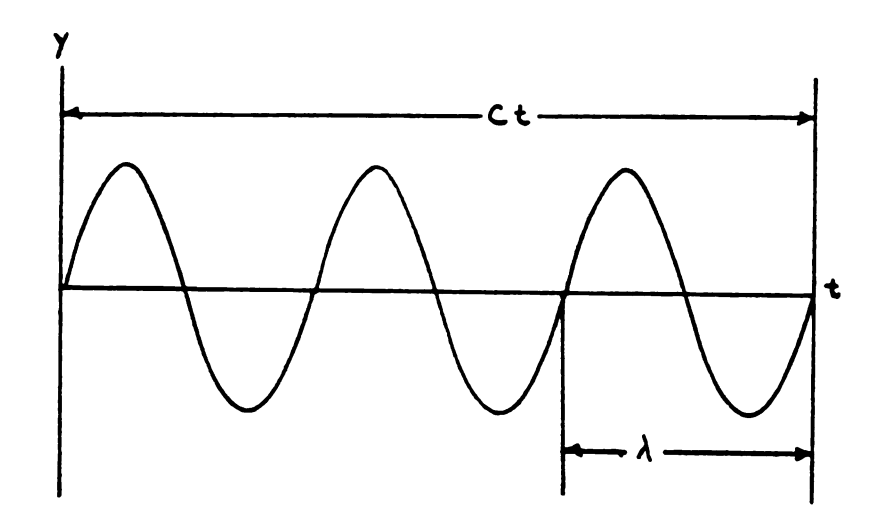


Figure 63 Source Stationary Distance/Wave Length Relationship

The wave length and wave speed are related by

$$n\lambda = ct$$
 (distance traveled =  $\lambda n$ )

or

$$n = \frac{ct}{\lambda} \tag{6.1}$$

where n = the number of cycles, c = velocity of light and <math>t = time.

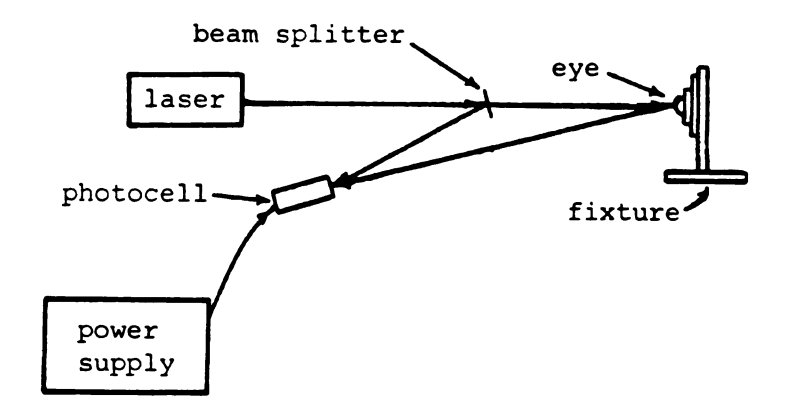


Figure 64 Source Moving Pathway

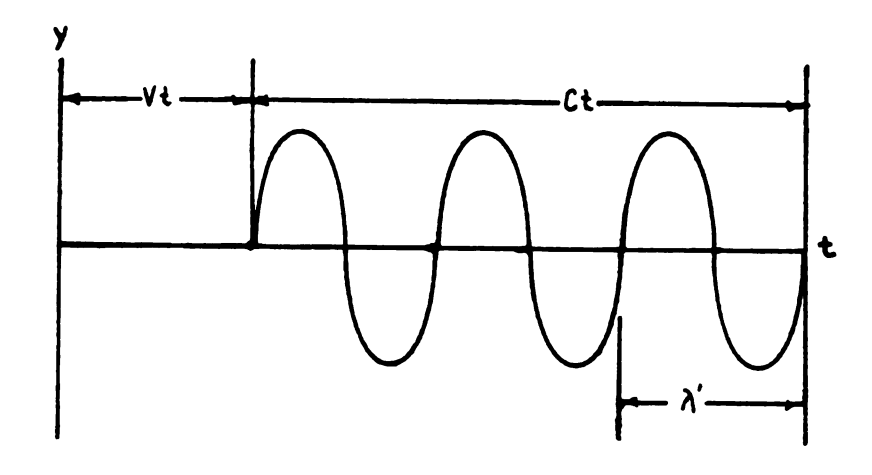


Figure 65 Source Moving, Distance/Wave Length Relationship

When considering both the incident and reflected beams, the equation becomes

$$n = \frac{t}{\lambda^{1}} (c - 2v) \tag{6.2}$$

If 
$$f = \frac{c}{\lambda}$$
, then  $f^1 = \frac{c}{\lambda^1}$  and  $\lambda^1 = \frac{c}{f^1}$ 

Substitute  $\lambda^1 = \frac{c}{f^1}$  into equation 6.2 yielding

$$n = \frac{t}{\frac{c}{f^1}} (c - 2v)$$

or

$$n = \frac{tf^{1}}{c} (c - 2v) \tag{6.3}$$

Also, if  $f = \frac{c}{\lambda}$  is substituted into equation 6.1,

$$n = ft ag{6.4}$$

Now, combining equations 6.3 and 6.4 yields

$$ft = tf^{1} (1 - \frac{2v}{c})$$

or

$$f = f^1 \left(1 - \frac{2v}{c}\right)$$

This is rearranged to give

$$f^{1} = \frac{f}{\left(1 - \frac{2v}{c}\right)} \tag{6.5}$$

Equation 6.5 can be written as follows:

$$f^{1} = \frac{f}{(1 - \frac{2v}{c})(1 + \frac{2v}{c})} = \frac{f(1 + \frac{2v}{c})}{1 - \frac{4v^{2}}{c^{2}}}$$
 if  $c >> v$ 

We know that

$$\frac{4v^2}{c^2} \longrightarrow 0$$

so that

$$f^1 \longrightarrow f (1 + \frac{2v}{c})$$

Finally, we use the approximation

$$f^{1} \simeq f \left(1 + \frac{2v}{c}\right) \tag{6.6}$$

where f = frequency of wave from cornea, v = velocity of corneal surface and c = laser light velocity.

The beat frequency is simply the difference between the frequency of the wave from the beam splitter and the frequency of the wave from the corneal surface. That is,

$$\Delta f = f^1 - f$$

or, with equation 6.6

$$\Delta f = f \left(1 + \frac{2v}{c}\right) - f$$

$$= \frac{2v}{c} f$$
(6.7)

Since c = constant (laser light velocity), the beat frequency is a direct function of corneal velocity.

Thus it is shown that the frequency of radiation as would be observed depends upon the velocity of the corneal surface and would provide an approach to measuring the velocity in a noncontacting way. In general, it is not possible to observe optical frequencies with sufficient accuracy in a direct way. An effective method is to mix the light from the moving scattering source with a reference beam from the laser and to measure the frequency of the beat which will be generated by a photo detector.

6.5.3 Measurement of Doppler Frequency Shift
Consider the optical system shown in Figure 66
below.

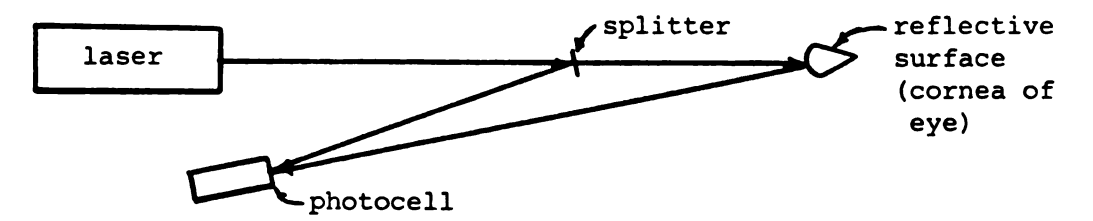


Figure 66 Simple Doppler Frequency Shift Measurement Apparatus

See Figure 67 for a sketch of the incoming waves to the photo diode.

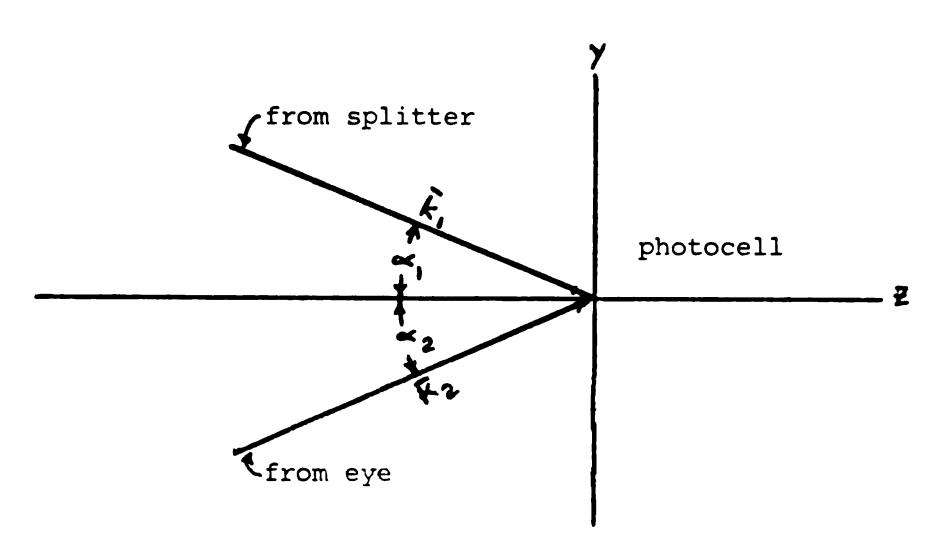


Figure 67 Incoming Waves to Photo Diode

The wave numbers are given by

$$\overline{k}_1 = \frac{2\pi}{\lambda_1} \hat{\alpha}_1$$
,  $\overline{k}_2 = \frac{2\pi}{\lambda_2} \hat{\alpha}_2$ , and  $\alpha_1 = -\alpha_2$ 

In complex algebra, the amplitude of the incoming waves defined by wave vectors  $\overline{k}_1$  and  $\overline{k}_2$  can be expressed as

$$E_{1} = R_{e} e^{i\overline{k}_{1} \cdot \overline{r}} e^{i\omega_{1}t} = \frac{1}{2} (e^{i\overline{k}_{1} \cdot \overline{r}} e^{i\omega_{1}t} + e^{-i\overline{k}_{1} \cdot \overline{r}}$$

$$e^{-i\omega_{1}t})$$

$$E_{2} = R_{e} e^{i\overline{k}_{2} \cdot \overline{r}} e^{i\omega_{2}t} = \frac{1}{2} (e^{i\overline{k}_{2} \cdot \overline{r}} e^{i\omega_{2}t} + e^{-i\overline{k}_{2} \cdot \overline{r}}$$

$$e^{-i\omega_{2}t})$$

So at the photocell, where  $\mathbf{E}_1$  and  $\mathbf{E}_2$  are joined,

$$E_p = E_1 + E_2 = \frac{1}{2} (e^{i\overline{k}} 1^{\cdot \overline{r}} e^{i\omega} 1^t + e^{-i\overline{k}} 1^{\cdot \overline{r}} e^{-i\omega} 1^t)$$

$$+ \frac{1}{2} \left( e^{i\overline{k}} 2 \cdot \overline{r} e^{i\omega} 2^{t} + e^{-i\overline{k}} 2 \cdot \overline{r} e^{-i\omega} 2^{t} \right)$$

$$E_{p} = \frac{1}{2} \left[ e^{i\overline{k}} 1 \cdot \overline{r} e^{i\omega} 1^{t} + e^{-i\overline{k}} 1 \cdot \overline{r} e^{-i\omega} 1^{t} + e^{i\overline{k}} 2 \cdot \overline{r} e^{i\omega} 2^{t} + e^{-i\overline{k}} 2 \cdot \overline{r} e^{-i\omega} 2^{t} \right]$$

Since the intensity is the square of the amplitude and the photocell responds to the time average, it can be written as

$$I_p = \langle E_p E_p^* \rangle$$

where < > designates the time average

$$= |_{\overline{k}} \left[ (e^{i\overline{k}}1 \cdot \overline{r} e^{i\omega_1 t})^2 + (e^{-i\overline{k}}1 \cdot \overline{r} e^{-i\omega_1 t})^2 \right.$$

$$+ (e^{i\overline{k}}2 \cdot \overline{r} e^{i\omega_2 t})^2 + (e^{-i\overline{k}}2 \cdot \overline{r} e^{-i\omega_2 t})^2$$

$$+ (e^{i\overline{k}}1 \cdot \overline{r} e^{i\omega_1 t}) (e^{-i\overline{k}}1 \cdot \overline{r} e^{-i\omega_1 t})$$

$$+ (e^{i\overline{k}}1 \cdot \overline{r} e^{i\omega_1 t}) (e^{i\overline{k}}2 \cdot \overline{r} e^{i\omega_2 t})$$

$$+ (e^{i\overline{k}}1 \cdot \overline{r} e^{i\omega_1 t}) (e^{-i\overline{k}}2 \cdot \overline{r} e^{-i\omega_2 t})$$

$$+ (e^{-i\overline{k}}1 \cdot \overline{r} e^{-i\omega_1 t}) (e^{i\overline{k}}2 \cdot \overline{r} e^{-i\omega_2 t})$$

$$+ (e^{-i\overline{k}}1 \cdot \overline{r} e^{-i\omega_1 t}) (e^{i\overline{k}}2 \cdot \overline{r} e^{i\omega_2 t})$$

$$+ (e^{-i\overline{k}}1 \cdot \overline{r} e^{-i\omega_1 t}) (e^{i\overline{k}}2 \cdot \overline{r} e^{i\omega_2 t})$$

$$+ (e^{-i\overline{k}}1 \cdot \overline{r} e^{-i\omega_1 t}) (e^{-i\overline{k}}2 \cdot \overline{r} e^{-i\omega_2 t})$$

$$+ (e^{i\overline{k}}2 \cdot \overline{r} e^{-i\omega_2 t}) (e^{i\overline{k}}1 \cdot \overline{r} e^{-i\omega_1 t})$$

+ 
$$(e^{i\overline{k}_2 \cdot \overline{r}} e^{i\omega_2 t}) (e^{-i\overline{k}_1 \cdot \overline{r}} e^{-i\omega_1 t})$$
  
+  $(e^{i\overline{k}_2 \cdot \overline{r}} e^{i\omega_2 t}) (e^{-i\overline{k}_2 \cdot \overline{r}} e^{-i\omega_2 t})$   
+  $(e^{-i\overline{k}_2 \cdot \overline{r}} e^{-i\omega_2 t}) (e^{i\overline{k}_1 \cdot \overline{r}} e^{i\omega_1 t})$   
+  $(e^{-i\overline{k}_2 \cdot \overline{r}} e^{-i\omega_2 t}) (e^{-i\overline{k}_1 \cdot \overline{r}} e^{-i\omega_1 t})$   
+  $(e^{-i\overline{k}_2 \cdot \overline{r}} e^{-i\omega_2 t}) (e^{i\overline{k}_2 \cdot \overline{r}} e^{i\omega_2 t})]$ 

where  $E_{p}^{*}$  represents the complex conjugate of  $E_{p}$ 

The various terms are multiplied as indicated to give

$$\begin{split} \mathbf{I}_{p} &= \left| \frac{1}{4} \left[ (e^{2i\overline{k}}\mathbf{1} \cdot \overline{r} \ e^{2i\omega_{1}t}) \ + \ (e^{-2i\overline{k}}\mathbf{1} \cdot \overline{r} \ e^{-2i\omega_{1}t}) \right. \\ &+ \ (e^{2i\overline{k}}\mathbf{2} \cdot \overline{r} \ e^{2i\omega_{2}t}) \ + \ (e^{-2i\overline{k}}\mathbf{2} \cdot \overline{r} \ e^{-2i\omega_{2}t}) \\ &+ \ (e^{\circ}e^{\circ}) \ + \ (e^{i(\overline{k}}\mathbf{1} + \overline{k}\mathbf{2}) \cdot \overline{r} \ e^{i(\omega_{1} + \omega_{2})t}) \\ &+ \ (e^{i(\overline{k}}\mathbf{1} - \overline{k}\mathbf{2}) \cdot \overline{r} \ e^{i(\omega_{1} - \omega_{2})t}) \ + \ (e^{\circ}e^{\circ}) \\ &+ \ (e^{i(\overline{k}}\mathbf{2} - \overline{k}\mathbf{1}) \cdot \overline{r} \ e^{i(\omega_{2} - \omega_{1})t}) \\ &+ \ (e^{-i(\overline{k}}\mathbf{1} + \overline{k}\mathbf{2}) \cdot \overline{r} \ e^{-i(\omega_{1} + \omega_{2})t}) \\ &+ \ (e^{i(\overline{k}}\mathbf{2} + \overline{k}\mathbf{1}) \cdot \overline{r} \ e^{i(\omega_{2} - \omega_{1})t}) \\ &+ \ (e^{i(\overline{k}}\mathbf{2} - \overline{k}\mathbf{1}) \cdot \overline{r} \ e^{i(\omega_{2} - \omega_{1})t}) \ + \ (e^{\circ}e^{\circ}) \\ &+ \ (e^{i(\overline{k}}\mathbf{1} - \overline{k}\mathbf{2}) \cdot \overline{r} \ e^{i(\omega_{1} - \omega_{2})t}) \\ &+ \ (e^{-i(\overline{k}}\mathbf{2} + \overline{k}\mathbf{1}) \cdot \overline{r} \ e^{-i(\omega_{2} + \omega_{1})t}) \ + \ (e^{\circ}e^{\circ}) \right] \end{split}$$

Collecting terms we have

$$\begin{split} I_{p} &= | \frac{1}{4} \left[ (e^{2i\overline{k}_{1} \cdot \overline{r}} e^{2i\omega_{1}t}) + (e^{-2i\overline{k}_{1} \cdot \overline{r}} e^{-2i\omega_{1}t}) \right. \\ &+ (e^{2i\overline{k}_{2} \cdot \overline{r}} e^{2i\omega_{2}t}) + (e^{-2i\overline{k}_{2} \cdot \overline{r}} e^{-2i\omega_{2}t}) \\ &+ 2(e^{i(\overline{k}_{1}} + \overline{k}_{2}) \cdot \overline{r} e^{i(\omega_{1}} + \omega_{2})t) \\ &+ 2(e^{i(\overline{k}_{1}} - \overline{k}_{2}) \cdot \overline{r} e^{i(\omega_{1}} - \omega_{2})t) \\ &+ 2(e^{i(\overline{k}_{2}} - \overline{k}_{1}) \cdot \overline{r} e^{i(\omega_{2}} - \omega_{1})t) \\ &+ 2(e^{-i(\overline{k}_{1}} + \overline{k}_{2}) \cdot \overline{r} e^{-i(\omega_{1}} + \omega_{2})t) + 4 \right] | \end{split}$$

Since the terms involving the difference between frequencies contribute to the "beat" while the sum terms do not, the sum terms will be omitted at this time. The sum terms are at too high a frequency to be observed and simply add a D.C. bias.

$$I_{p} = k + | \frac{1}{2} e^{i(\overline{k}_{1} - \overline{k}_{2}) \cdot \overline{r}} e^{i(\omega_{1} - \omega_{2})t}$$

$$+ \frac{1}{2} e^{i(\overline{k}_{2} - \overline{k}_{1}) \cdot \overline{r}} e^{i(\omega_{2} - \omega_{1})t} |$$

$$= k + | \frac{1}{2} e^{i(\overline{k}_{1} - \overline{k}_{2}) \cdot r} e^{i(\omega_{1} - \omega_{2})t}$$

$$+ \frac{1}{2} e^{-i(\overline{k}_{1} - \overline{k}_{2})} e^{-i(\omega_{1} - \omega_{2})t} |$$

$$= k + \cos [(\overline{k}_{1} - \overline{k}_{2}) \cdot r + (\omega_{1} - \omega_{2})t]$$

$$= k + \cos (\overline{k}_{1} - \overline{k}_{2}) \cdot r \cos (\omega_{1} - \omega_{2})t$$

$$- \sin (\overline{k}_{1} - \overline{k}_{2}) \cdot r \sin (\omega_{1} - \omega_{2})t$$

since  $\omega=2\pi f_1$ ,  $\overline{k}_1=\frac{2\pi\hat{\alpha}_1}{\lambda_1}$  and  $\overline{k}_2=\frac{2\pi\hat{\alpha}_2}{\lambda_2}$ . This is put in the form

$$I_{p} = k + \cos \left(\frac{2\pi\hat{\alpha}_{1}}{\lambda_{1}} - \frac{2\pi\hat{\alpha}_{2}}{\lambda_{2}}\right) \cdot \overline{r} \cos \left(2\pi f_{1} - 2\pi f_{2}\right) t$$

$$- \sin \left(\frac{2\pi\hat{\alpha}_{1}}{\lambda_{1}} - \frac{2\pi\hat{\alpha}_{2}}{\lambda_{2}}\right) \cdot \hat{r} \sin \left(2\pi f_{1} - 2\pi f_{2}\right) t$$

Taking the scaler product of the unit vectors  $\overline{\alpha}_1$  and  $\overline{\alpha}_2$  with the position vector  $\overline{r}$  at the photocell surface where x=z=o,

$$I_{p} = \cos \left(\frac{2\pi\alpha_{1}y}{\lambda_{1}} - \frac{2\pi\alpha_{2}y}{\lambda_{2}}\right) \cos \left(2\pi f_{1} - 2\pi f_{2}\right)t$$

Hence, we have

- 
$$\sin \left(\frac{2\pi\alpha_1 y}{\lambda_1} - \frac{2\pi\alpha_2 y}{\lambda_2}\right) \sin \left(2\pi f_1 - 2\pi f_2\right) t$$

since  $\alpha_1 = -\alpha_2$ . Using the appropriate trigometric identity, there results

$$I_{p} = k + \cos 2\pi \left(\frac{\alpha_{1}}{\lambda_{1}} + \frac{\alpha_{1}}{\lambda_{2}}\right) y \cos 2\pi (f_{1} - f_{2}) t$$

$$- \sin 2\pi \left(\frac{\alpha_{1}}{\lambda_{1}} + \frac{\alpha_{1}}{\lambda_{2}}\right) y \sin 2\pi (f_{1} - f_{2}) t$$

$$= k + \cos 2\pi\alpha_{1} \left( \frac{1}{\lambda_{1}} + \frac{1}{\lambda_{2}} \right) y \cos 2\pi (f_{1} - f_{2}) t$$

$$- \sin 2\pi\alpha_{1} \left( \frac{1}{\lambda_{1}} + \frac{1}{\lambda_{2}} \right) y \sin 2\pi (f_{1} - f_{2}) t$$

$$= k + \cos 2\pi\alpha_{1} \left( \frac{f_{1}}{c} + \frac{f_{2}}{c} \right) y \cos 2\pi (f_{1} - f_{2}) t$$

$$- \sin 2\pi\alpha_{1} \left( \frac{f_{1}}{c} + \frac{f_{2}}{c} \right) y \sin 2\pi (f_{1} - f_{2}) t$$

$$= k + \cos \frac{2\pi\alpha_{1}}{c} (f_{1} + f_{2}) y \cos 2\pi (f_{1} - f_{2}) t$$

$$- \sin \frac{2\pi\alpha_{1}}{c} (f_{1} + f_{2}) y \sin 2\pi (f_{1} - f_{2}) t$$

The frequency sum terms are at optical frequencies that would not be detected by the photocell except as a total flooding at some intensity I'. Since the contribution by those terms would not affect the photo detector output (except as a d-c bias), for clarity, those terms will be represented by a constant  $k_1$  or  $k_2$ . This results in

$$I_{p} = k + k_{1} \cos 2\pi (f_{1} - f_{2})t$$

$$- k_{2} \sin 2\pi (f_{1} - f_{2})t \qquad (6.8)$$

The photo diode responds to the light input or moving fringe pattern generating an output which can be represented by the integral of the intensity.

Output = 
$$k + k_3 \sin 2\pi (f_1 - f_2)t$$
  
+  $k_4 \cos 2\pi (f_1 - f_2)t$  (6.9)

where  $k_3$  and  $k_4$  are new constants. The frequency difference ( $f_1 - f_2$ ) is a "beat" frequency which can be detected by a photo diode output. See Figure 68 for a sketch of the photo diode output.

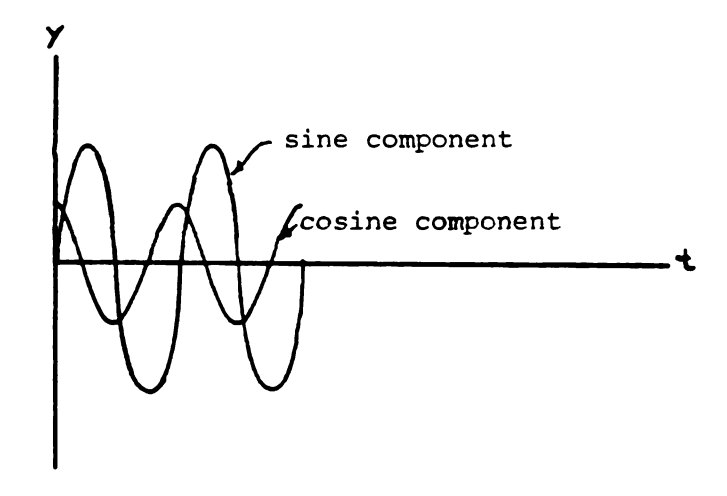
 $\Delta f$  is the difference in optical frequency between the two paths and is the "beat" frequency. Referring to Equation 6.7 one can see that this frequency is the corneal response frequency.

Observations that can be made at this time include the following:

- Beat frequencies will occur at any frequencies to which the eye will respond.
- 2. The "beat" signal will be detected by a photocell.
- 3. The photocell need have a frequency response only through the range of excitation frequencies (it need not respond at frequencies of light).

## 6.6 Modifier System

Modifier systems were evaluated for possible use in invitro and invivo tests as reported in Chapters 5 and 8. In the following discussion, reasons for the various modifiers used are presented.



The combined output in equation form can be written as:

Output = 
$$k + \sqrt{k_3 + k_4} \cos [2\pi (f_1 - f)t - \phi]$$
 (6.10)

where  $(f_1 - f_2) = \Delta f$  and  $\phi$  is the phase shift as shown by the graphical representation of equation 6.10.

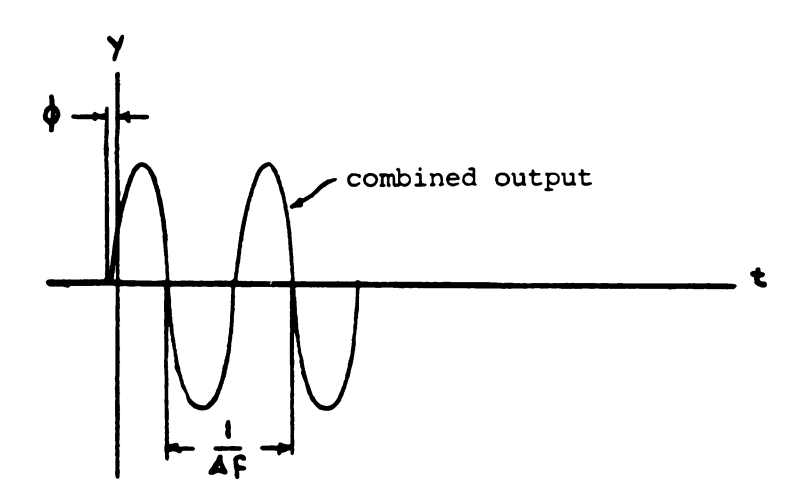


Figure 68 Component and Combined Output from Photo Diode

A Tektronix Type O operational amplifier was used to amplify the signal output from the photocell. In Experimental Set Up #1 (Figure 33) a Krohn-Hite model 335 R variable filter was used in the band pass mode to eliminate extraneous frequencies. A limitation of the Krohn-Hite unit was that the low pass and high pass filter slopes were not steep enough for effective separation of the noise from the signal. The low pass and high pass frequencies of the Krohn-Hite unit were adjusted to the audio oscillator frequency and were swept through the frequency range of interest in unison manually. The variable filter characteristics of the unit are presented in Figure 69.

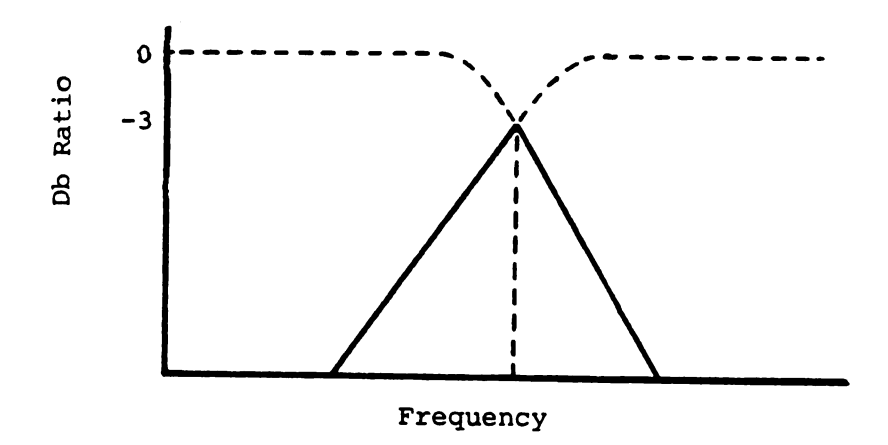


Figure 69 Variable Filter Characteristics in the Band Pass Mode

When the low pass and high pass frequencies of the variable filter were tuned to the oscillator frequency, the nonlinearity due to roll off was eliminated. Also, since the oscillator was adjusted to the mid-frequency of the band pass range of the filter, minimum (zero) phase change should occur between input and output signals due to instrumentation. Phase variation between input and output signals might be a key issue in the determination of normal response frequencies of the cornea in invivo tests with specially designed sweep oscillators and tracking filters. See Figure 70 for a sketch of the signal modifier system.

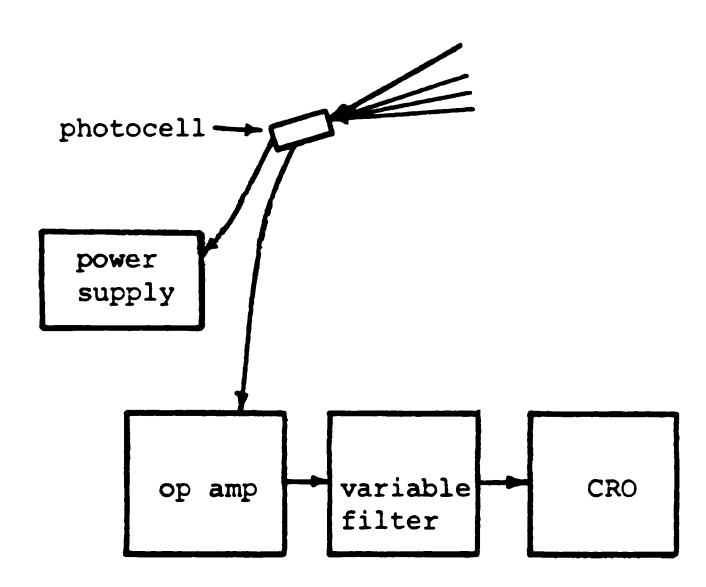


Figure 70 Signal Modifier System

The output from the variable filter was the input to the Tektronix 551 CRO where final signal modification took place. The CRO also served as the readout in Experimental Set Up #1.

#### 6.7 Experimental Procedures

The procedures developed for invitro IOP measurement were patterned after those developed for the diaphragm model presented in Section 5.3.

All eye data reported in the investigation were obtained from freshly excised lambs' eyes. The eyes were removed in about one minute each using the instruments shown in Figure 71 and the procedure outlined below. The procedure for eye removal was:

- Snip the inner lid tissue from a portion of the eye with the curved scissors.
- 2. Clamp an orbital muscle with the clamp.
- 3. Insert curved scissors between lid and eye and snip around eye, severing eye from socket holding eye stationary with clamp.
- 4. When eye appears to be loose, place curved scissors behind eye globe and bring eye out until it can be grasped with two fingers.
- Finish trimming orbital muscles, inner eye lid and optic nerve.
- 6. Remove eye and place in Ringer's solution.



Figure 71 Instruments for Eye Removal

Before a series of tests was performed, all equipment was turned on and allowed to come to operating temperature. The room air conditioner and humidifier were turned on to maintain the room at approximately 20°C and 40% relative humidity to minimize temperature and humidity effects on the eyes.

When all equipment was in operation and warmed up, an eye was selected, rinsed in distilled water, the posterior globe dried and the eye placed in the loading fixture. A hypodermic needle was then carefully inserted into the anterior chamber of the eye. The needle was connected to the manometer by a tubing and valve system. Any tubing in the neighborhood of the eye was supported

to eliminate corneal loading. The speaker cone was placed within a few centimeters of the eye. The laser was then trained on the eye. Adjustments were made in the positions of the beam splitter, collimating lens and model frame to obtain the proper balance at the photocell between the two optic paths. Proper balance was assumed to be attained between the pathways when a maximum output was recorded on the CRO for a given signal input. A double check was made on the eye to insure no leaking at the needle and no wrinkles in the cornea indicating corneal loading. The valve between the manometer and eye was opened. The following procedure was adhered to initially:

- Distilled water was added to the manometer to a predetermined level.
- Frequency of the audio oscillator was adjusted to 100 Hz.
- 3. The variable filter's high and low pass roll off frequencies were adjusted to the audio oscillator frequency.
- 4. The output amplitude of the photocell was obtained from the CRO.
- 5. The audio oscillator was then adjusted to the previous reading plus 10 Hz (except in the

immediate neighborhood of the corneal normal response frequency where the exact frequency was dialed\*).

6. Repeat steps 3 - 6.

Water was then added to the manometer and a completely new set of tests was run following procedures 2 - 6.

After a degree of familiarity with the response frequency range of the eye was developed, an abbreviated procedure was followed. The new procedure was:

- Distilled water was added to the manometer to a predetermined level.
- 2. Frequency of the audio oscillator and the variable filter's high and low pass roll off frequencies were tuned in unison to the corneal normal response frequency as evidenced by a maximum output on the CRO (performed 5 times for each eye at each IOP).

Water was then added to the manometer and procedure 2 was rerun for each IOP. A photograph of the IOP measurement apparatus is included in Figure 72.

The exact frequency (or as close to exact as possible) was dialed because the normal response frequency might land somewhere between the two measured frequencies if the 10 Hz criteria were to be adhered to. Since the frequency range of interest was approximately 5 Hz, the entire range of frequencies could have been omitted.



Figure 72 Invitro IOP Measurement Apparatus

The abbreviated procedure reduced the amount of time required to obtain a set of data from several hours to several minutes with no loss of necessary information or data quality. This procedure was used to obtain all data on excised eyes reported in the investigation.

#### CHAPTER 7

#### DATA ANALYSIS AND RESULTS

### 7.1 Data Analysis

All data reported in this dissertation were obtained from freshly excised lambs' eyes using the procedure described in Section 6.7. The data are presented in Table 2. The presented data were obtained from two days of experimentation. Data from April 22, 1976 appear to have less variance than the data of March 9, 1976 which were assumed to be a function of the increased skill of the experimenter. However, both sets of data were treated equally and the results presented and conclusions drawn are from all the data.

Referring to the data of March 9 and April 22, it can be noted that an odd number of eyes was reported on each occasion. Since it is well known that eyes come in pairs in lambs, a word of explanation seems necessary. In both instances, air was mistakenly introduced into the anterior chamber of an eye. Even when the amount of air introduced was small, it affected the normal response frequencies of the eyes significantly. For this reason,

Table 2 Mean Frequencies for Lamb Eye Data

65°F 40%	40% relative humidity	humidity		March 9,	, 1976						
Eyes 1 hr	hr. old at	at beginning	of test	(10:30 A.M.)	м.)						
IOP	Eye #1	Eye #2	Eye #3	Eye #4	Eye #5	Eye #6	Eye #7	Eye #8	Eye #9	Eye #10 Eye	e #11
5" H <sub>2</sub> 0	243	241	242	244	242	243	242	242	244		
	242	243	242	243	243	243 243	243	243	243		
	243	243	243	242	243	243	243	243	244		
	243	244	242	243	244	244	243	243	244		
mean Hz	242.6	242.8	242.4	243.2	243.2	243.2	242.8	242.8	243.8		
10" H <sub>2</sub> 0	243	245	243	244	245	244	244	245	245		
7	244	245	244	246	245	245	245	244	245		
	244	245	244	245	245	245	245	245	244		
	244	245	243	245	245	245	245	245	245		
	244	244	243	245	245	245	245	245	245		
mean Hz	243.8	244.8	243.4	245	245	244.8	244.8	244.8	244.8		
15" H <sub>2</sub> 0	245	246	244	247	246	245	245	247	246		
	245	247	244	246	246	245	246	248	245		
	244	246	244	246	246	246	247	247	246		
	245	246	245	247	246	246	246	247	246		
	244	247	245	247	246	245	246	248	246		
mean Hz	244.6	246.4	244.4	246.6	246	245.4	246	247.4	245.8		

Table 2 (Continued)

65°F 40%	relative	40% relative humidity		March 9,	1976						
Eyes 1 hr	hr. old at	at beginning of	test	(10:30 A.M.)	M.)						
IOP	Eye #1	Eye #2	Eye #3	Eye #4	Eye #5	Eye #6	Eye #7	Eye #8	Eye #9	Eye #10	Eye #11
25" H <sub>2</sub> 0	246	247	246	248	247	246 246	247	248	247		
	245	248	246	250	248	246	247	248	248		
	245 246	248 248	247 248	250 250	249 248	246 246	246 246	248 247	248 248		
mean Hz	245.6	247.6	246.8	249.4	247.8	246	246.6	248	247.8		
35" H <sub>2</sub> 0	246	250	249	252	251	247	248	248	249		
1	246 247	250 251	249 249	251 252	250 251	248 246	248 247	249 248	248 248		
	247	251	250	251	251	246	248	249	248		
	246	251	249	252	249	248	248	249	247		
mean Hz	246.4	250.6	249.8	251.6	250.4	247	247.8	248.6	248		
65°F 50%	relative	50% relative humidity		April 22,	, 1976						
Eyes 1 hr.	old at	beginning	of tests	(10:20 A.M.)	(.M.)						
5" H,O	242	243	241	242	244	242	243	243	242	242	244
7	242	243	243	243	243	243	243	243	242	243	244

Table 2 (Continued)

65°F 50%	relative	50% relative humidity		April 22, 1976	9, 1976						
Eyes 1 hr	1 hr. old at	at beginning	g of tests	(10:20 A.M.)	1.M.)						
IOP	Eye #1	Eye #2	Eye #3	Eye #4	Eye #5	Eye #6	Eye #7	Eye #8	Eye #9	Eye #10	Eye #11
5" H,0	243	242	242	242	242	243	244	243	243	243	244
7	243	242	242	242	243	243	244	243	242	243	244
(court)	243	242	242	243	243	242	242	242	242	244	244
mean Hz	242.6	242.4	242	242.4	243	242.6	243.2	242.8	242.2	243	244
10" H,O	244	244	245	244	246	245	245	245	245	244	245
7	244	244	244	246	245	244	245	244	244	245	245
	244	245	244	245	245	244	245	244	244	244	245
	244	244	244	245	245	245	245	245	244	245	245
	244	245	244	245	244	244	245	244	245	245	245
mean Hz	244	244.4	244.2	245	245	244.4	245	244.4	244.4	244.6	245
15" H <sub>2</sub> 0	246	246	246	246	246	246	246	247	247	246	246
7	245	245	246	247	246	246	245	246	246	247	247
	245	246	246	247	246	246	246	246	246	247	246
	245	247	246	246	245	246	246	246	246	246	246
	245	246	246	246	246	246	246	246	246	246	247
mean Hz	245.8	246	246	246.4	245.8	246	245.8	246.8	246.8	246.4	246.4

Table 2 (Continued)

65°F 50%	50% relative humidity	humidity		April 22,	2, 1976							
Eyes 1 h	r. old at	Eyes 1 hr. old at beginning of tests	g of tests	s (10:20 A.M.)	).M.)							
IOP	Eye #1	Eye #2	Eye #3	Eye #4	Eye #5	Eye #6	Eye #7	Eye #8	Eye #9	Eye #10	Eye #11	
25" H <sub>2</sub> 0	246	246	247	247	247	247	246	247	248	247	247	
l	246 246	247 246	247 248	248 248	246 246	247 246	247 246	247 246	246	247 248	247	
	246	248	247	248	246	246	246	247	246	246	246	
	246	247	247	248	246	247	246	247	247	247	247	1
mean Hz	246	246.8	247.2	247.8	246.8	246.6	246.2	246.8	246.8	247	246.8	.23
35" H <sub>2</sub> O	246	248	247	249	246	246	246	247	248	247	247	
<b>v</b>	246	247	248	248	247	247	246	247	246	247	247	
	246	248	248	248	246	247	246	246	246	247	247	
	246	248	248	249	247	247	246	246	247	247	247	
	246	248	248	248	247	247	246	247	248	248	247	
mean Hz	246	247.8	247.8	248.6	246.6	246.8	246	246.6	246.8	247.2	247	

the data from the eyes with air in the anterior chamber were omitted.

After the frequency-IOP data were obtained for a 20 eye sample, the mean normal response frequency for each IOP was calculated. The equation used for the calculation was

$$\overline{f} = \begin{cases} \frac{f_i}{N} \\ i = 1 + N \end{cases}$$
 (7.1)

where f is the mean normal response frequency,  $f_1$  is the normal response frequency and N is the number of eyes.

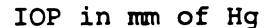
When the raw data were plotted, it was noted that scattering existed particularly at high IOP levels. Errors at higher IOP levels (above 20" H<sub>2</sub>O) were larger in magnitude than at lower IOP levels, but were less important to this study. IOP values of 20" H<sub>2</sub>O (37.3 mm Hg) and higher are generally considered physiologically out of range.

Various means of data examination were employed.

First, the raw data were plotted and a cueve drawn between the mean frequencies of the 20 eye sample as shown in Figure 73.

Since the IOP data are all in inches of H<sub>2</sub>O and the accepted unit in the medical field is in mm Hg, both units will be used with the mm of Hg in parenthesis ().

<sup>\*\*</sup>IOPs as high as 37" H<sub>2</sub>O (65.4 mm Hg) and higher have been observed (34); however, routine tonometry is not needed at such pressures to confirm glaucoma.



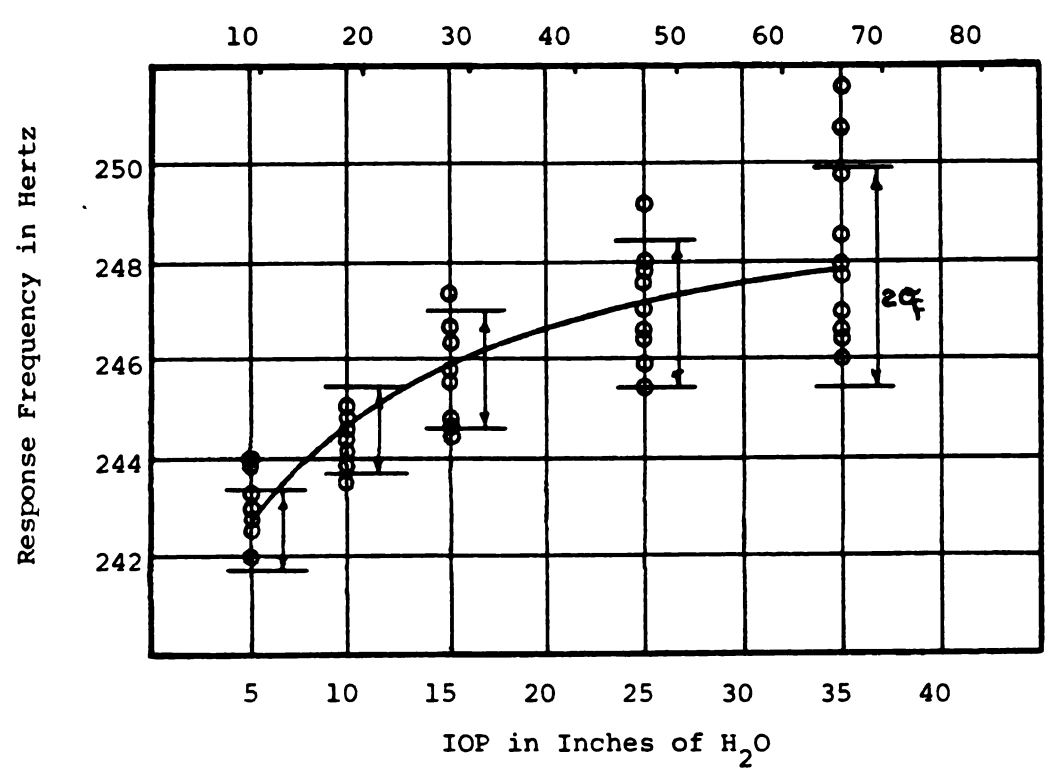


Figure 73 Frequency vs IOP for 20 Lamb Eyes

Next, the root-mean-square deviation  $\sigma_{\mathbf{f}}$  (standard deviation) of frequency was calculated for each IOP. The standard deviation of the population is defined as follows:

$$\sigma_{f} = \begin{bmatrix} N \\ \Sigma & (f_{i} - \overline{f})^{2} \\ \frac{i=1}{N-1} \end{bmatrix}^{\frac{1}{2}}$$
(7.2)

Data outside the  $\overline{f}$  ±  $2\sigma_f$  were eliminated and new values for  $\overline{f}$  and  $\sigma_f$  were calculated for each IOP. Sample calculations for  $\overline{f}$  and  $\sigma_f$  for an IOP of 5" H<sub>2</sub>O (9.34 mm Hg) are presented in Table 3. The remainder of the calculations are found in Appendix C.

Table 3 Sample Calculations

f <sub>i</sub>	$(f_i - \overline{f})$	$f_i - \overline{f})^2$
242.8	04	.0016
242.8	04	.0016
243.8	.96	.9216
242.6	24	.0576
242.8	04	.0016
242.4	44	.1936
243.2	.36	.1296
243.2	.36	.1296
243.2	.36	.1296
242.6	24	.0576
242.4	44	.1936
242	84	.7056
242.4	44	.1936
243	.16	.0256
242.6	24	.0576
243.2	.36	.1296
242.8	04	.0016
242.2	64	.4096
243	.16 1.16*	.256
244*	1.16	1.3456*

1st Run	2nd Run
$\overline{f} = \frac{4856.8}{20} = 242.84 \text{ Hz}$	$f = \frac{4612.8}{19} = 242.78 \text{ Hz}$
$\sigma_{f} = .4979$	$\sigma_{f} = .4293$
$f_L = 242.849958$	$f_L = 242.78859$
= 241.84 Hz	= 241.82 Hz
$f_{H} = 242.84 + .9958$	$f_{H} = 242.78 + .859$
= 243.84  Hz	= 243.64  Hz

where  $\boldsymbol{f}_L$  is the low frequency recorded and  $\boldsymbol{f}_H$  is the high frequency recorded.

<sup>\*</sup>Eliminated with  $\overline{f} \pm 2\sigma_{f}$  criteria

All data were tested for normality using a histogram technique and a program named "DAP" from the Chevrolet Product Assurance Program Library developed by G. F. Gruska, K. Mirkhani and L. R. Lamberson at General Motors Technical Center. The tests performed indicated that the data were not "non-normal" in distribution.

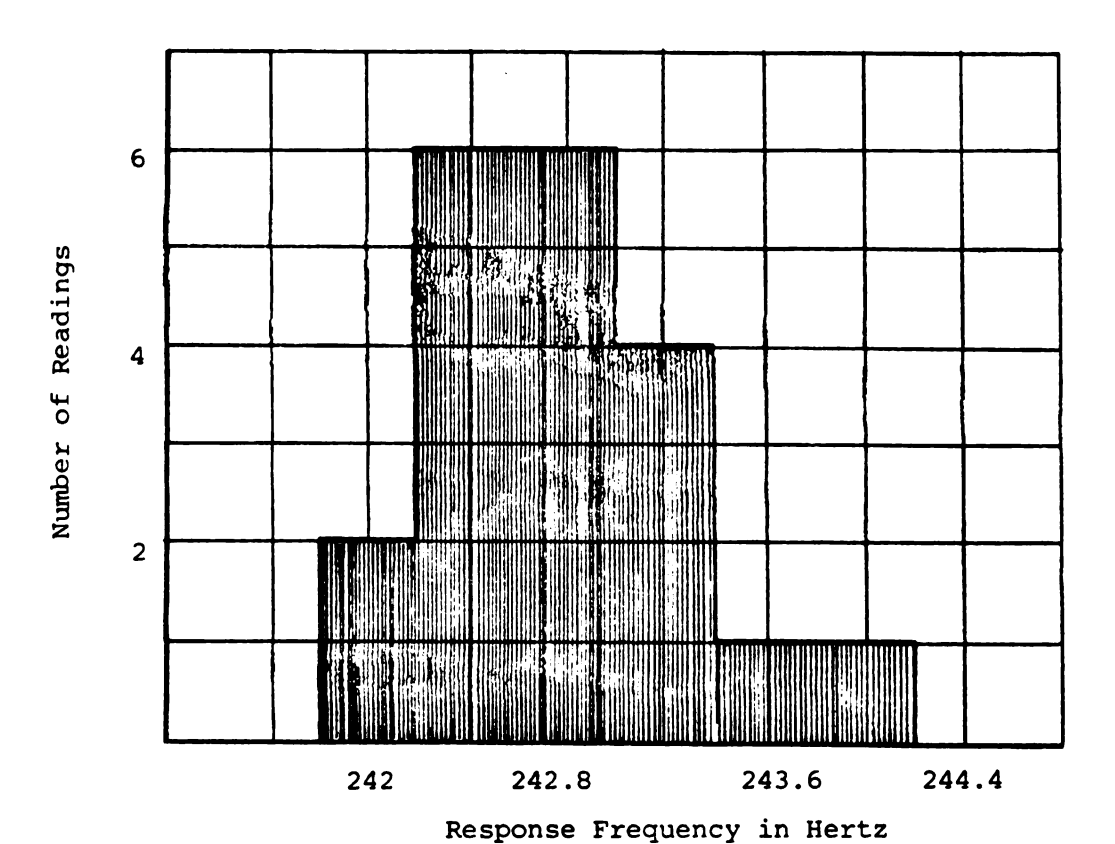
While some data fall out of range for a normal distribution as far as frequency of occurrence is concerned, this is generally acceptable within reason for a small sample size.

A sample histogram of the data obtained for the 5"  $\rm H_2O$  (9.34 mm Hg) IOP is presented in Figure 74. All other histograms and supporting data can be found in Appendix C. The histograms of the data at all IOP levels showed that the normal distribution technique for eliminating data were valid and corrected values for  $\overline{f}$  and  $\sigma_f$  were calculated. The  $\overline{f}$  ±  $2\sigma_f$  limits were used to tighten up the mean and standard deviation.

Standard error of  $\sigma_{\mbox{\bf f}}$  was calculated for the various IOP levels. Standard error is defined as follows:

$$\overline{e} = \frac{\sigma_f}{(N-1)^{\frac{1}{2}}} \tag{7.3}$$

No recommendations or inferences will be drawn from the standard error values calculated since the data as represented by the histograms indicated that some of



Interval Frequency (of occurrence)
241.8 242.8 2
242.2 242.6 6
242.6 243 6
243 243.4 4
243.4 243.8 1

243.8 244.4

Figure 74 Histogram, 5"  $H_2O$  (9.34 mm Hg) IOP

the data do not lend themselves to satisfactory standard error calculations.  $\overline{f}$ ,  $\sigma_{f}$  and  $\overline{e}$  for the IOP values investigated are presented in Table 4.

IOP in. H <sub>2</sub> O	IOP mm Hg	Ē	<sup>σ</sup> f	ē
5	9.34	244.78	.4293	.1013
10	18.68	244.69	.3160	.0767
15	28.02	246.14	.3922	.0981
25	46.7	246.97	.6778	.16

247.34

1.0217

.2554

Table 4 Mean, Standard Deviation and Standard Error

After the elimination of the data outside of the  $\overline{f} \pm 2\sigma_f$  limits, the remaining data were plotted and are shown in Figure 75. It is significant to note that the response frequency was most effected by IOP variations at pressures below 20" H<sub>2</sub>O (37.3 mm Hg) as can be observed from the changing slope of the curve.

65.38

35

Interestingly enough, the data in the physio-logical range of IOPs (5-20"  $\rm H_2O$  or 9.34 - 37.3 mm  $\rm Hg)$ 

<sup>\*</sup>Calculations of the standard deviation, probable error of the mean and other properties determined mainly by the bulk of the readings for distributions with pronounced tail or tails can be treated mathematically as normal distributions. However, when questions of the limit of error (standard error of  $\sigma_f$ ) or minimum value arise, the presence of a tail or tails must be taken into account (45).

have lower standard deviation of frequency  $(\sigma_{\mathbf{f}})$  and lower error of standard deviation of frequency  $(\bar{\mathbf{e}})$  than the range of IOPs from 20"  $\mathrm{H_2O}$  (37.3 mm Hg) and higher. This is evidence for greater credibility of the lower

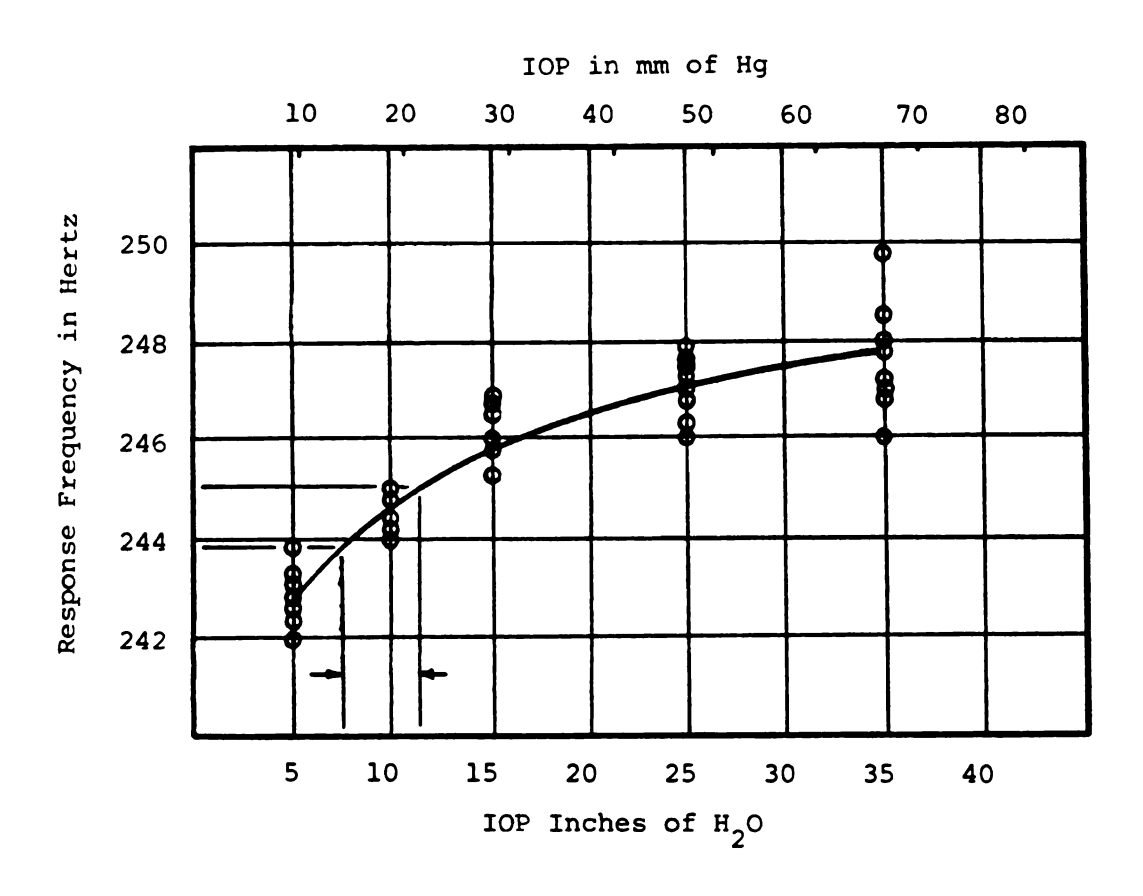


Figure 75 Response Frequency vs IOP

# 7.2 An Empirical Relationship

Since one desired output of the investigation was an empirical algebraic relationship between response frequency and IOP, the data were linearized using a natural log plotting technique. Several linearization techniques were investigated. The simplest technique

of those that showed promise was the square root of the natural log of the IOP on the absissa and frequency on the ordinate. It was felt that when more and better data are obtained, more sophisticated data-handling techniques would be applied. The calculations and semilog data plot are shown in Figure 76.

The "Y" intercept (c) in the equation "Y = c + m(ln IOP) was obtained through extrapolating the "X" axis to zero while (m) was a simple "rise over run" relationship. The calculations are as follows:

Y intercept = 233.65

m (slope) = 
$$\frac{\text{rise}}{\text{run}} = \frac{5.84}{.8} = 7.3 \text{ for H}_2\text{O}$$

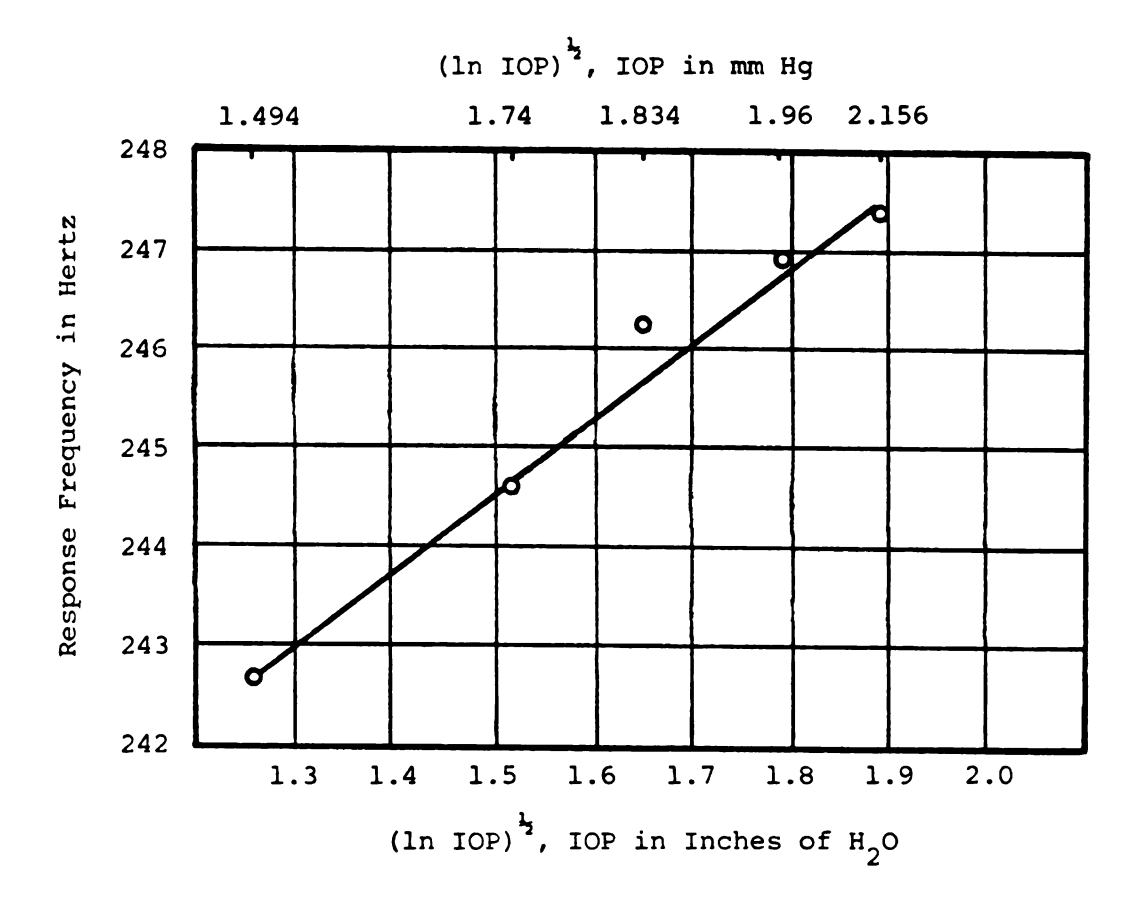
The equation relating  $f_{i}$  and IOP is determined to be

$$f_i = 233.7 + 7.3(\ln IOP)^{\frac{1}{2}} \text{ in. } H_2O$$
 (7.4)

or

$$f_i = 233.7 + 6.9(\ln IOP)^{\frac{1}{2}} mm Hg$$

Equation 7.4 is the relationship obtained from the data for lambs' eyes. The validity of Equation 7.4 can be established through further experimental work.



		Inches	of H <sub>2</sub> O		mm of	Hg
Ī	IOP	ln IOP	(ln IOP) 1/2	IOP	ln IOP	(ln IOP)
242.78	5	1.609	1.269	9.34	2.23	1.494
244.69	10	2.303	1.517	18.68	2.93	1.74
246.14	15	2.708	1.646	28.02	3.38	1.834
246.97	25	3.219	1.794	46.7	3.84	1.96
247.34	35	3.555	1.886	65.38	4.17	2.156

Figure 76 Linearized Data Plot

# 7.3 Discussion of Data Scatter

The plotted data still have significant scatter.

The following reasons are cited as being among the major contributors to the scatter.

- 1. Equipment-induced scatter. All equipment used to obtain data was general purpose "off the shelf" equipment and not designed for this specific application.
- 2. Operator-induced scatter. Since the voltage (amplitude) vs frequency curve for the eye, a damped system, has a gradual slope approaching and retreating from the response frequency of the eye, an exact reading of the peak of that hill with the equipment employed was nearly impossible.\*

As can be seen in Figure 77, there is a relatively flat region near the normal response frequency of the cornea. Since the variation of the normal response frequency with IOP extends over a range of only about 5 Hz from 5 to 35" of H<sub>2</sub>O (9.34 to 65.3 mm Hg), exact frequency determination is critical. (See Appendix E for "basic validity of approach" test.)

<sup>\*</sup>This difficulty with the "peak on the hill" determination was felt to be due to both the general purpose signal modifiers used and heavy system damping in the eye.

3. Physiological scatter. Variation between eyes due to size variation, variation in scleral rigidity and variation attributed to aging and/or injury.

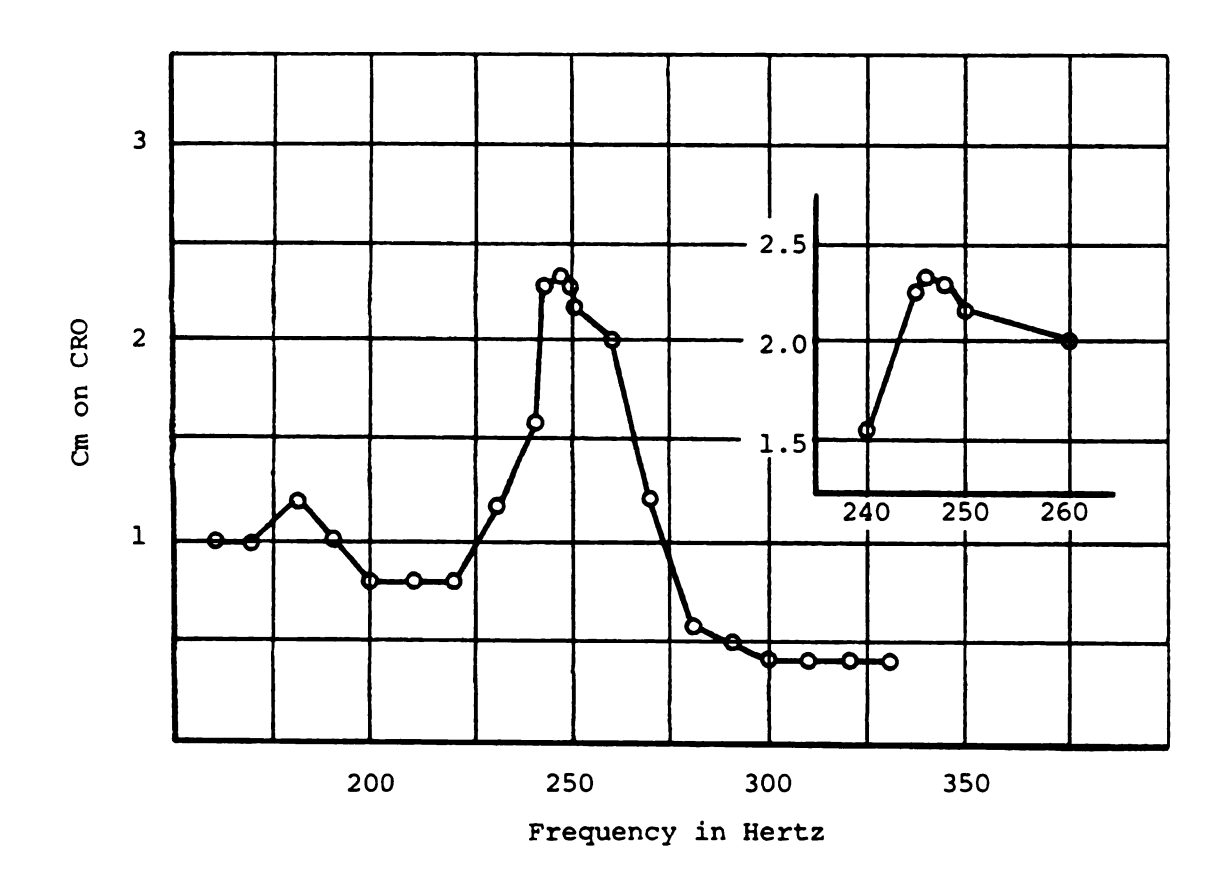


Figure 77 Lamb Eye Frequency Response

At this time, a comparison with clinical tonometers would be helpful in assessing the probably useful potential of the proposed measurement system. Experimenters with contemporary clinical tonometer systems consider the IOP measured as the dependent variable, while with the proposed system, IOP is the independent variable. However, for the sake of the comparison, this

difference in data treatment will be ignored. Refer to Figure 76 and consider a situation where the patient has an IOP of 10" H<sub>2</sub>O which would translate to 18.68 mm Hg. An IOP of 18.68 mm Hg is generally considered to be in the physiologically normal range. The frequency scatter as represented by  $\overline{f}~\pm~2\sigma_{\text{f}}$  for an eye with an IOP 10"  ${\rm H_2O}$  would place that eye within a pressure range from 7.5" H<sub>2</sub>O to 11.5" H<sub>2</sub>O. In millimeters of Hg, the range would be expressed as  $17.74 \pm 2.8$  mm Hg. This  $\pm$  2.8 mm Hg scatter translates to a  $\pm$  1.4 mm Hg standard deviation. The standard deviation of ± 1.4 mm Hg is less than that reported for contemporary clinical tonometers (31, 34, 48 and 53), but does give cause for concern. If the scatter were totally physiological and not partially due to instrumentation, this new system of tonometry would have little advantage over other tonometer methods in the areas of repeatability and accuracy.

A precise determination of the relative importance of each contribution to the total scatter is not possible with the existing data. It is reasonable, however, to assume that the scatter is not totally physiological and that it may be reduced through improved instrumentation. Some sources of instrumentation related errors are listed as follows:

- 1. Equipment-induced scatter.
  - A. Stimulation system. It is suggested that a sound lens be used to focus the sound on the cornea. A sound lens would reduce the ambient level of sound by up to 20 db and would also enable the operator to precisely direct the acoustic energy.
  - B. Close coupled oscillator and tracking filter.

    The close coupled oscillator and tracking
    filter would insure the midrange of the band
    pass filter coinciding with the stimulation
    frequency. The close coupling would help to
    minimize signal attenuation through faulty
    tuning of the filter.
  - C. Band pass filter. A band pass filter with high and low pass filter slopes of 48 to 96 db/octave is desired. Steep filter slopes would enable effective separation of noise from signal.
- 2. Operator-induced scatter. The operator-induced scatter would be reduced because of the increased quality of amplitude vs frequency data with the improved instrumentation suggested in A and B above. Other information such as the phase relationship between the stimulation frequency

and the corneal normal response frequency could be utilized with a phase meter to reduce further the quality of human judgment required.

# 7.4 Summary

The following summarizes the major findings resulting from this investigation.

- Standard deviation of pressure for the excised eyes was about ± 1.4 mm Hg in the physiological range of IOPs investigated.
- 2. An imperical relationship between normal response frequency and IOP for freshly excised lambs' eyes was derived. The relationship for lambs' eyes is represented by Equation 7.4 and is found on page 131.

### CHAPTER 8

#### A PRELIMINARY INVIVO STUDY ON DOGS

### 8.1 Introduction

A second series of tests was run with the proposed optical tonometer system. These tests were run invivo on live dogs in the Veterinary Clinic at Michigan State University. This series of tests was designed mainly to aid in the development of recommendations for improving the IOP measuring system for future work. The tests yielded data that were supportive of the trends observed with the invitro tests. Although the data were supportive, the data values were not as well defined. The invivo data were very difficult to obtain with the present measurement system since the operator required about a minute to tune in on the normal response frequency. The eye, being alive in the invivo tests, responded physiologically to the induced high pressures. The pressures in the eye decreased rapidly after being brought to the elevated values. This time rate of change of pressure made it impossible to catch reasonable accurate normal response frequencies at pressures

above 20"  $\rm H_2O$  (37.3 mm Hg). At pressures below 20"  $\rm H_2O$  (37.3 mm Hg), repeatable data were obtained. Several points of data were taken and are presented in Section 8.3.

### 8.2 General Procedures

The procedures used to obtain data from the dogs were as follows:

- Set up optical IOP measurement system. Plug in and turn on all electrical instrumentation.
   See Figure 78 for a photograph of the measurement system. This system is the same as is illustrated diagrammatically in Figure 33.
- 2. Anesthetize the dog with a barbituate (Phenobar-bital). A reduction of baseline IOP was noted (also reported in Section 4.1.1) as a result of the barbituate, but did not interfere with this series of tests. For future work, however, other anesthetics that will not repress the blood pressure resulting in IOP reduction will be used.
- 3. Clamp and suture lid open and eye in position as shown in Figure 79.

If the eye was not sutured in position, it rotated upward until only the sclera could be observed.



Figure 78 IOP Instrumentation for Invivo Measurements



Figure 79 Preparation of Eye for Examination

- 4. Insert a 22-gauge hypodermic needle into the anterior chamber of the eye (see Figure 80).

  The needle was connected to an electronic pressure measurement system (Electronics for Medicine, Inc. Model DR-8) capable of displaying a pressure vs time output on a CRT. The syringe and lines of the system were filled with a hypertonic lactated Ringer's solution to prevent the travel of blood to the transducer.
- 5. Bathe eye periodically with an isotonic lacrimal fluid to keep cornea moist during examination (Tearsol by Alcon Laboratories was used).
- 6. Use syringe to set pressure in anterior chamber to a pre-determined level. See Figure 81 for a sketch of this set-up.
- 7. Using the optical IOP measurement system, measure the normal response frequency of the eye.
- 8. Re-adjust pressure in anterior chamber with syringe and repeat procedures 7 and 8.
- After completion of the tests, replace dog in his pen to recover from the effects of the anesthetic.

During the course of obtaining data with the proposed tonometer system, data were also taken with the Schiotz and EMT 20 applanation tonometers. These data



Figure 80 Inserting Needle into Anterior Chamber

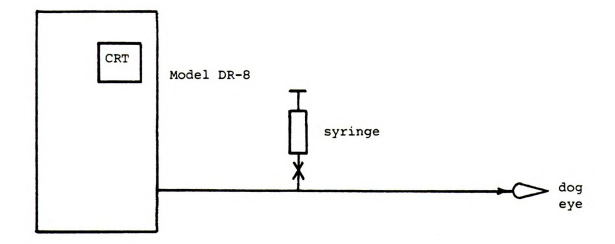


Figure 81 Pressure Monitoring System

were taken to verify the pressures induced and measured by the electronic pressure measurement system and syringe thereby providing a cross check on the proposed system.

### 8.3 Invivo Data

The data obtained from the eyes of live dogs are presented in Table 5.

Table 5 Normal Response Frequency for Dogs, Run Invivo

March 11, 1976		
IOP Inches of H <sub>2</sub> O	Average Value of Response Frequency	Range of Response Frequencies
5		
10	254	(253-255)*
15	255	(253-257)
20	NA	too much drift in pressure

<sup>\*</sup>Several readings were taken at this IOP.

Data were taken at IOP values of up to 75"  $\rm H_2O$  (140 mm Hg) without destroying the eye. The CRT display in the Electronics for Medicine Model DR-8 indicated a significant and rapid decay of IOP with time at IOP values above 15"  $\rm H_2O$  (28.02 mm Hg). This IOP decay was attributed to causes including the following:

 Live eyes respond physiologically to the induced high IOP. 2. Syringe which was used to induce the high IOPs perhaps was "backing off" thereby reducing the induced pressure value.

# 8.4 Summary

This phase of the total investigation, while encouraging as to the applicability of the proposed system for invivo tests, revealed the following areas in need of improvement:

- An anesthetic that would not induce a reduction of IOP.
- 2. A modification of the electronic pressure measurement system to enable it to hold elevated pressures for extended periods of time.
- 3. Modifications of the proposed tonometry system as referred to in Section 8.1 to provide for rapid and accurate tuning of the normal response frequency.

#### CHAPTER 9

#### CONCLUSIONS AND RECOMMENDATIONS

### 9.1 Conclusions

1. An apparatus, procedure and measurement system were developed for exploring the vibrational response of enucleated eyes (Chapters 4 and 6).

Experimental Set Up #1 (Figure 33) was satisfactory with the diaphragm model and with the invitro eye tests. The major limitation was that the measurement of frequency data was subjective. The subjectivity of the data was a function of operator judgment as to when the exact normal response frequency was reached. It was assumed that the normal response frequency was reached when the output on the CRO was a maximum for a constant amplitude corneal stimulation signal. It was difficult to determine a maximum amplitude at a discrete frequency because the eye has significant damping and, therefore, did not have a clearly defined response peak (Figure 71). Since the frequency range of the eye in physiological IOPs is limited (Figure 71),

the lack of a clearly defined peak was serious. Even with the stated difficulties, useful IOP data were obtained (Section 7.1).

Experimental Set Ups #2 and #3 (Figures 34 and 35) were highly satisfactory with the diaphragm model with air in the cavity but were unsatisfactory with the invitro eye tests. It was noted that the energy required to effect a measurable frequency response in eyes was many times greater than that for the diaphragm. This increase in energy requirement was considered to be due to factors including:

- a. Greater thickness to diameter ratio in the eye than in the diaphragm
- b. Medium viscosity liquid in eyes compared with air behind the diaphragm
- c. Scleral rigidity value much larger in the eye than the rigidity value for the latex diaphragm
- d. Tissue is more highly damped than latex

While the signal generator coupled with an audio amplifier of Experimental Set Up #1 could supply the necessary energy to stimulate the cornea, the random noise generator with an audio amplifier could not. The energy level necessary for corneal stimulation with the present modifiers was about 110 db at discrete frequencies. To achieve this same energy level at discrete

frequencies with the random noise generator and amplifier would require a total energy output beyond the range of the output transducer (speaker). See Section 5.4.

- 2. The relationship between mean normal response frequency and IOP is real and measurable (Section 7.1).
- 3. The normal response frequency was determined to be most affected by IOP variation in the physiological range of IOP values (Section 7.1).
- 4. The relationship between normal response frequency and IOP has greatest credibility in the physiological range of IOP values (Section 7.1).
- 5. An empirical relationship between vibrational response and IOP was developed (Section 7.1).
- 6. High-speed films taken of existing clinical tonometers applanating corneas of dogs and humans (Section 4.1), visually support the existence for blunt object trauma as indicated by measured hypotony reported in the literature (Section 3.3).
- 7. Invivo tests run in the Veterinary Clinic indicate that this optical IOP measurement system with modifications could be practical (Chapter 8).

### 9.2 Recommendations

1. Replace signal generator and variable filter of Experimental Set Up #1 with a close coupled sweep oscillator and tracking filter. The sweep oscillator should have a range of 1-1000 Hz with a 1 Hz band width and variable sweep rates. The tracking filter should have about 96 db per octave high and low pass filter slopes for effective separation of signal from noise with a 1 Hz band width and variable sweep rate (refer to discussion in Section 7.1).

- 2. Add a phase detection device to aid in the discrimination process when approaching the normal response frequency of the cornea. This device could detect minute phase variations between the "beat" signal and the stimulation signal and could thereby increase the quality of judgment.
- 3. Since about 110 db was required to stimulate the cornea, it is suggested that a sound lens (or reflector) be used with a small, high-intensity speaker. The sound lens (or reflector) would be used to focus the sound on the cornea and reduce the dispersion. A suggested reflector would be Barone's reflector (see Figure 82).

A requirement of Barone's reflector is that the sound source be behind the reflector. The incident wave coming from the sound source is changed to a cylindrical wave by the 90° cone. The cylindrical wave is reflected by the paraboloid section where it is converted into a spherical wave converging to the focus "f." The system

must be designed so that the waves reflected by the parabolic section are not obstructed by the cone (2). It is also necessary that the specific acoustic impedance of the reflector material be as different as possible from the fluid for maximum gain. The maximum possible gain from a reflector coupled with an incident sound source is about 20 db (23). The sound level outside the focal point of the reflector would then be substantially less than the sound level of the incident wave.

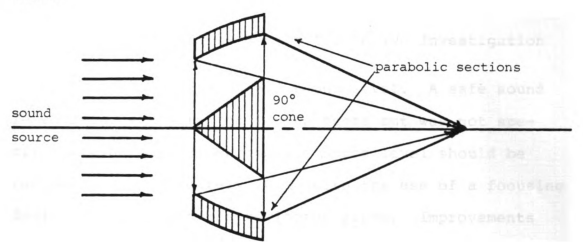


Figure 82 Cross-Section through Barone's Reflector

- 4. Reduce the power of the laser beam from 4.8 mw to a value well under the "safe" physiological limit for eyes.
- Improve the optical components for more distinct focusing of the laser on eye and photocell.
- $\begin{tabular}{ll} \bf 6. & Possible system for invivo investigation \\ \end{tabular}$

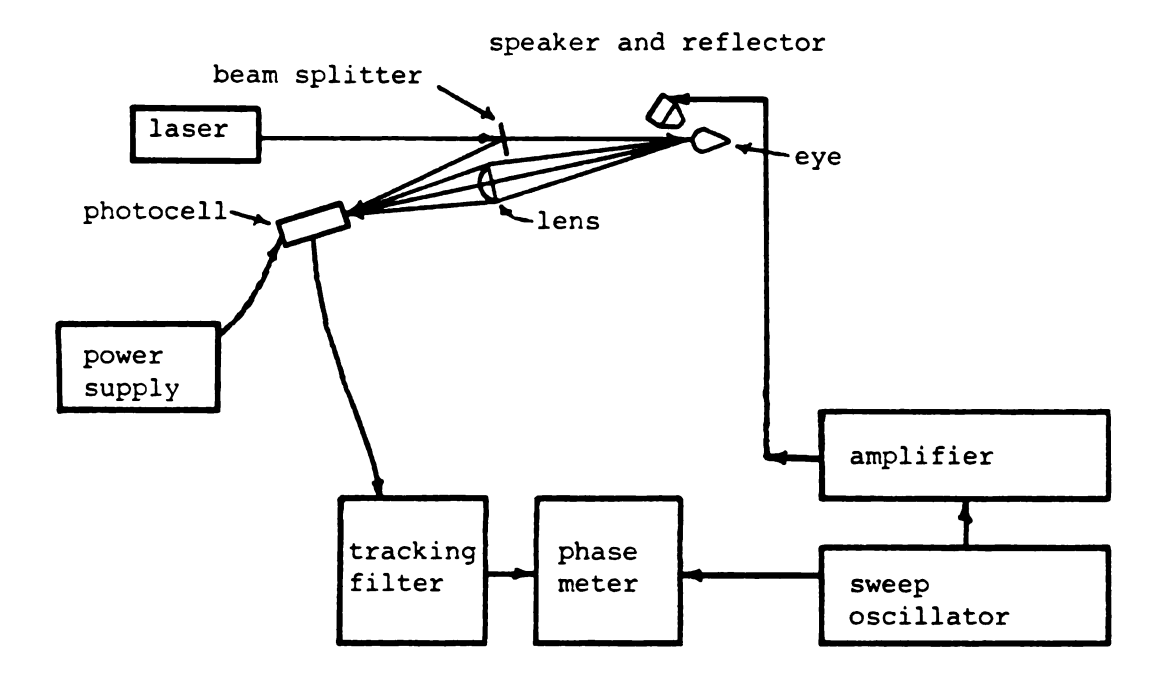
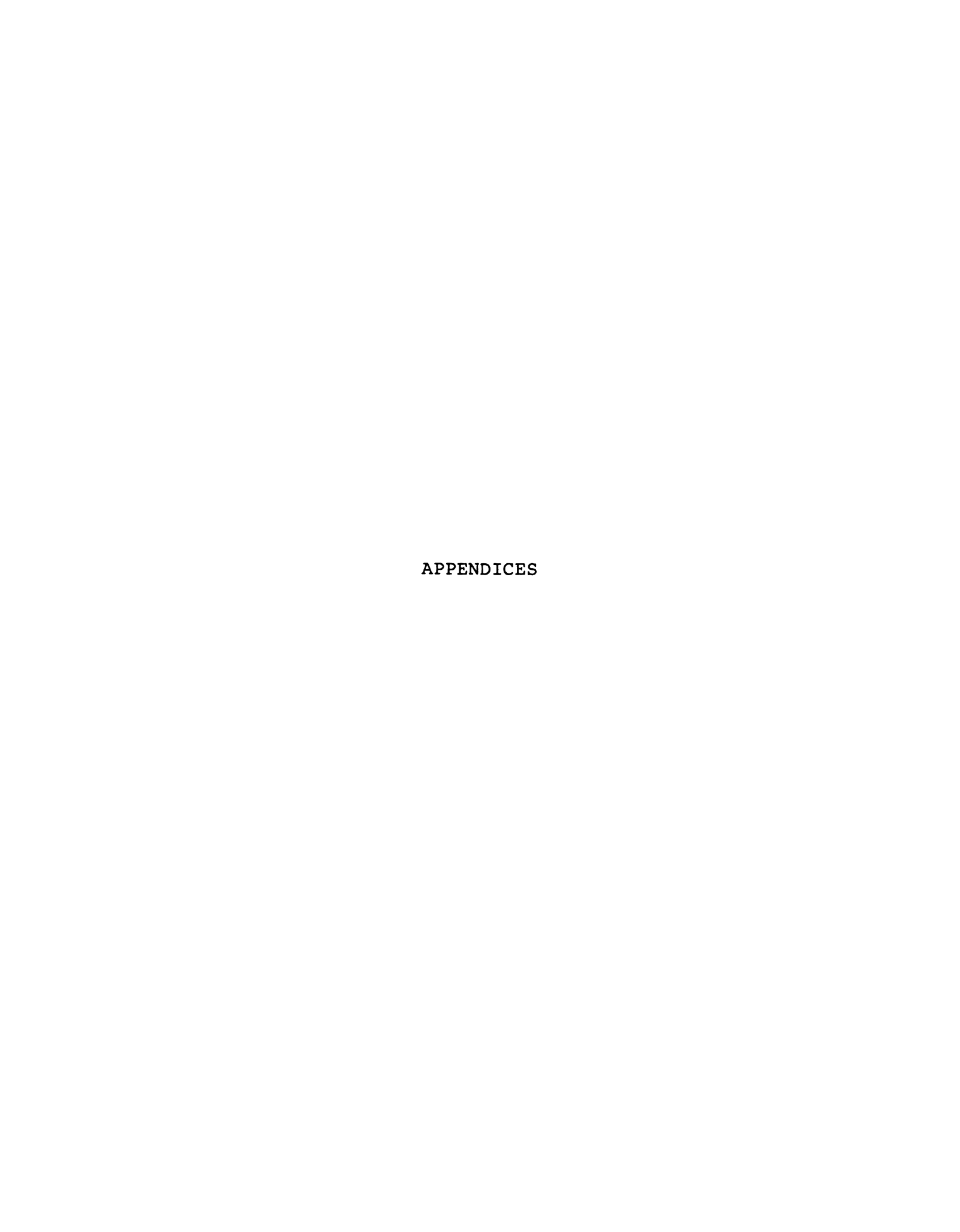


Figure 83 Possible System for Invivo Investigation

- 7. Investigate safe sound level. A safe sound level is a necessity for invivo tests but was not specifically addressed because the sound level should be reduced by approximately 20 db with the use of a focusing device such as Barone's reflector alone. Improvements in the optics, signal modifiers and readouts should very well reduce the energy input to the eye still further.
- 8. The final recommendation is that this work be continued beginning with the system of Figure 83 applied to excised eyes. Once a degree of familiarity with the system has been developed and repeatable data obtained, then proceed directly to invivo testing.

# 9.3 Afterword

It is realized that much investigation has to be performed with this system before it can be applied to humans. However, it is felt that based on the results from the investigation, more work is justified. The system has demonstrated promise to be quick and painless, would not require an anesthetic, could be performed without the patients being made aware of the test and would not require the services of an ophthalmologist.



# APPENDIX A

THE 11 GLAUCOMA RULES

#### APPENDIX A

#### THE 11 GLAUCOMA RULES

By

#### Dr. Theodore Schmidt

- All patients age 40 or above, as well as myopes (over -3.0 sph) age 20 or above, should be examined with the Applanation Tonometer. This examination should be performed at least once a year in patients who are frequently examined.
- 2. If the ocular pressure is 21 mm Hg or higher, a visual field examination should be performed at a subsequent visit.
- 3. If perimetry is performed because of suspicion of glaucoma, this examination should be followed by measurement of the intraocular pressure.
- 4. When the intraocular pressure is between 21 and 22.5 mm Hg, and the visual fields are normal, repeat the perimetric examination and the tonometry in one year.
- 5. If the intraocular pressure is higher than 22.5 mm Hg and the visual fields are normal, the intraocular pressure should be checked in one week, and a perimetric examination should be repeated in 6 months.
- 6. If intraocular pressures higher than 22.5 mm Hg are repeatedly recorded, or intraocular pressure at one measure higher than 22 mm Hg, or if the typical perimetric changes associated with glaucoma is found, the following examinations should be performed: Charting of the intraocular pressure changes in the hospital, or if possible this may be done on an ambulatory basis (2 measures of the intraocular pressure by Applanation and a measure of the morning pressure in bed in a darkened room with a Schiotz tonometer; the patient should continue his normal pattern of life throughout the day), gonioscopy, a determination of the ocular rigidity, perimetric examination, examination of the optic disc with a contact lens at the Slit Lamp.

- 7. If during the plotting of the intraocular pressure curve, several pressures above 22.5 mm Hg are measured, medical treatment should be instituted, at first with pilocarpind drops at night. The intraocular pressure should be normalized during the measurement of the diurnal pressure curve (the tension should remain below 20 mm Hg for 2 successive days), then checked after 1 week, then in 2 weeks.
- 8. Alterations of the visual fields with an intraocular pressure below 22.5 mm Hg indicates the need for medical treatment.
- 9. If, despite careful medical treatment intraocular pressures above 22.5 mm Hg are obtained, or if despite a normal intraocular pressure (never higher than 22.5 mm Hg) the visual field continues to deteriorate, the medication should be changed during a diurnal pressure curve. After change in medication, the intraocular pressure should fall a minimum of 2 mm Hg.
- 10. If despite optimal medication, the intraocular pressure oscillates between 22.5 and 26 mm Hg, the visual field must be rechecked every 2 months. Surgery would be advised if the visual field undergoes modification, or if despite optimal treatment the intraocular pressure remains above 26 mm Hg.
- 11. In the case of intraocular pressure normalized below 20 mm Hg the visual field should be checked every 4 months. If the pressure is normalized between 20 and 22.5 mm Hg the visual field should be redone every month.

Procedure in applanation tonometry: First a trial measurement and then 3 measurements and calculation of the mean value.

First examination of the field of vision: Examination of the whole visual field (4 isopters and the blind spot).

Checking of the visual field: Examination of the central field of vision (2 to 3 isopters within 30" and the blind spot).

APPENDIX B

EQUIPMENT LIST

#### APPENDIX B

### EQUIPMENT LIST

Spectra Physics Model 134 laser, 4.8 milliwatt

General Radio Random Noise Generator Type 1390-B

Harrison Laboratories 6204A DC Power Supply

Bogen Charger, Audio Amplifier

Hewlett Packard Model 200 Cd Audio Oscillator

Hewlett Packard Model 521 A Counter

Quantech Model 304T Wave Analyzer

Krohn-Hite Model 335 R Variable Filter

Tektronix Type O Operational Amplifier with Type 132 Power Supply

Moseley Type 7035B XY Plotter

Fastax Model WF-17 16mm Camera with Fastax Raptar No. D17217 2" lens with extension

Federal Scientific, Ubiquitous Spectrum Analyzer, Model US-7B

Schiotz Tonometer, Stotz Laboratories

American Optical Air Jet Optical Tonometer

EMT 20 Digital Applanation Tonometer

Electronics for Medicine, Inc., Model DR-8

Lo-Cam, High Speed Movie Camera, Red Lake Laboratories

Photocell, see Reference 5

# APPENDIX C

CALCULATIONS AND HISTOGRAMS

### APPENDIX C

#### CALCULATIONS AND HISTOGRAMS

## First Run Frequency Mean

$$\frac{5" \text{ H}_2\text{O}}{\sum_{i=1}^{N} f_i} = 4856.8 \qquad \frac{N}{\sum_{i=1}^{N} f_i} = 4891.6$$

$$\overline{f} = \frac{1}{N} \sum_{i=1}^{N} f_i = 242.84 \qquad \overline{f} = \frac{1}{N} \sum_{i=1}^{N} f_i = 244.58$$

$$\frac{15" \text{ H}_2\text{O}}{\sum_{i=1}^{N} f_i} = 4920.8 \qquad \frac{25" \text{ H}_2\text{O}}{\sum_{i=1}^{N} f_i} = 4940.4$$

$$\overline{f} = \frac{1}{N} \sum_{i=1}^{N} f_i = 246.04 \qquad \overline{f} = \frac{1}{N} \sum_{i=1}^{N} f_i = 247.02$$

$$\frac{35" \text{ H}_2\text{O}}{\sum_{i=1}^{N} f_i} = 4957.4$$

$$\overline{f} = \frac{1}{N} \sum_{i=1}^{N} f_i = 247.87$$

First Run Calculations

$5 \text{ H}_2\text{O}, \ \overline{f} = 242.84 \text{ Hz}$			10" $H_2O$ , $\overline{f} = 244.58 \text{ Hz}$			
f <sub>i</sub>	$(f_i - \overline{f})$	$(f_i - \overline{f})^2$	f <sub>i</sub>	$(f_i - \overline{f})$	$(f_i - \overline{f})^2$	
242.8	04	.0016	244.8	.22	.0484	
242.8	04	.0016	244.8	.22	.0484	
243.8	.96	.9216	244.8	.22	.0484	
242.6	24	.0576	243.8*	78*	.6084*	
242.8	04	.0016	244.8	.22	.0484	
242.4	44	.1936	243.4*	-1.18*	1.3924*	
243.2	.36	.1296	245	.42	.1764	
243.2	.36	.1296	245	.42	.1764	
243.2	.36	.1296	244.8	.22	.0484	
242.6	24	.0576	244	58	.3364	
242.4	44	.1936	244.4	18	.0324	
242	84	.7056	244.2	38	.1444	
242.4	44	.1936	245	.42	.1764	
243	.16	.0256	245	.42	.1764	
242.6	24	.0576	244.4	18	.0324	
243.2	.36	.1296	245	.42	.1764	
242.8	04	.0016	244.4	18	.0324	
242.2	64	.4096	244.4	18	.0324	
243	.16	.0256	244.6	.02	.0004	
244*	1.16*	1.3456*	245	.42	.1764	

<sup>\*</sup>Eliminated with  $\overline{f} \pm 2\sigma$  criteria

157

First Run Calculations

15" $H_2O$ , $\overline{f} = 246.04 Hz$			25" $H_2O$ , $\overline{f} = 247.02 Hz$			
f <sub>i</sub>	$(f_i - \overline{f})$	$(f_i - \overline{f})^2$	f <sub>i</sub>	$(f_i - \overline{f})$	$(f_i - \overline{f})^2$	
246	.04	.0016	246.6	42	.1764	
247.4*	.96*	.9216*	248	.98	.9604	
245.8	24	.0576	247.8	.78	.6084	
244.6*	-1.44*	2.0736*	245.6*	-1.42*	2.0164*	
246.4	.36	.1296	247.6	.58	.3364	
244.4*	-1.64*	2.6896*	246.8	.22	.0484	
246.6	.56	.3136	249.4*	1.62*	2.6244*	
246	04	.0016	247.8	.78	.6084	
245.4	64	.4096	246	42	.1764	
245.8	24	.0576	246	42	.1764	
246	04	.0016	246.8	22	.0484	
246	04	.0016	247.2	.18	.0324	
246.4	.36	.1296	247.8	.78	.6084	
245.8	24	.0576	246.8	22	.0484	
246	04	.0016	246.6	42	.1764	
245.8	24	.0576	246.2	82	.6724	
246.8	.76	.5776	246.8	22	.0484	
246.8	.76	.5776	246.8	22	.0484	
246.4	.36	.1296	246.8	22	.0484	
246.4	.36	.1296	247	02	.0004	

<sup>\*</sup>Eliminated with f  $\pm$  2 $\sigma$  criteria

First Run Calculations

35"  $H_2O$ ,  $\overline{f} = 247.87 Hz$ 

fi	(f <sub>i</sub> - <del>f</del> )	$(f_i - \overline{f})^2$
247.8	07	.0049
248.6	.73	.5329
248	.13	.0169
246.4	-1.47	2.1609
250.6*	2.73*	7.4529*
249.8	1.93	3.7249
251.6*	3.73*	13.9129*
250.4*	2.53*	6.4009*
247	87	.7569
246	-1.87	3.4969
247.8	07	.0049
247.8	07	.0049
248.6	.73	.5329
246.6	-1.27	1.6129
246.8	-1.07	1.1449
246	-1.87	3.4969
246.6	-1.27	1.6129
246.8	-1.07	1.1449
247.2	67	.4489
247	87	.7569

<sup>\*</sup>Eliminated with f ± 2σ criteria

## First Run Calculations

5" 
$$H_2O$$

$$f_i = \overline{f} \pm 2\sigma_f \qquad \sigma_f = .4979$$

$$f_L = 242.84 - .9958 = 241.84 Hz$$

$$f_H = 242.84 + .9958 = 243.84 Hz$$

10" 
$$H_2O$$

$$f_i = \overline{f} \pm 2\sigma_f \qquad \sigma_f = .4538$$

$$f_L = 244.58 - .9076 = 243.57 \text{ Hz}$$

$$f_H = 244.58 + .9076 = 245.49 \text{ Hz}$$

15" 
$$H_2O$$
  
 $f_i = \overline{f} \pm 2\sigma_f$   $\sigma_f = .6977$   
 $f_L = 246.04 - 1.3954 = 244.64 Hz$   
 $f_H = 246.04 + 1.3954 = 247.44 Hz$ 

25" 
$$H_2O$$

$$f_i = \overline{f} \pm 2\sigma_f \qquad \sigma_f = .8655$$

$$f_L = 247.02 - 1.7310 = 245.29 \text{ Hz}$$

$$f_H = 247.02 + 1.7310 = 248.75 \text{ Hz}$$

35" 
$$H_2O$$

$$f_i = \overline{f} \pm 2\sigma_f \qquad \sigma_f = 1.6095$$

$$f_L = 247.87 - 3.3190 = 244.55 \text{ Hz}$$

$$f_H = 247.87 + 3.3190 = 257.2 \text{ Hz}$$

### Second Run Mean

5" 
$$H_2O$$
 $\sum_{i=1}^{N} f_i = 4612.8$ 
 $\sum_{i=1}^{N} (f_i - \overline{f})^2 = 3.3664$ 
 $\overline{f} = 242.78$ 
 $\sigma_f = .4293$ 

10" 
$$H_2O$$

$$\sum_{i=1}^{N} f_i = 4648.2 \qquad \sum_{i=1}^{N} (f_i - \overline{f})^2 = 2.5192$$

$$\overline{f} = 244.64 \qquad \sigma_f = .3687$$

15" 
$$H_2O$$
 $\sum_{i=1}^{N} f_i = 4184.4$ 
 $\sum_{i=1}^{N} (f_i - \overline{f})^2 = 2.6352$ 
 $\overline{f} = 246.14$ 
 $\sigma_f = .3937$ 

25" 
$$H_2O$$

$$\sum_{i=1}^{N} f_i = 4445.4 \qquad \sum_{i=1}^{N} (f_i - \overline{f})^2 = 4.776$$

$$\overline{f} = 246.97 \qquad \sigma_f = .6778$$

35" 
$$H_2O$$

N

 $\Sigma_{i=1} f_i = 4705.8$ 
 $\overline{f} = 247.67$ 

N

 $\Sigma_{i=1} (f_i - \overline{f})^2 = 35.309$ 
 $\sigma_f = 1.386$ 

## Second Run Calculations

5" 
$$H_2O$$
  
 $f_i = \overline{f} \pm 2\sigma_f$   $\sigma_f = .4293$   
 $f_L = 242.78 - .8586 = 241.82 \text{ Hz}$   
 $f_H = 242.78 + .8586 = 243.64 \text{ Hz}$ 

10" 
$$H_2O$$

$$f_i = \overline{f} \pm 2\sigma_f \qquad \sigma_f = .3687$$

$$f_L = 244.64 - .7374 = 243.80 \text{ Hz}$$

$$f_H = 244.64 + .7374 = 245.38 \text{ Hz}$$

15" 
$$H_2O$$

$$f_i = \overline{f} \pm 2\sigma_f \qquad \sigma_f = .5261$$

$$f_L = 246.14 - 1.0521 = 246.09 Hz$$

$$f_H = 246.14 + 1.0521 = 247.2 Hz$$

25" 
$$H_2O$$
  
 $f_i = \overline{f} \pm 2\sigma_f$   $\sigma_f = .6778$   
 $f_L = 246.97 - 1.3556 = 245.61 Hz$   
 $f_H = 246.97 + 1.3556 = 247.33 Hz$ 

35" 
$$H_2O$$

$$f_i = \overline{f} \pm 2\sigma_f \qquad \sigma_f = 1.386$$

$$f_L = 247.67 - 2.772 = 244.9 \text{ Hz}$$

$$f_H = 247.67 + 2.772 = 250.44 \text{ Hz}$$

### Third Run Mean and Calculations

10" 
$$H_2O$$
 $\Sigma_{i=1}^{N} f_i = 4404.4$ 
 $\Sigma_{i=1}^{N} (f_i - \overline{f})^2 = 1.911$ 
 $\overline{f} = 244.69$ 
 $\sigma_f = .316$ 

35" 
$$H_2O$$
 $\Sigma_{i=1}^{N} f_i = 4204.8$ 
 $\Sigma_{i=1}^{N} (f_i - \overline{f})^2 = 21.455$ 
 $\overline{f} = 247.34$ 
 $\sigma_f = 1.0217$ 

10" 
$$H_2O$$

$$f_i = \overline{f} \pm 2\sigma_f$$

$$f_L = 244.69 - .632 = 244.06 Hz$$

$$f_H = 244.69 + .632 = 245.32 Hz$$

35" 
$$H_2O$$

$$f_i = \overline{f} \pm 2\sigma_f$$

$$f_L = 247.34 - 2.04 = 245.3 Hz$$

$$f_H = 247.34 + 2.04 = 249.38 Hz$$

# Mean f and $\sigma_{\rm c}$ values

5" 
$$_{12}^{00}$$
  $_{16}^{0}$  = 242.78 Hz Standard error  $_{16}^{0}$  =  $_{16}^{0}$   $_{16}^{0}$  = .0966  $_{16}^{0}$   $_{16}^{0}$  = .4293  $_{16}^{0}$  N = 19 True value  $_{16}^{0}$  =  $_{16}^{0}$  = .0768  $_{16}^{0}$   $_{16}^{0}$  = .3160  $_{16}^{0}$  = 18 True value  $_{16}^{0}$  =  $_{16}^{0}$  = .0768  $_{16}^{0}$  = .3922  $_{16}^{0}$  = .3922  $_{16}^{0}$  = .17 True value  $_{16}^{0}$  =  $_{16}^{0}$  = .0955  $_{16}^{0}$  = .246.97 Hz Standard error  $_{16}^{0}$  =  $_{16}^{0}$  = .1214  $_{16}^{0}$  = .6778  $_{16}^{0}$  = .1214  $_{16}^{0}$  = .6778  $_{16}^{0}$  = .1214  $_{16}^{0}$  = .247.34 Hz Standard error  $_{16}^{0}$  =  $_{16}^{0}$  = .247.34 Hz Standard error  $_{16}^{0}$  =  $_{16}^{0}$  = .2716

True value  $q = \overline{f} \pm e_{\overline{f}}$ 

 $\sigma_{f} = 1.0217$ 

N = 17

# Histogram Intervals

5" H <sub>2</sub> O			25" H <sub>2</sub> (	25" H <sub>2</sub> O			
Interval		Number	Inte	Interval			
241.8	242.2	2	245.4	245.8	1		
242.2	242.6	6	245.8	246.2	3		
242.6	243	6	246.2	246.6	2		
243	243.4	4	246.6	247	7		
243.4	243.8	1	247	247.4	1		
243.8	244.2	1	247.4	247.8	4		
10" н <sub>2</sub> С	)		247.8	248.2	1		
Inter	val	Number	248.2	248.6	0		
243	243.4	1	248.6	249	0		
243.4	243.8	1	249	249.4	1		
243.8	244.2	2	35" н <sub>2</sub> (				
244.2	244.6	5	Inte		Number		
244.6	245	11	245 8	246.4	3		
15" H <sub>2</sub> C	)		246.4		6		
Inter	val	Number		247.6	1		
244	244.4	1	247.6	248.2	4		
244.4	244.8	1	248.2		2		
244.8	245.2	0	248.8		0		
245.2	245.6	1	249.4		1		
245.6	246	9	250		2		
246	246.4	4		251.2	0		
246.4	246.8	3		251.8	1		
246.8	247.2	0					
247.2	247.6	1					

APPENDIX D

DIAPHRAGM IOP DATA

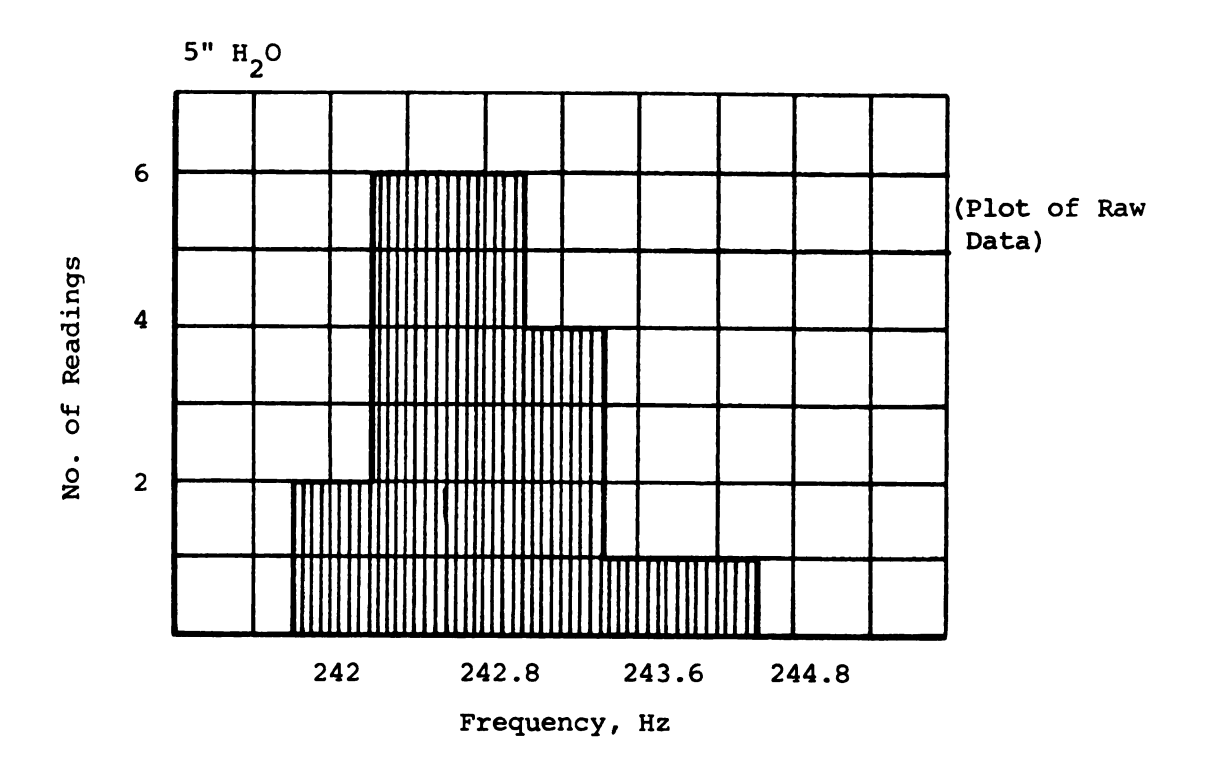


Figure C-1 Histogram, 5" H<sub>2</sub>O IOP

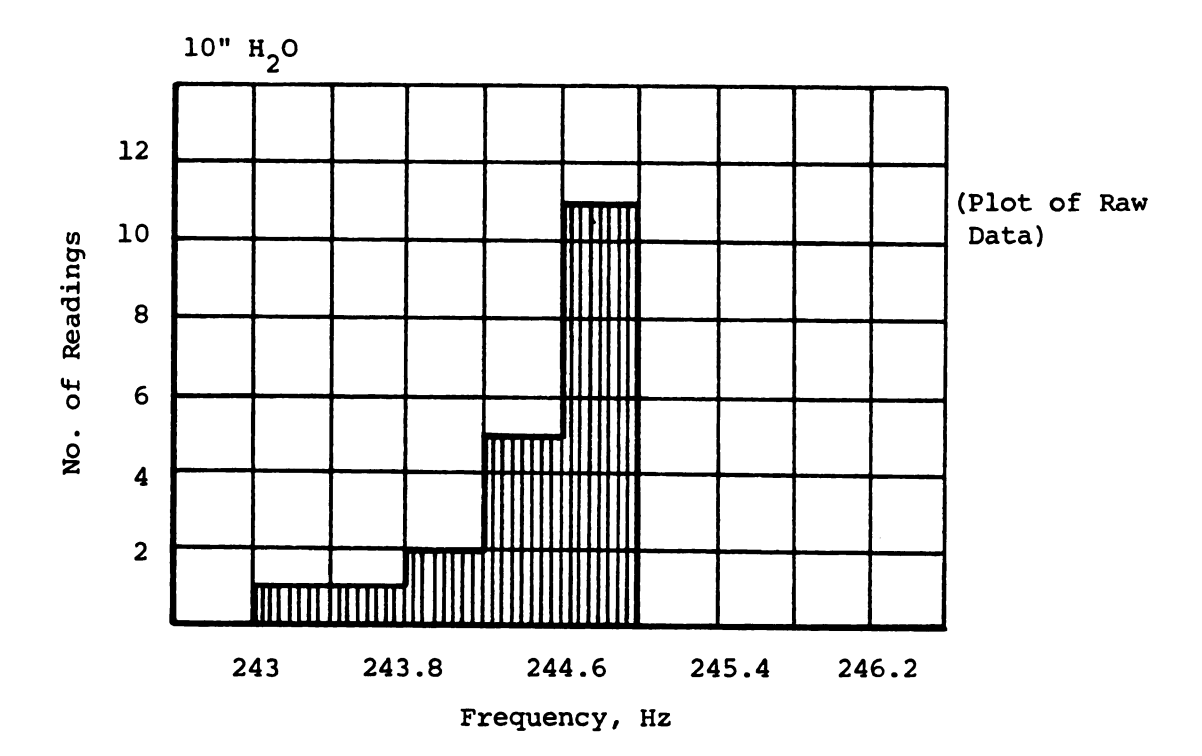


Figure C-2 Histogram, 10" H<sub>2</sub>O IOP

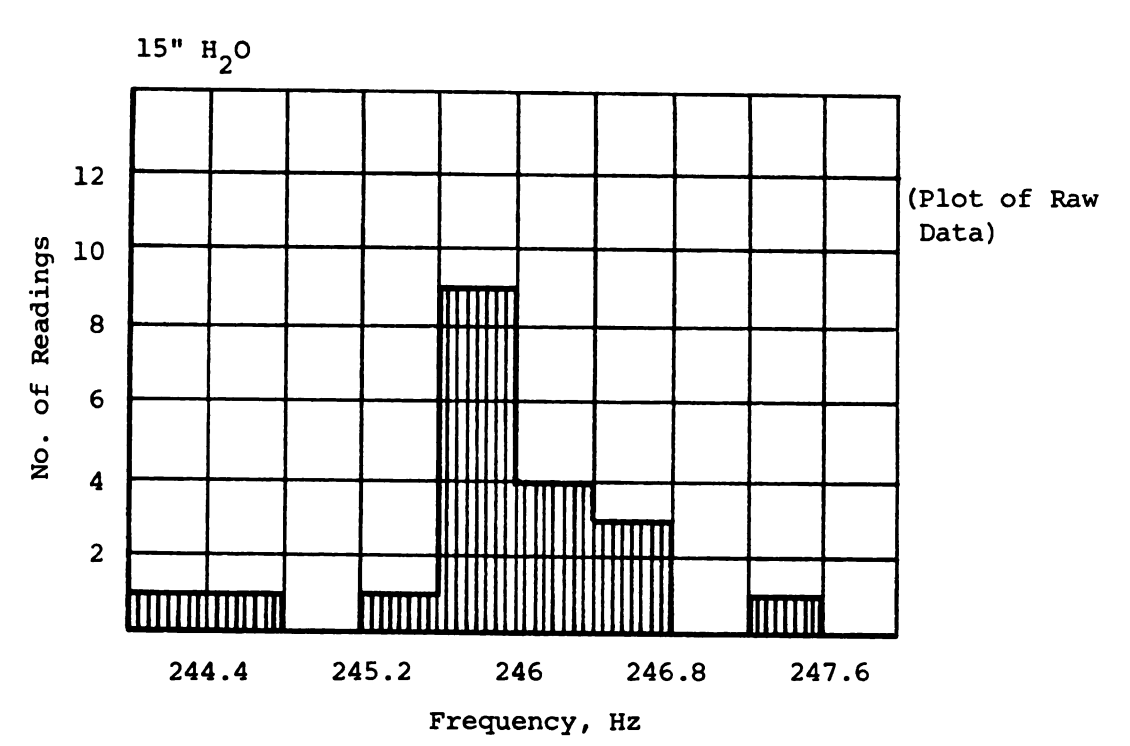


Figure C-3 Histogram, 15" H<sub>2</sub>O IOP

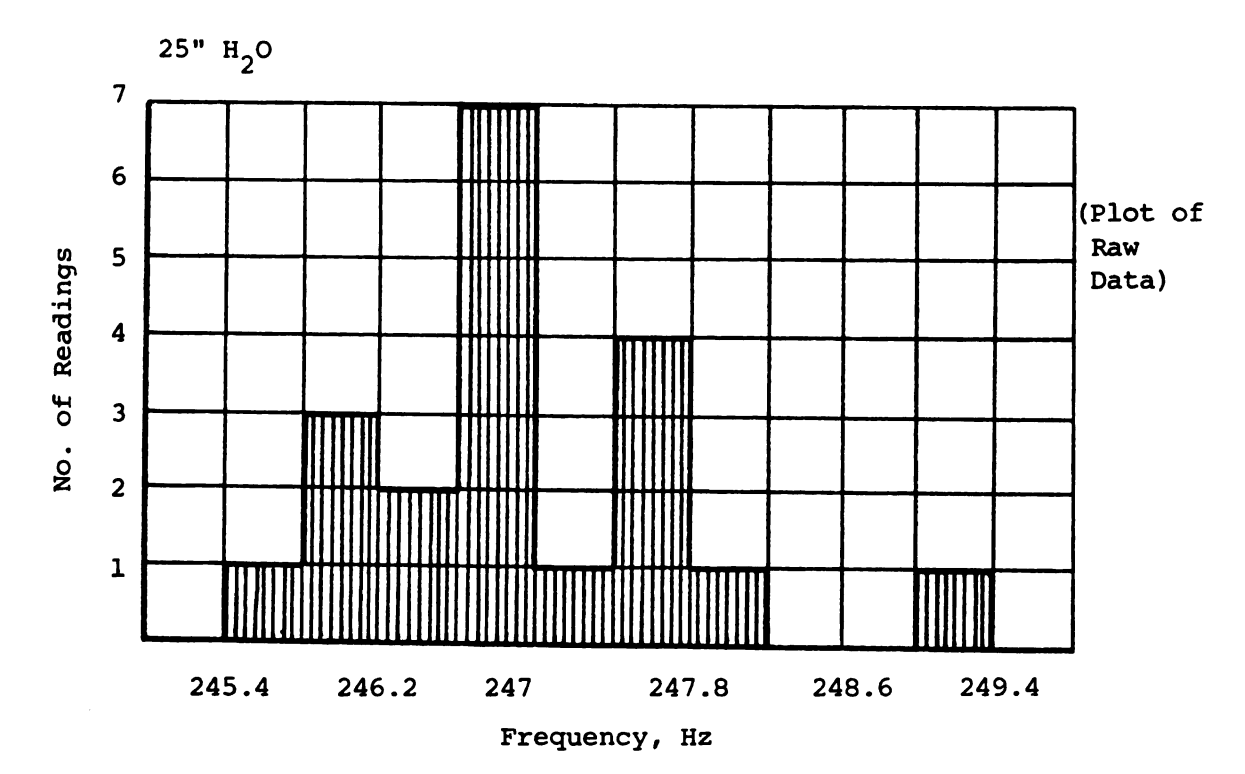


Figure C-4 Histogram, 25" H<sub>2</sub>O IOP

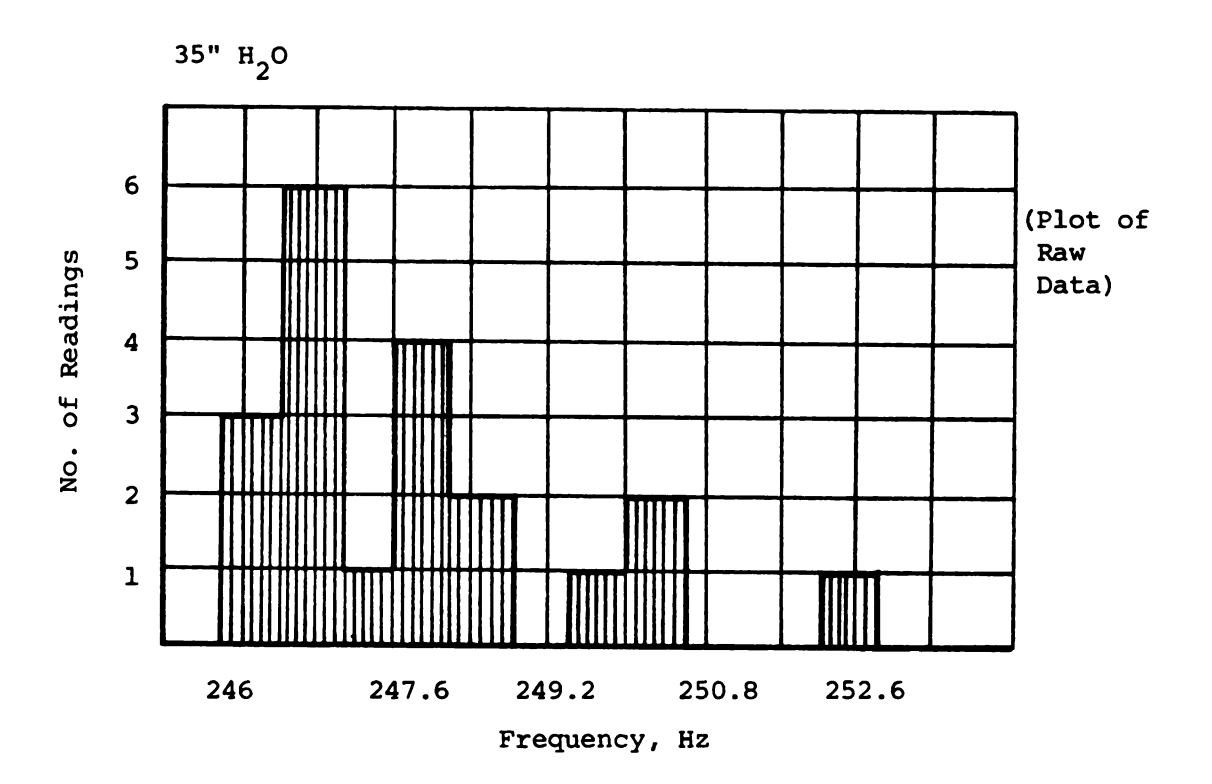


Figure C-5 Histogram, 35" H<sub>2</sub>O IOP

APPENDIX D

DIAPHRAGM IOP DATA

Table D-1 Data Set I-B

September 26, 1975							
Frequency	Speaker Input	Speaker Out	Ratio	5" H <sub>2</sub> O	7.5" H <sub>2</sub> O	10" H <sub>2</sub> O	12.5" н <sub>2</sub> 0
100	2	1.8	.09			.2	.2
110		1.8	.09	.2		.2	.2
120		1.8	.09	.4	.2	.2	.4
130		1.9	.095	.6	. 4	. 4	.4
140		1.9	.095	.8	.6	.4	.6
150		2.0	.1	.6	.2	.4	.4
160		2.0	.1	.4	.2	.2	.2
170		1.8	.09	.2	.2	.2	.2
180		1.6	.08	.2	.2	. 4	.4
190		1.2	.06	.2	.2	.4	.4
200		.7	.035	.4	.4	.6	.6
210		1.0	.05	.4	. 4	1.2	.8
220		1.6	.08	.6	.6	1.2	1.2
230	$\downarrow$	1.8	.09	1.6	.8	1.8	1.4
240		1.7	.085	3.6	2.0	2.5	1.0
250		1.7	.085	2.2	2.4	2.8	1.0

Table D-1 (Continued)

September 26, 1975							
Frequency	Speaker Input	Speaker Out	Ratio	5" H <sub>2</sub> O	7.5" н <sub>2</sub> 0	10" н <sub>2</sub> 0	12.5" н <sub>2</sub> 0
260	2	1.8	.09	1.0	2.2	2.8	1.1
270		1.8	.09	.8	2.0	2.4	1.2
280		1.8	.09	.6	1.4	2.2	1.3
290		1.8	.09	.6	1.0	1.2	1.0
300		1.7	.085	.4	.8	1.0	1.0
310		1.6	.08	.6	.8	1.0	1.2
320		1.6	.08	.6	.8	.9	1.2
330		1.6	.08	.8	.6	.9	1.0
340		1.6	.08	.6	.8	1.0	.9
350		1.6	.08	.5	1.1	1.0	.8
360		1.6	.08	.4	1.7	1.1	.9
370		1.6	.08	.4	1.9	1.6	1.0
380		1.6	.08	.5	1.4	1.8	1.0
390		1.6	.08	.6	1.2	1.9	1.0
400		1.5	.075	.6	1.0	1.8	.9
410		1.4	.07	.8	1.0	1.8	.8
420		1.5	.075	.9	.8	1.8	.7
430	₩	1.4	.07	.8	.8	1.6	.6
440		1.4	.07	.8	.9	1.2	.6
450		1.3	.065	.7	.8	.8	.6
460		1.3	.065	.7	.6	.6	.6
470		1.2	.06	.7	.6	.7	.8

170

Table D-1 (Continued)

September 26, 1975 Speaker Speaker Ratio 5"  ${\rm H_2O}$  7.5"  ${\rm H_2O}$  10"  ${\rm H_2O}$  12.5"  ${\rm H_2O}$ Frequency Out Input 480 2 1.2 .06 .7 .6 1.3 .9 1.1 490 .055 .5 .8 1.3 .9 .7 500 1.0 .05 .4 1.2 .8 .5 510 1.0 .05 . 4 1.0 .8 520 1.0 .05 .5 . 4 1.0 .6 530 1.0 .05 .4 .4 1.0 . 4 540 1.0 .05 .4 . 4 1.0 . 4 .05 550 1.0 .4 . 4 1.0 .6 560 1.0 .05 .4 .8 .6 .4 570 1.0 .05 .5 .5 . 4 .4 580 1.1 .055 . 4 .4 . 4 . 4 590 1.2 .06 . 4 . 4 .6 . 4

1.2

.06

. 4

.4

.7

. 4

600

# APPENDIX E

BASIC VALIDITY OF APPROACH TEST

#### APPENDIX E

### BASIC VALIDITY OF APPROACH TEST

The "basic validity of approach" test was a simple test designed to illustrate that the measurement system would yield repeatable data on a system other than an eye or diaphragm. The procedure used in the test was as follows:

- 1. Calibrate a 4" speaker (see Figure E-1 for the calibration curve) with the instrumentation package of Experimental Set Up #1 (see Figure 21 for a sketch of Experimental Set Up #1).
- 2. Set up the 4" speaker with Experimental Set Up #1 as illustrated in Figure E-2.
- 3. Tune oscillator and variable filter (in band pass mode) to natural frequency of small speaker as evidenced by a maximum amplitude on the CRO.
- 4. Repeat procedure #3 twenty times.

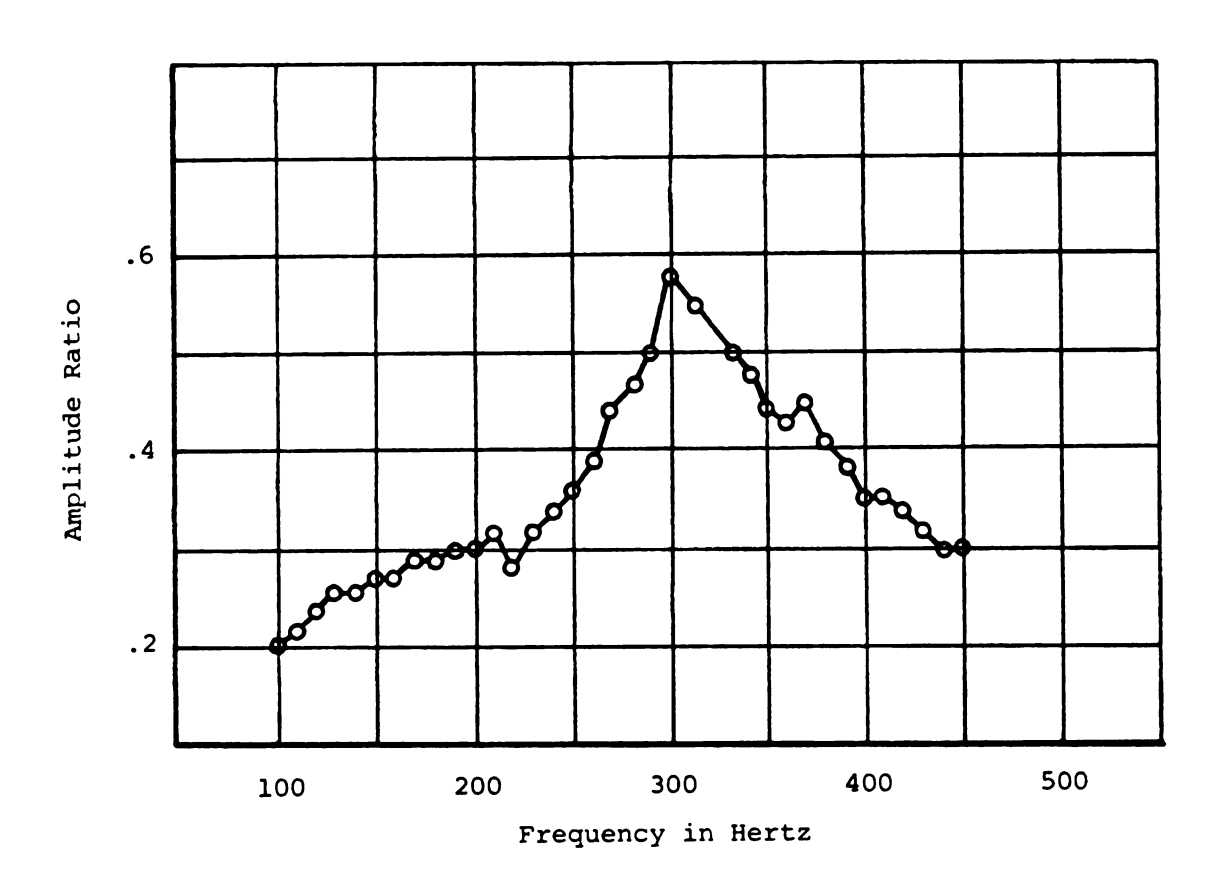


Figure E-l Calibration Curve, 4" Speaker

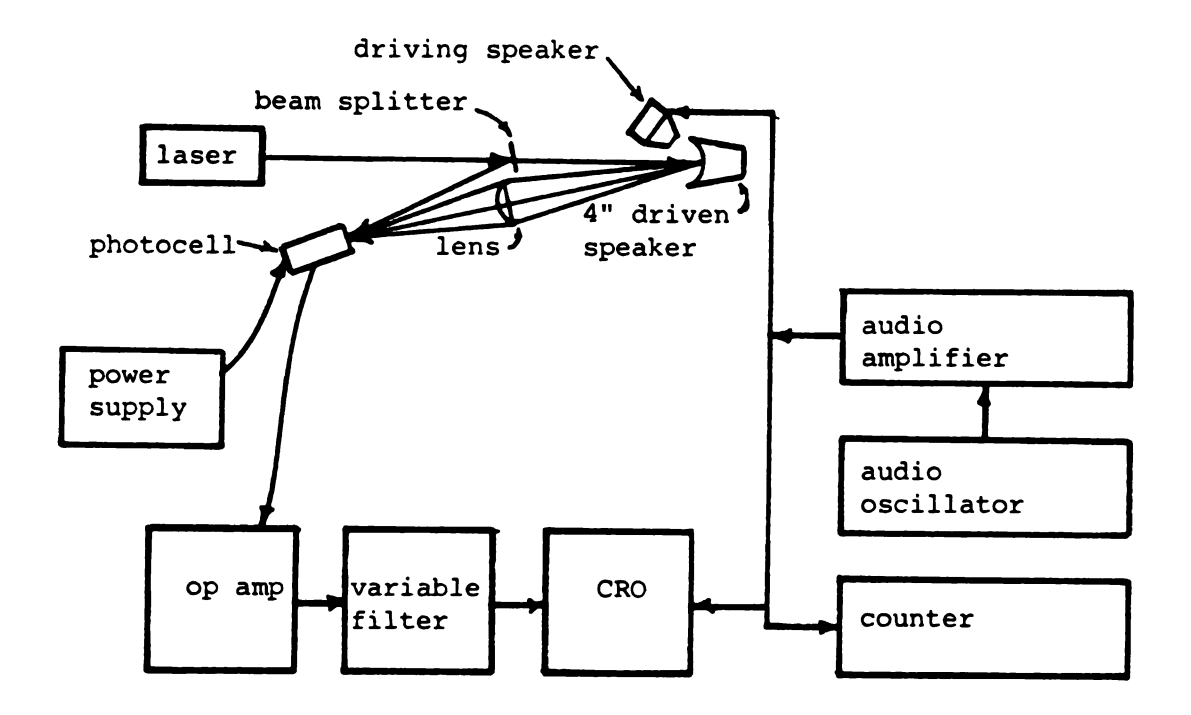
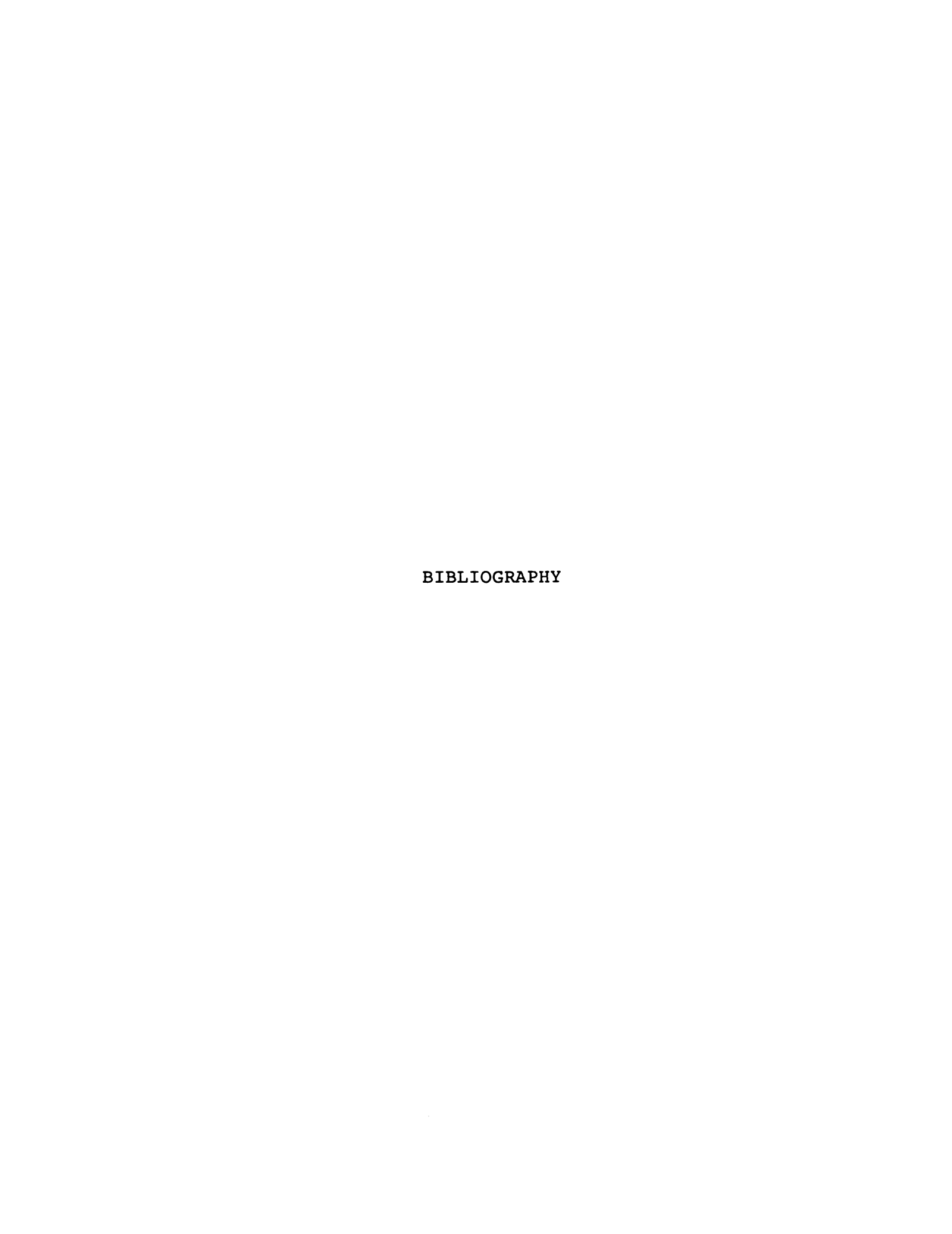


Figure E-2 Basic Validity Experimental System

The natural frequency of the driven speaker system was simple to obtain. The speaker had a well-defined maximum at 305 Hz. The 20 data points all fell in the range of 305  $\pm$  ½ Hz or 305 Hz with a standard deviation of  $\pm$  ½ Hz.



#### **BIBLIOGRAPHY**

- Archer, R. R. "On the Influence of Uniform Stress States on the Natural Frequencies of Spherical Shells." Transactions of the ASME, Journal of Applied Mechanics, 502-505 (September 1962).
- 2. Barone, A. "Sound Reflection." Acoustica, 2, 221 (1952).
- 3. Becker, B. and Gay, A. J. "Applanation Tonometry in the Diagnosis and Treatment of Glaucoma."

  AMA Archives of Ophthalmology, 62, 77-81

  (August 1959).
- 4. Buchhave, P. "Laser Doppler Velocimeter with Variable Optical Frequency Shift." Optics and Laser Technology, 11-16 (February 1975).
- 5. Cloud, G. L. "Infrared Photoelasticity, Principles, Methods and Applications." PhD Dissertation, Michigan State University (1966).
- 6. Cloud, G. L. "Practical Speckle Interferometry for Measuring In-Plane Deformations." Applied Optics, 14, 4, 878-884 (April 1975).
- 7. Engin, A. E. "Vibrations of Fluid-Filled Spherical Shells." Journal Acoust. Soc. Amer., 46, 1 (Part 2), 186-190 (1969).
- 8. Engin, A. E. and Engin, A. W. "Survey of Theoretical and Experimental Mechanics Applied to Head Injury." Shock and Vibration Digest, 7, 3, 1-13 (March 1975).
- 9. Engin, A. E. and Liu, Y. K. "Axisymmetric Response of a Fluid-Filled Spherical Shell in Free Vibrations," Journal of Biomechanics, Pergamon Press, 3, 11-22 (1970).

- 10. "Fastax Cameras, Handbook of Operating Instructions." Wollensak Optical Co., Rochester, N.Y. (1954).
- 11. Forbes, M., Pico Jr., G. and Grolman, B. "A Non-contact Applanation Tonometer." AMA Archives of Ophthalmology, 91, 134-139 (February 1974).
- 12. Friedenwald, J. S. "Contribution to the Theory and Practice of Tonometry." American Journal of Ophthalmology, 20, 10, 985-1024 (October 1937).
- 13. Friedenwald, J. S. "Variation of Corneal Curvature to Ocular Rigidity." American Journal of Ophthalmology, 20, 10 (October 1937).
- 14. Ganong, W. F. Review of Medical Physiology. 4th Edition, Lange Medical Publications, Los Altos, California (1969).
- 15. Gloster, J. and Perkins, E. S. "Distensibility of the Human Eye." British Journal of Ophthalmology, 43, 97, 97-101 (1959).
- 16. Goldmann, H. "Applanation Tonometry." Glaucoma, Trans. Second Conference, F. W. Newell (ed.), Sponsored by the Josiah Macy Jr. Foundation, New York, 167-220 (1956).
- 17. Goldmann, H. "Some Basic Problems of Simple Glaucoma." Presented at 28th Meeting of the Association for Research in Ophthalmology, Inc., Atlantic City, New Jersey, 213-220 (June 1959).
- 18. Gooberman, G. L. <u>Ultrasonics</u>, Theory and Application. The English Universities Press LTD, London (1958).
- 19. Green, D. G., Frueh, B. R. and Shapiro, J. M.

  "Corneal Thickness Measured by Interferometry."

  Journal of the Optical Society of America, 65, 2, 119-123 (February 1975).
- 20. Grolman, B. "A New Tonometer System." American Journal of Optometry and Archives of American Academy of Optometry, 49, 8, 646-660 (August 1972).
- 21. Hilton, G. F., and Schoffer, R. N. "Electronic Applanation Tonometry." American Journal of Ophthalmology, 62 (1966).

- 22. Junger, M. C. and Felt, D. <u>Sound, Structures and Their Interaction</u>. The MIT Press, Cambridge (1972).
- 23. Kenner, V. H. and Goldsmith, W. "Dynamic Loading of a Fluid-Filled Spherical Shell." International Journal of Mech. Sc., Pergamon Press, 14, 557-568 (1972).
- 24. Kobayashi, A. S., Staberg, L. G. and Schlegel, W. A. "Viscoelastic Properties of Human Cornea."

  Sponsored by the Bishop Eye Research Foundation and NIH Grant EY-272 and CM 634 G 03, University of Washington (1974).
- 25. Kobayashi, A. S. and Staberg, L. G. "Mechanics of Mackey-Marg Tonometer." ASME Publication No. 73-Wa Bio-21.
- 26. Kobayashi, A. S., Woo, S. L-Y., Lawrence, C. and Schlegel, W. A. "Analysis of the Corneo-Scleral Shell by the Method of Direct Stiffness." Journal of Biomechanics, 4, 323-330 (1971).
- 27. Mackay, R. S. and Marg, E. "Fast, Automatic Electronic Tonometers Based on an Exact Theory."

  Acta Ophthalmolgia, 37, 495-507 (1959).
- 28. Millard, N. D. and King, B. G. <u>Human Anatomy and Physiology</u>, 3rd. Ed., W. B. Saunders Company, Philadelphia (1951).
- 29. Morse, P. M. and Feshback, H. Methods of Theoretical Physics, Part II. McGraw Hill Book Company, Inc., New York (1953).
- 30. Moses, R. A. "The Goldmann Applanation Tonometer." American Journal of Ophthalmology, 46, 6, 865-869 (December 1958).
- 31. Moses, R. A. "Repeated Applanation Tonometry."
  Ophthalmologica, 142, 663-668 (1961).
- 32. Moses, R. A. and Grodzki, W. J. "Theory and Calibration of the Schiotz Tonometer." Investigative Ophthalmology, 589-591 (August 1971).
- 33. Moses, R. A., Marg, E. and Oechsli, R. "Evaluation of the Basic Validity and Clinical Usefulness of the Mackay-Marg Tonometer." Investigative Ophthalmology, 1, 1, 78-85 (February 1962).

- 34. Moses, R. A. and Tiu, C. H. "Repeated Applanation Tonometry." American Journal of Ophthalmology, 66, 1, 89-91 (July 1968).
- 35. Mow, C. C. "A Theoretical Model of the Cornea for Use in Studies of Tonometry." Bulletin of Mathematical Biophysics, 30, 437-453 (1968).
- 36. Newell, F. W. and Ernest, J. T. Ophthalmology. 3rd. Ed., C. V. Mosby Co., St. Louis (1974).
- 37. Nyquist, G. W. "The Corneal Lamella Anisotropic Elastic Constitutive Relation: Theory and Experiment." PhD Dissertation, Department of Metallurgy, Mechanics and Material Science, Michigan State University (1970).
- 38. Nyquist, G. W. "Rheology of the Cornea: Experiment Techniques and Results." Experimental Eye Research, 7, 183 (1968).
- 39. Nyquist, G. W. and Cloud, G. L. "Stress Dependent Dispersion of Corneal Birefringence: A Proposed Optical Technique for Intraocular Pressure Measurement." Journal of Biomechanics, 3, 249 (1970).
- 40. Phillips, C. I. and Shaw, T. L. "Model Analysis of Impression Tonometry and Tonography." Experimental Eye Research, 10, 161-182 (1970).
- 41. Piersol, G. A. (Editor). <u>Human Anatomy</u>, Volume II. Seventh Edition, J. B. Lippincott Company, Philadelphia (1919).
- 42. Post, D. and Gurland, J. E. "Corneal Studies by Photoelasticity." Experimental Mechanics, 7, 10, 419 (October 1967).
- 43. Rabinowicz, E. An Introduction to Experimentation.
  Addison-Wesley Publishing Company, Reading, Mass.
  (1970).
- 44. Rand, R. and DiMaggio, F. "Vibrations of Fluid-Filled Spherical and Spheroidal Shells." The Journal of Acoustical Society of America, 42, 6, 1278-1286 (December 1967).

- 45. Schwartz, N. J., Mackay, R. S. and Sackman, J. L.

  "A Theoretical and Experimental Study of the
  Mechanical Behavior of the Cornea with Application to the Measurement of Intraocular
  Pressure." Bulletin of Mathematical Biophysics,
  28, 585-643 (1966).
- 46. Stanworth, A. "The Cornea in Polarized Light."
  British Journal of Ophthalmologica, 48 (1970).
- 47. Stepanik, J. "The Mackay-Marg Tonometer." Acto Ophthalmologica, 48, 1140-1144 (1970).
- 48. Stocker, F. W. "On Changes in Intraocular Pressure after Application of the Tonometer." American Journal of Ophthalmology, 45, 192-195 (1958).
- 49. Tierney, J. P. and Rubin, M. L. "A Clinical Evaluation of the Electronic Applanation Tonometer."

  American Journal of Ophthalmology, 263-273

  (August 1966).
- 50. Vasek, A. G. "Ocular Rigidity and the Mechanical Properties of the Sclera." PhD Dissertation, University of Detroit (1970).
- 51. Walker, R. E. and Litovitz, T. L. "An Experimental and Theoretical Study of the Pneumatic Tonometer." Experimental Eye Research, 13, 14-23 (1972).
- 52. Wang, C. P. and Snyder, D. "Laser Doppler Velocimetry: Experimental Study." Applied Optics, 13, 1, 98-103 (January 1974).
- 53. Wittenberg, S. "Repeated Applanation Tonometry with the Noncontacting Tonometer." Journal of the American Optometric Association, 44, 1, 50-56 (January 1973).
- 54. Woo, S. L-Y., Kobayashi, A. S., Lawrence, C. and Schlegel, W. A. "Mathematical Model of the Corneal-Scleral Shell as Applied to Intraocular Pressure-Volume Relations and Applanation Tonometry." Annals of Biomedical Engineering, 1, 87-98 (1972).
- 55. Woo, S. L-Y., Kobayashi, A. S., Schlegel, W. A. and Lawrence, C. "Nonlinear Material Properties of Intact Cornea and Sclera." Experimental Eye Research, 14, 1, 29-39 (July 1972).